DISSERTATION

CONTROL OF PROTEIN ADSORPTION, CELL MORPHOLOGY AND INTRACELLULAR SIGNAL TRANSDUCTION USING SELF-ASSEMBLED MONOLAYERS OF ALKYLTHIOLATES ON GOLD

Submitted by

Kristin Beth McClary

Department of Biochemistry and Molecular Biology

In partial fulfillment of the requirements

For the Degree of Doctor of Philosophy

Colorado State University

Fort Collins, Colorado

Spring 1999

COLORADO STATE UNIVERSITY

March 26, 1999

WE HEREBY RECOMMEND THAT THE DISSERTATION PREPARED UNDER OUR SUPERVISION BY KRISTIN BETH MCCLARY ENTITLED CONTROL OF PROTEIN ADSORPTION, CELL MORPHOLOGY AND INTRACELLULAR SIGNAL TRANSDUCTION USING SELF-ASSEMBLED MONOLAYERS OF ALKYLTHIOLATES ON GOLD BE ACCEPTED AS FULFILLING IN PART REQUIREMENTS FOR THE DEGREE OF DOCTOR OF PHILOSOPHY.

Committee on Graduate Work

Robert W. Woody

Adviser

Department Head/Director

ABSTRACT OF DISSERTATION

SURFACE CHEMISTRY CONTROL OF PROTEIN ADSORPTION, CELL MORPHOLOGY AND INTRACELLULAR SIGNAL TRANSDUCTION

Self-assembled monolayers of terminally-functionalized alkylthiolates on gold have been used to interrogate cell-biomaterial surface interactions at the extracellular and intracellular level. The goal of this research was to provide molecular level information on the surface determinants necessary to produce predictable, controllable biological responses to implanted materials.

Various players in "outside-in" communication between a cell and a material's surface were investigated. Surfaces of a variety of alkylthiol chemistries were used to monitor protein adsorption and subsequent Swiss 3T3 fibroblast adhesion, spreading and growth. Distinct alkylthiol substrate chemistry-dependent differences were observed. Formation of focal contacts and stress fibers, early indicators of effective signaling, was observed to be surface-chemistry dependent. These responses could be correlated with protein dynamics on different surface chemistries. Relative deposition and conformations of fibronectin were shown to be dependent on surface chemistry. Results indicate that observed differential cell adhesion, spreading and growth on derivatized surfaces is mediated through modulations of adsorbed ECM molecules (e.g., fibronectin).

The primary regulators of the events investigated above were examined. Well-controlled alkylthiol surface chemistries were used to monitor the activation state of RhoA. Activation states of RhoA were determined and shown to be surface chemistry-dependent. RhoGDI levels and intracellular localization were also shown to be surface-chemistry dependent. Cells cultured on -CH_3 terminated SAMs, which normally exhibit a

cultured on -CH_3 terminated SAMs, which normally exhibit a low growth phenotype, were transfected with a constitutively active RhoA mutant. Transfected cells exhibited significant increases in cell length. However, no focal contact formation was observed. These results show that genetic alteration of intracellular regulators is incapable of overcoming the lack of extracellular stimuli, in the form of adsorbed ECM proteins, present on –CH_3 terminated SAM surfaces.

In summary, extracellular and intracellular information indicates that surface chemistry is capable of modulating communication between a cell and its extracellular environment. These data provide new, valuable molecular level information necessary to develop rational cause and effect relationships between a material's surface chemistry and biological response. This information should prove useful to develop biomaterials capable of producing predictable biological responses.

Kristin Beth McClary
Biochemistry and Molecular
Biology Department
Colorado State University
Fort Collins, CO 80523
Spring 1999

ACKNOWLEDGMENT

First and foremost, I would like to thank my advisor and friend, Dr. David Grainger, for his guidance and support in both my professional and personal endeavors. His continuous faith in my scientific ability and willingness to expose me to new challenges has helped me become the scientist I am today. I would also like to thank Dr. Guoquiang Mao, Rob Holcomb and Joe Caballaro for synthesizing and characterizing the derivatized alkylthiols I used throughout my research, Dr. David Castner at NESAC/Bio for performing XPS measurements and finally, the National Science Foundation and National Institutes of Health for the financial support to make this research possible.

DEDICATION

To my family, for getting me this far and to my fiancé, for being my future.

TABLE OF CONTENTS

CHAPTER 1. CELLS AND SURFACES

1.1. INTRODUCTION..... 1

1.2. SURFACE PROPERTIES OF BIOMATERIALS..... 5
1.2.1. Introduction..... 5
1.2.2. Self-Assembled Monolayers (SAMs)..... 7
1.3. EXPERIMENTAL..... 12
1.3.1. Surface Preparation..... 12
1.3.2. Contact Angle Analysis..... 12
1.3.3. Ellipsometry..... 13
1.3.4. X-Ray Photoelectron Spectroscopy..... 13

1.4. RESULTS AND DISCUSSION..... 14
1.4.1. Contact Angle Analysis..... 14
1.4.2. Ellipsometry..... 14
1.4.3. X-Ray Photoelectron Spectroscopy..... 14

1.5. CONCLUSIONS..... 18

1.6. ENDNOTES..... 20

CHAPTER 2. EXTRACELLULAR MATRIX PROTEINS AND CELLS ON SURFACES

2.1. INTRODUCTION..... 25
2.1.1. Protein Adsorption at Biomaterials Interfaces 25
2.1.2. Influence of Surface Properties on Protein Adsorption..... 26
2.1.3. Conformation and Orientation of Proteins at Interfaces..... 27
2.1.4. The Role of Adsorbed Proteins in Cell Interactions with Solid Surfaces..... 29
2.1.5. Cells on SAMs..... 31

2.2. EXPERIMENTAL..... 33
2.2.1. Fibronectin Adsorption to Derivatized SAM Surfaces..... 33
2.2.2. Availability of the Cell Binding Domain in Fibronectin Adsorbed on SAM Surfaces..... 34
2.2.3. Fibroblast Adhesion on SAM Surfaces..... 35

2.2.4. Fibroblast Growth on Derivatized SAM Surfaces..... 35
2.2.5. Primary Cell Line Experiments..... 36

2.3. RESULTS..... 36
2.3.1. Fibronectin Adsorption to SAM Surfaces Varies with Surface Chemistry..... 36
2.3.2. Adsorbed Fibronectin Conformation is Modulated by Surface Chemistry..... 38
2.3.3. Swiss 3T3 Fibroblast Adhesion and Growth on SAM Surfaces is Dependent Upon Composition of the Pre-Adsorbed Protein Mixture..... 41
2.3.4. Primary vs Secondary Cell Line Response to SAM Surfaces..... 43

2.4. DISCUSSION..... 47

2.5. ENDNOTES..... 51

CHAPTER 3. INTRACELLULAR SIGNALING ON MODEL CELL CULTURE SURFACES

3.1. INTRODUCTION..... 56
3.1.1. Cell Integrin Receptors are Involved in Cell-Surface Recognition of Adsorbed ECMs... 56
3.1.2. Early Integrin-Mediated Intracellular Events..... 57

3.2. EXPERIMENTAL..... 61
3.2.1. Immunocytochemistry..... 61
3.2.2. Primary Cell Line Experiments..... 63
3.2.3. Analysis of Tyrosine Phosphorylation of Focal Adhesion Proteins..... 63

3.3. RESULTS..... 65
3.3.1. Swiss 3T3 Fibroblast Stress Fiber and Focal Contact Formation on SAM Surfaces is Dependent Upon the Composition of the Pre-Adsorbed Protein Mixture..... 65
3.3.2. Comparisons of Swiss 3T3 Fibroblasts and Chick Skin Fibroblast Focal Contact and Stress Fiber Formation..... 70
3.3.3. Tyrosine Phosporylation of Focal Contact Proteins is Surface Chemistry-Dependent..... 72

3.4. DISCUSSION..... 79

3.5. ENDNOTES..... 82

CHAPTER 4. THE ROLE OF THE MOLECULAR WEIGHT GTPASE RHOA IN SURFACE CHEMISTRY-INDUCED CHANGES IN FIBROBLAST MORPHOLOGY

4.1. INTRODUCTION..... 87

4.2. EXPERIMENTAL..... 90
4.2.1. Cells and Culture Substrates..... 90
4.2.2. Cytosolic/Membrane Fractionation..... 91
4.2.3. Western Blot Analysis..... 91
4.2.4. Mutant RhoA Expression..... 92

4.3.RESULTS..... 92
4.3.1. Intracellular Localization of RhoA..... 93
4.3.2. Rho-GDI Levels are Higher in Cells Plated on $-CH_3$ Terminated SAMs..... 96
4.3.3. C3 Toxin Inactivation of RhoA in Cells Plated on –COOH Terminated SAM Surfaces 96
4.3.4. Mutant RhoA Expression Effects on Transfected Fibroblasts Plated on $-CH_3$ Terminated SAM Surfaces..... 99

4.4. DISCUSSION..... 106

4.5. ENDNOTES..... 114

CHAPTER 5:SUMMARY

5.1. INTRODUCTION..... 118

5.2. FUTURE WORK..... 125

5.5. ENDNOTES..... 127

LIST OF TABLES

Table		Page
1.1.	Water Contact Angle Data of Functionalized Alkylthiolate Self-Assembled Monolayers on Gold Surfaces.....	15
1.2.	Ellipsometry Film Thickness Data of Functional Alkylthiolate Self-Assembled Monolayers on Gold Surfaces.....	16
1.3.	XPS Atomic Percent Data of CH_3-$(CH_2)_{11}$-SH Self-Assembled Monolayers on Gold Before and After UV Sterilization and Overnight Buffer Exposure.....	19

LIST OF FIGURES

Figure		Page
1.1	The Structure of Self-Assembled Monolayers of Alkylthiols On Gold <111> Surfaces.....	9
1.2.	XPS Spectra of Different SAMs.....	17
2.1.	Fibronectin Adsorption to Derivatized SAM Surfaces.....	37
2.2.	Scatchard Plots of Binding Data for the Interaction of Anti-RGD Antibody with SAM Surface Adsorbed Fn.....	39
2.3.	Summary of Cell Binding Domain Exposure in Fn Adsorbed to SAM Surfaces Probed by Monoclonal Antibodies.....	40
2.4.	Fibroblasts Adhesion to Derivatized SAM Surfaces.....	42
2.5.	Fibroblast Growth on Derivatized SAM Surfaces.....	44
2.6.	Comparison of Swiss 3T3 Fibroblast and Chick Skin Fibroblast Adhesion to Derivatized Sam Surfaces.....	45
2.7.	Comparison of Swiss 3T3 Fibroblast and Chick Skin Fibroblast Growth on Derivatized SAM Surfaces.....	46
3.1.	Vinculin and F-Actin Immunostaining in Attached Swiss 3T3 Fibroblasts on Derivatized SAM Surfaces.....	66
3.2.	Paxillin Immunostaining in Attached Swiss 3T3 Fibroblasts on Derivatized SAM Surfaces.....	68
3.3.	FAK Immunostaining in Attached Swiss 3T3 Fibroblasts on Derivatized SAM Surfaces.....	69
3.4.	Filamentous Actin Staining in Attached Chick Skin Fibroblasts on Derivatized SAM Surfaces.....	71
3.5.	Immunostaining in Attached Chick Skin Fibroblasts on Derivatized SAM Surfaces.....	73
3.6.	Phosphotyrosine Immunostaining in Attached Fibroblasts Derivatized SAM Surfaces.....	74

3.7.	Immunoprecipitations of Paxillin (68K) and FAK (125K) from Whole Cell Extracts of Swiss 3T3 Fibroblasts Plated on Derivatized SAM Surfaces.....	76
3.8.	Westerns of FAK (125 K) immunoprecipitations of whole cell extracts of Swiss 3T3 fibroblasts plated on derivatized SAM surfaces.....	77
3.9.	Phosphotyrosine Westerns of Paxillin (68K) and FAK (125K) from Immunoprecipitations of Whole Cell Extracts of Swiss 3T3 Fibroblasts Plated on Derivatized SAM Surfaces.....	78
4.1.	RhoA Western of Whole Cell Extracts of Swiss 3T3 Fibroblasts Plated on Derivatized SAM Surfaces.....	94
4.2	RhoA Westerns of Cytosol/Membrane Fractions From Swiss 3T3 Fibroblasts Plated on Derivatized SAM Surfaces.....	95
4.3.	Rho-GDI Western of Whole Cell Extracts of Swiss 3T3 Fibroblasts Plated on Derivatized SAM Surfaces	97
4.4.	Rho-GDI Westerns of Cytosol/Membrane Fractions From Swiss 3T3 Fibroblasts Plated on Derivatized SAM Surfaces	98
4.5.	Phase Contrast Images of Swiss 3T3 Fibroblasts in the Presence of C3 Transferase.....	100
4.6.	Expression of constitutively active RhoA in fibroblasts cultured on –COOH terminated SAM surfaces leads to a loss of growth morphology.....	101
4.7.	Expression of constitutively active RhoA in fibroblasts cultured on $-CH_3$ terminated SAM surfaces causes an initial increase in cell spreading followed by cell retraction	102

Chapter 1: Cells and Surfaces

1.1. Introduction

Interactions between cells and surfaces play a major role in controlling cellular behavior. Cells in tissues in higher organisms are surrounded by a proteinaceous scaffold that is vital to their normal functioning. Earlier in the century, when researchers began to first explore the art of culturing cells *ex-vivo*, it was determined that most cells require attachment to a solid matrix to proliferate [1]. When normal fibroblast cells are cultured in suspension and therefore are rounded up, the probability of entering the S phase (synthesis) of the cell cycle averages 8% at any particular time. The percent of cells that progress through the cell cycle increases with cell spreading in intimate contact with a surface and its adsorbed proteins [2]. Most normal fibroblasts must be attached to a matrix or solid substrate to progress through the cell cycle and proliferate; a phenomenon referred to as 'anchorage dependence'. Loss of anchorage dependence is a common sign of viral transformation and strongly correlates to tumorgenicity [3, 4]. The work of Penman and co-workers demonstrated that most metabolic processes in normal cells are also dependent on adhesion [5, 6].

Anchorage control has been shown to operate at the G_1 checkpoint, meaning that cells require anchorage to pass this point in the cell cycle. Fibroblasts undergo cell cycle arrest in the G_1 phase of the cell cycle when cultured in suspension [7-9]. Beyond a defined time point in G_1, cells are no longer dependent on adhesion to complete the cell

cycle [10]. Anchorage dependence can be traced to the necessary induction of several growth-associated genes. Cell adhesion has been shown to induce specific mRNA expression of c-fos, c-myc, actin [11], collagenase, stromelysin [12], collagen [13], fibronectin and laminin [14], as well as cause global messenger RNA and protein synthesis induction [5]. In addition to growth, the interaction of anchorage-dependent cells with ECM proteins plays a key role in the formation and maintenance of tissue integrity and organization, regulation of cell motility as well as influencing many other aspects of cell physiology including activation of intracellular processes and differentiation [15-20].

In addition to the important role cell-surface interactions play in normal cellular function within the body, the growth of cells on solid substrates is of fundamental importance in the fields of biotechnology and biomedical/biomaterials engineering. The growth of anchorage-dependent mammalian cells in large-scale bioreactors is useful in the production of gene products that must be appropriately modified (i.e., glycosylated) after translation in order to be biologically active. These systems are commonly used for the production of monoclonal antibodies, growth factors, hormones, enzymes and vaccines [21].

More recently, new biomedical applications require the growth of cells entrapped inside of or seeded onto polymeric devices. These systems have been used in new therapeutic approaches to treat diabetes, Parkinson's disease, liver failure and nerve regeneration [22]. For example, cells engineered to produce a therapeutic agent are seeded in a reservoir onto hollow polymeric fibers. Fluid is passed through the fiber, which acts as a semi-permeable membrane, to selectively deliver nutrients and filter off

the cellular product of interest [23]. Polymeric materials are also being exploited as scaffolds to enhance the regrowth of damaged tissue, including liver, nerve and bone. In these applications, biodegradable, biocompatible polymeric scaffolds are placed in areas where tissue damage has occurred. Often, the polymer scaffolds are infused with growth factors (e.g., bone morphogenic protein) that, upon progressive degradation of the polymer, are released to signal cell growth and infiltration into the implant site.

Quite possibly the most important area of need for better understanding of cell-surface interactions is in the field of biomaterials. Biomaterials scientists are challenged to modify the effects of implantation of synthetic materials into the body to augment or replace the structure or function provided by a tissue or organ that has failed. These devices can be either permanent or temporary and commonly include pacemakers, catheters, stints, hip joints, and contact lenses. Implanted or cell-seeded biomaterials maintain intimate contact with host cells or tissue via their outer surfaces and often are intended to integrate and promote tissue replacement or neogenesis. Consequently, current technologies demand new materials and methods to control and exploit cell/surface interactions in biological scenarios to enhance or replace natural tissue function.

After 30 years of research and development, numerous materials are now commonly used in the manufacture of implanted medical devices. Over 2500 biomedical devices currently marketed in the US rely on a diverse array of synthetic biomaterials, including titanium, silicone rubber, polyurethane, hydrogel, stainless steel, aluminum and Teflon™. Many of these biomaterials are in fact approved for biomedical and surgical use by historical precedent and were never designed specifically for surgical uses. Most

biomaterials, while performing adequately in a number of implant applications, fall drastically short of being ideal, "biocompatible" replacement materials. All these materials, when implanted into the body, elicit a typical foreign body response. The implant site with the material in place represents a wound site that cannot heal properly using normal processes. As is typical for the normal inflammatory reaction, the site will be infiltrated with neutrophils, followed by macrophages and foreign body giant cells. However, the implanted material surface, with an assorted array of adsorbed, denatured proteins activates giant cells, T-cells and macrophages abnormally. Eventually, fibroblasts will attach to the surface of the implant and form a fibrous, avascular capsule around the implant, effectively "walling it off" from the body's defenses. This response, when tolerated by the host in the appropriate context, is commonly referred to as "biocompatibility" in the biomaterials field [24]. In some cases, this response is adequate, although not ideal, for the requisite properties of the implant. However, if exchange of fluids and nutrients between the implant and the body is necessary, as in the case of cell encapsulation, this typical biocompatibility encapsulation response is undesirable. In addition, millions of surgeries are performed each year to retrieve implants that become infected or seriously, pathologically rejected over time by the body [25]. The biomaterials research community has spent over 30 years attempting to understand the molecular basis for the complex relationship between a material's surface properties and cell proliferation in order to improve implant performance. Compelling, unsolved technological and medical needs continue to drive such research.

1.2. Surface Properties of Biomaterials

1.2.1. Introduction

Several surface properties have been documented to affect biological responses to implanted biomaterials. In general, cell physiological responses have been shown to be influenced by surface topography (including roughness, texture and porosity), chemistry, wettability, and charge.

Implant surface topography has been shown to influence cell behavior *in vitro* and tissue response *in vivo*. In a study comparing textured and smooth polytetrafluoroethylene (PTFE), it was demonstrated that fibroblasts cultured on textured PTFE showed more attachment and growth than those cultured on smooth PTFE [26]. Other researchers have shown that ridges and grooves promote directional orientation responses in cells cultured on these surfaces. Oakley and Brunette correlated texture-dependent orientation of migration and elongation with the alignment of several cytoskeletal elements including microtubules, microfilaments and focal adhesion contacts [27]. Meyle and coworkers demonstrated that focal adhesions are primarily found on the tops of ridges as opposed to in the grooves [28]. Overall, previous data supports cell discrimination of orientation by surface topography within texture dimensions of 1-3 μm width and 0.5-1.0 μm depth [28].

Surface chemistry has been widely studied for its ability to promote or discourage biological interaction. Historically, the design of implant materials has focused to some degree on understanding the ability of biomaterial surface chemistries to provide specific, predictable control over physiological responses. Deconvoluting the contributions of each chemistry to cellular responses would provide the information necessary to rationally

design surfaces capable of predictably controlling biological responses. Despite decades of research effort, the specific surface determinants controlling and modulating cell, tissue and many biocompatibility responses (e.g., immunogenicity, thrombogenicity) are not well understood.

Currently, the most commonly used cell culture surface is corona-oxidized polystyrene (tissue culture polystyrene). This surface has proven to be very effective in supporting cell attachment, spreading and growth. By using a corona, high-voltage discharge under air or inert gas and then exposing to oxygen, a wide array of oxidized carbon species are produced at the polystyrene surface. These are known to include carbonyl, alcohol, epoxide and carboxylate chemistries. Unfortunately, no control of surface chemistry is possible or attempted with this method, and no correlations between oxidized chemistry and specific molecular biology have been reported. In contrast, Teflon™ is widely used as a non-adhesive polymer substrate. Although commonly used, tissue culture polystyrene and Teflon™ are polymers with very different surface chemistries. The aspects of these chemistries or the combination of these chemistries that makes them successful or unsuccessful in supporting cell growth are unknown, but thought to reside in their interfacial behavior with proteins.

A recognized major limitation to investigating and understanding cellular responses to biomaterials surfaces has been the inability to accurately control the chemistries presented [29]. Careful surface analytical research has demonstrated that virtually all biomaterial surfaces--polymers, metals, ceramics-- have variable, poorly defined and poorly controlled surface properties at the level of the protein or cellular response. A range of chemistries, both native to the material and contaminating

adsorbates, are present on all materials. Additionally, surface chemistry is dynamic, responding to environmental influences.

Due to their desirable physical and mechanical properties, polyurethanes have been used for decades as materials for biomedical applications. Chen and Ruckenstein used contact angle measurements and electron spectroscopy for chemical analysis (ESCA) to demonstrate that polyurethane surfaces undergo rearrangement when the external environment changes. Specifically, they noted that hydrophobic regions of the polymer (polymethane hard segments) were exposed at the surface in hydrophobic environments (air) while hydrophilic moieties (soft segments) were exposed under hydrophilic conditions (water). Similar trends have been documented for Teflon™ [30] and numerous block copolymers [31]. The current inability to design improved biomaterials for many applications results in part from this lack of control over surface design features that heavily influence cell and protein interactions. Recent advances in surface preparation and characterization now provide a new ability to accurately and consistently present cells and tissue with well-controlled surfaces presenting a wide array of functional groups organized at the molecular level.

1.2.2. Self-Assembled Monolayer (SAMs)

Self-assembled organic monolayers are "molecular assemblies that are formed spontaneously by the immersion of an appropriate substrate into a solution of an active surfactant in organic solvent [32]." Long chain alkyl compounds terminated with thiol, disulfide, isonitrile, silane, or pyridine groups have been studied with regard to their film forming behaviors on solid surfaces [32]. Molecules bearing these specific functional

terminal groups will spontaneously adsorb to solid surfaces such as polymers, metals, and metal oxides. This self-assembly process leads to the formation of highly organized, stable, organic monolayers having all the requisite properties for molecular-level surface modifications to improve biomaterial interfacial response.

SAMs of organic thiols on coinage metals were first reported by Nuzzo and Allara [33]. Sulfide, disulfide and thiol groups have been shown to be effective anchor groups for self-assembly on metals such as gold, silver and copper. Much of the work on SAMs has been done on gold, mainly because of the fact that gold does not have a stable oxide and thus can be handled in ambient conditions [34]. The surface reaction is a chemisorption event between the 'anchor' groups and the substrate. A slightly polar, gold-sulfur bond is formed, resulting in a stable interaction with bond energies of about half a covalent bond (~40-45 kcal/mol). (Figure 1.1).

The process of organic film self-assembly is mediated by an epitaxial event set up by the gold surface itself. Gold exists in a crystalline lattice. Alkylthiolate molecules spontaneously assemble via sulfur-gold thiolate bonds into the three-fold hollow sites on the gold <111> crystal faces of the gold lattices, as these sites are the most stable. The placement of the three-fold gold hollow sites in the atomic crystal lattice force an epitaxial hexagonal adlayer of adsorbed for self-assembled molecules on the surface. Alkyl chains of length C12 or greater terminated in thiol or disulfide groups will assemble spontaneously onto many clean metals to form chemisorbed monolayers. These monolayers are stabilized by van der Waals forces between adsorbed alkyl chains. On gold surfaces, FTIR has shown that well-organized alkyl chains of SAMs tilt 27° from the surface normal in an all-trans conformation. Alkylthiols have been shown to form

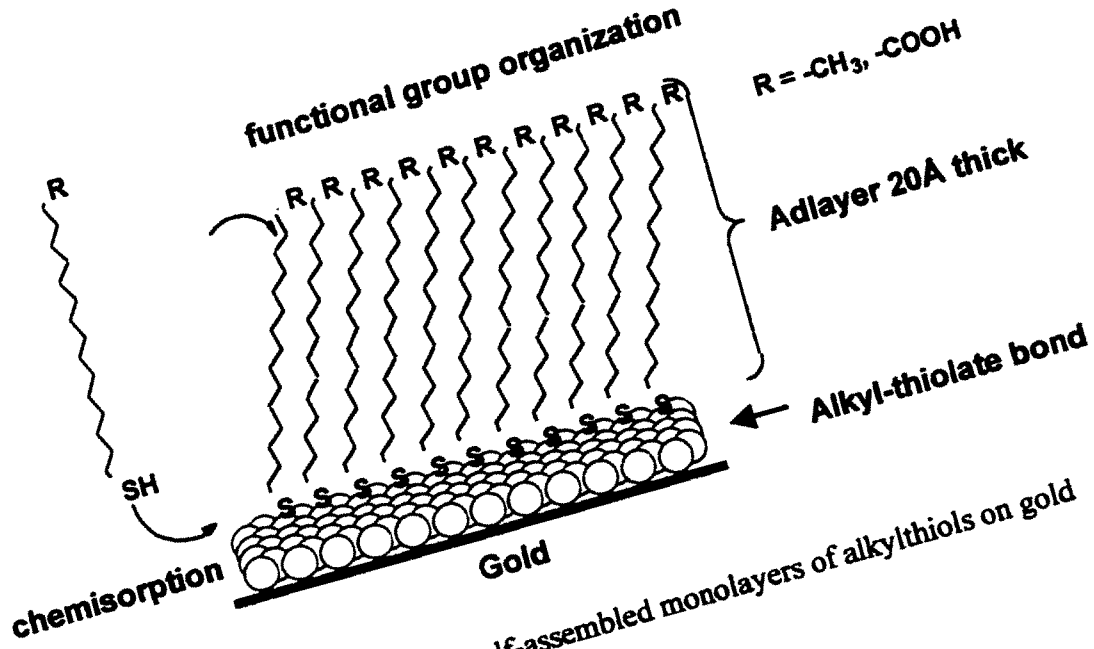

Figure 1.1. The structure of self-assembled monolayers of alkylthiols on gold <111> surfaces

well-ordered thiolate-anchored monolayers 20Å thick on metal surfaces, yielding relatively stable arrays of dense-packed alkyl chains projecting from the surface [35-38].

In addition to bearing terminal anchoring groups on one end, alkyl chains can be asymmetrically functionalized at their non-anchoring terminus with several other functional groups. Alkylthiol monolayers terminally derivatized with $-CF_3$ [39], -COOH [40], -OH [41], and $-NH_2$ [42] have been reported. In addition to basic functional groups, complex molecules (biotin) [43], sugars [44], antibodies [45] and phospholipids [46] have also been introduced onto solid surfaces through self-assembly. Control of the surface functional group density is a spontaneous product of the underlying anchor-group epitaxy on the metal surface.

Methods are also available for laterally and spatially varying self-assembling chemistries on surfaces. Early in the development of patterning techniques, numerous researchers used e-beam writing [47, 48], photolithography [49, 50] and micromachining [51] methods to pattern SAMs on surfaces. These processes involve selectively removing or destroying the integrity of SAMs to create a pattern on the surface. Recently, Whitesides' group at Harvard has developed numerous techniques to actively pattern self-assembled monolayers on solid surfaces [52]. Perhaps the most useful and versatile method of pattern formation is microcontact printing. In microcontact printing an elastomeric stamp is produced by casting poly(dimethysiloxane) (PDMS) onto an appropriate master. The stamp is then inked with an ethanolic solution of alkylthiols and placed in contact with a gold surface. After removal of the stamp, the gold surface can be immersed in a dilute ethanolic solution of alkanethiol with a different terminal functional group. Features as small as 200 nm have been generated using this technique [52]. This

technique has also been used to pattern SAMs with submicrometer features on curved surfaces with radii of curvature as small as 25 micrometers [53]. Another technique called microwriting involves dispensing alkylthiols from the tip of a fine pen or capillary onto the surface of a gold film. SAMs with lateral dimensions of 10 μm can be routinely prepared using this method [52]. These strategies provide a facile route to fabricating functionalized, spatially variable surface chemistries using self-assembling monolayers.

Characterization of structure and organization in these organic monolayer self-assembled films (SAMs) is extensive and well documented [32, 54]. Contact angle and wettability measurements have been used to provide information on the free energy of the terminal functional groups that comprise the outer layer of SAMs. The angle of an applied drop of liquid on a solid surface is the result of the balance between the cohesive forces in the liquid and the adhesive forces between the solid and the liquid. These forces result in a measurable contact angle. For instance, if there is no interaction between the solid and the liquid (non-wetting), the contact angle will be 180°. When water is used to interrogate SAMs, hydrophobic functional groups such as $-CF_3$ and $-CH_3$ exhibit high contact angles, as there is little interaction between the liquid (water) and the solid. The opposite case is observed for hydrophilic terminal functional groups such as –COOH and -OH. Ellipsometry data complements contact angle data by providing accurate adsorbed film thickness and mass data on solid surfaces.

In an x-ray photoelectron spectroscopy (XPS) experiment, a sample is exposed to monochromatic x-rays and the properties of the inner-shell electrons are probed. By varying the angle of the sample, numerous sample depths can be interrogated. For instance, at a grazing angle to the surface, information about surface atoms can be

obtained. XPS is particularly useful in determining the integrity of SAMs of alkylthiols on gold. For example, thiols are susceptible to oxidation into sulfonates or sulfinates. Oxidation of alkylthiol molecules in SAMs can lead to disruption of the gold-sulfur bond at the surface. Significant oxidation could cause desorption of the monolayer from the gold surface. XPS can identify oxidation by monitoring the sulfur2p peak in the XPS surface spectra. Oxidation leads to a shift in the binding energy of the sulfur atoms present at the surface.

1.3. EXPERIMENTAL

1.3.1. Surface Preparation. ω–Functionalized alkylthiols bearing terminal methyl ($-CH_3$), perfluoromethyl ($-CF_3$), hydroxyl (-OH) and carboxylate (-COOH) functional groups were synthesized and provided by Dr. G. Mao as cited in his Ph.D dissertation. Self-assembled monolayer (SAM) films of these compounds were fabricated on gold-coated Mylar surfaces (Courtaulds Performance Films, FM-1 gold coating, 99.99% purity, deposited to 70-90 Å thickness by evaporative deposition on 0.0007 gauge PET substrate). These clean, gold-coated substrates were immersed in 1 mM solutions of the alkylthiol compounds in nitrogen-purged ethanol for 24 hours. Substrates were then rinsed in ethanol and blown dry in a stream of nitrogen gas.

1.3.2. Contact Angle Analysis. Sessile drop contact angle analysis (Rame-Hart 100 Goniometer) used purified water (Millipore 18MΩcm resistivity) drops (2 μl) on three separate spots on each film surface in a controlled environment (100% relative humidity). Measurements were taken on both sides of water drops at ambient temperature

approximately 30 seconds after drops were applied to the surfaces. Contact angle data report the average of three drops at different spots.

1.3.3. Ellipsometry. All ellipsometry experiments were performed by G. Mao as described in his Ph.D dissertation. Film thicknesses were measured on a Gaertner L117 ellipsometer (wavelength 632.8 nm, incident angle 70°) referenced to clean gold pieces. The measurements reported represent the average of three different spot measured for each piece sample.

1.3.4. X-Ray Photoelectron Spectroscopy. In collaboration with Professor D.G. Castner (NESAC/Bio, University of Washington), x-ray photoelectron spectroscopy (XPS) experiments were performed on a Surface Science SSX-100 Spectrometer equipped with a monochromatic Al Kα source, hemispherical analyzer, and a multichannel detector. Typically, spectra were collected on the analyzer at 55° with reference to the sample surface normal, and the operating pressure was approximately $3x10^{-9}$ Torr. High resolution spectra were obtained at a pass energy of 50 eV using a 1000 μm spot size. The binding energy (BE) scales for all spectra were referenced to the Au ($4f_{7/2}$) peak at 84.00 eV. Peak fitting of the high resolution spectra was done using Gaussian peak shapes with commercial software supplied by Surface Science Instrument. For calculation of XPS elemental composition, the analyzer transmission function was assumed not to vary with photoelectron kinetic energy (KE), the photoelectron escape depth was assumed to vary as KE, and Scofields's photoelectron cross sections were used. Experiments were performed on freshly assembled SAMs, as well as SAMs which had been exposed to ultraviolet radiation and overnight buffer submersion.

1.4. Results and Discussion

1.4.1. Contact Angle Analysis. Results from the contact angle analysis are reported in Table 1.1. Water contact angles of these monolayers show that the solid surface energies of SAMs are strongly dependent on the terminal functional group [55]. Average aqueous static contact angles for SAM surfaces derivatized with –COOH, -OH, -CF_3 and -CH_3 functional groups are presented. In all cases, measurements consistent with the expected monolayer and surface compositions for the various functional groups were obtained. The contact angle of the -CH_3 and –CF_3 terminated SAMs on the gold substrate are 108° and 115°, respectively, consistent with reported alkylthiol SAMs with highly organized structures. The contact angles of the –COOH and –OH terminated SAMs on gold surfaces are less than 20°, indicating wetting and full coverage of those terminal functional groups on the gold surface.

1.4.2. Ellipsometry. The ellipsometry thicknesses of these SAMs on gold substrates demonstrate the assembly of the films into monolayer structures. Results from the ellipsometry are reported in Table 1.2. Results show that the thicknesses of SAMs are strongly dependent on the chemical composition of the monolayer. Average thicknesses for SAM surfaces derivatized with –COOH, -OH, -CF_3 and -CH_3 functional groups are presented. In all cases, measurements consistent with the expected monolayer and surface compositions for the various functional groups were obtained.

1.4.3. X-Ray Photoelectron Spectroscopy. Surface compositional results from XPS analysis of fresh SAMs, shown in Figure 1.2, verify a clean presentation of defined surface chemistry reflecting each SAM terminal group. The XPS C1s spectra shown quantitatively exhibit the carbon functional group expected at each surface and no

Table 1.1. Water contact angle data of functional alkylthiolate self-assembled monolayers on gold surfaces.

Thiolate Films on Gold	Contact Angle ($°H_20$) (+/- 2 °)
CF_3-$(CF_2)_8$-CH_2-CH_2-SH	115 °
CH_3-$(CH_2)_{11}$-SH	108 °
HOOC-$(CH_2)_{10}$-SH	17 °
HO-$(CH_2)_{11}$SH	18 °

Table 1.2. Ellipsometry film thickness data of functional alkylthiolate self-assembled monolayers on gold surfaces.

Thiolate Films on Gold	Thickness (Å)
CF_3-$(CF_2)_8$-CH_2-CH_2-SH	11 Å
CH_3-$(CH_2)_{11}$-SH	17 Å
HOOC-$(CH_2)_{10}$-SH	14 Å
HO-$(CH_2)_{11}$SH	14 Å

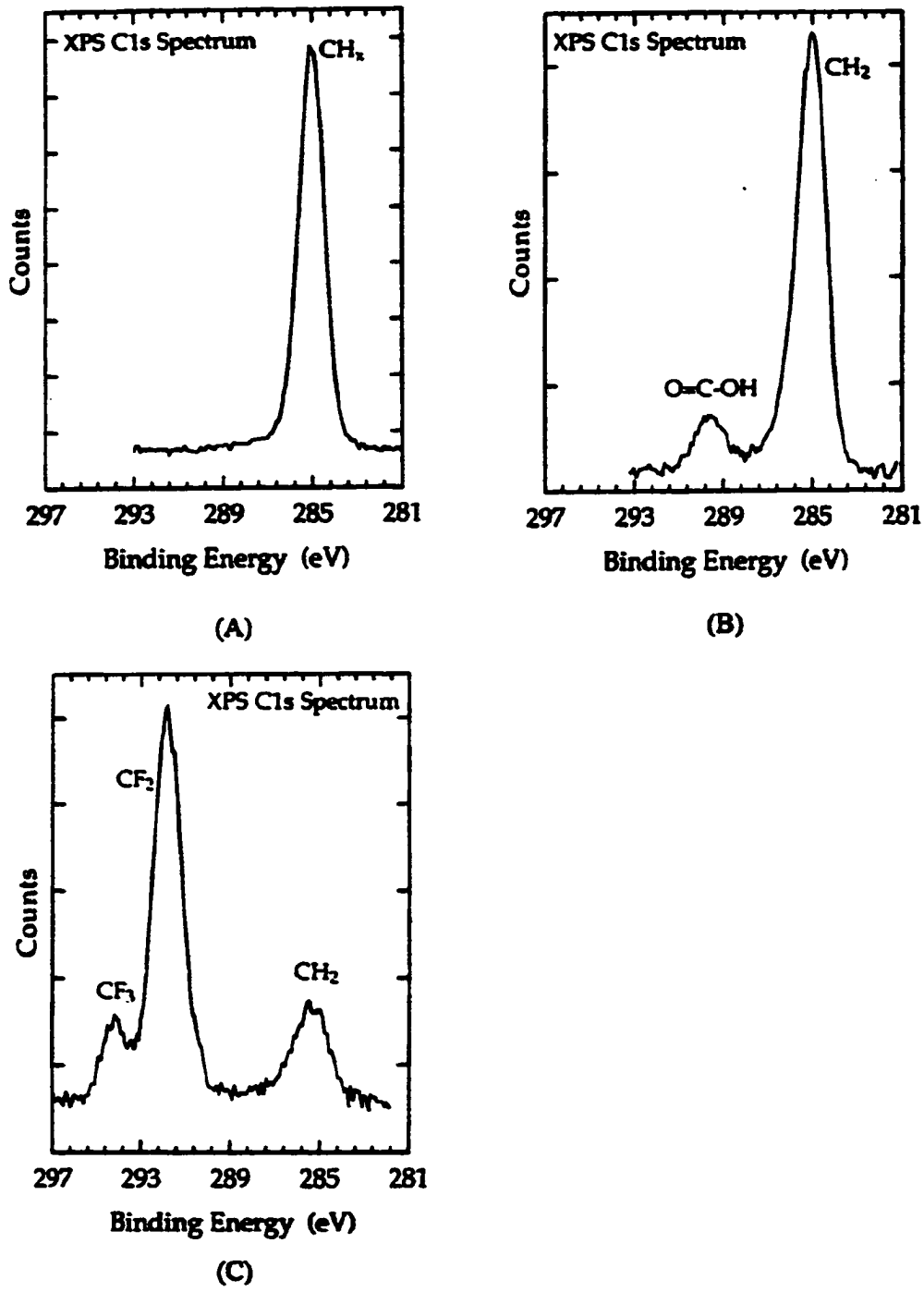

Figure 1.2. XPS spectra of different SAMs on gold. (A) CH_3-$(CH_2)_{11}$-SH, (B) HOOC-$(CH_2)_{10}$-SH, and (C) CF_3-$(CF_2)_8$-CH_2-CH_2-SH.

observable contamination. These SAM films were also tested under cell culture conditions including overnight phosphate-buffered saline (PBS) exposure and ultraviolet sterilization for 15 minutes. Following exposure, XPS characterization indicates that alkylthiol monolayer films retain their stability and integrity under cell culture conditions (Table 1.3). An increase in carbon and oxygen species, as well as a decrease in the gold species indicated that contamination from the buffer had deposited on or displaced some of the SAM. However, differences were not believed to be significant enough to affect their utility in biomaterials studies. Overall, surface analysis supports stable, predictable presentation of defined functional group chemistry. Increased oxygen content indicates inclusion of some new species on or within these surfaces, but sulfur content before and after treatment is constant, indicative of film stability. This is consistent with what is known and typical for SAM films.

1.5. Conclusions

Self-assembled monolayers of ω-functionalized alkylthiol molecules on gold were assembled for use as model cell culture surfaces. SAMs were characterized by contact angle, ellipsometry and XPS. In all cases, measurements consistent with the expected monolayer and surface compositions for the various functional groups were obtained. These well-controlled surfaces will be used as a model biomaterial to accurately and consistently present cells and tissue with consistent chemistry comprising a wide array of functional groups organized at the molecular level.

Table 1.3. XPS atomic percent data of CH_3-$(CH_2)_{11}$-SH self-assembled monolayers on gold before and after UV sterilization and overnight buffer exposure.

Treatment	XPS Atomic Percent				
	Au	F	C	S	O
No treatment	**28.0**	**42.7**	**26.7**	**1.4**	**1.3**
30 min. UV exposure	**29.0**	**42.6**	**26.3**	**1.0**	**1.1**
30 min. UV + 24 hour PBS	**24.7**	**40.7**	**30.8**	**1.5**	**2.4**

1.6. Endnotes

1. MacPherson, I. and L. Montagnier, Virology, **23** : p. 291-294 (1964).
2. O'Neil, C., P. Jordan, and G. Ireland, Cell, **44** : p. 489-496 (1986).
3. Shin, S., V.H. Freedman, R. Risser, and R. Pollack, Proc. Nat. Acad. Sci. USA, **72** (4435-4439): p. 4435-4439 (1975).
4. Vasiliev, J.M., Spreading of non-transformed and transformed cell, Biochim. Biophys. Acta., **780** : p. 21-65 (1985).
5. Benecke, B.J., A. Ben-Ze'ev, and S. Penman, The control of mRNA production, translation and turnover in suspended and reattached anchorage-dependent fibroblasts, Cell, **14** : p. 931-939 (1978).
6. Benecke, B.J., A. Ben-Ze'ev, and S. Penman, J. Cell Physiol., **103** : p. 247-254 (1980).
7. Guadagno, T.M. and R.K. Assoian, G1/S control of anchorage-independent growth in the fibroblast cell cycle, J. Cell Biol., **115** : p. 1419-1425 (1991).
8. Matsuhisa, T. and Y. Mori, An anchorage-dependent locus in the cell cycle for the growth of 3T3 cells., Exp. Cell Res., **135** : p. 393-398 (1981).
9. Otsuka, H. and M. Moskowitz, Arrest of 3T3 cells in G1 phase in suspension cultures, J. Cell Physiol., **87** : p. 213-219 (1975).
10. Han, E.K., T.M. Guadagno, S.L. Dalton, and R.K. Assoian, A cell cycle mutational analysis of anchorage-independent growth: cell adhesion and TGF-beta control G1/S transit specifically., J. Cell Biol., **122** : p. 461-471 (1993).

11. Dike, L.E. and S.R. Farmer, Cell adhesion induces expression of growth-associated genes in suspension-arrested fibroblasts, Proc Natl Acad Sci U S A, **85** (18): p. 6792-6 (1988).

12. Werb, Z., P.M. Tremble, O. Behrendtsen, E. Crowley, and C.H. Damsky, Signal transduction through the fibronectin receptor induces collagenase and stromelysin gene expression, J Cell Biol, **109** (2): p. 877-89 (1989).

13. Dhawan, J. and S.R. Farmer, Regulation of alpha 1 (I)-collagen gene expression in response to cell adhesion in Swiss 3T3 fibroblasts, J Biol Chem, **265** (16): p. 9015-21 (1990).

14. Nagahara, S. and T. Matsuda, Cell-substrate and cell-cell interactions differently regulate cytoskeletal and extracellular matrix protein gene expression, J. Biomed. Mat. Res., **32** : p. 677-686 (1996).

15. Geiger, B., D. Ginsberg, D. Salomon, and T. Volberg, Cell Differ. Dev., **32** : p. 343-353 (1990).

16. Burridge, K., K. Fath, T. Kelly, G. Nuckolls, and C. Turner, Annu. Rev. Cell Biol., **4** : p. 487-525 (1988).

17. Geiger, B., T. Volk, T. Volberg, and R. Bendori, J. Cell Sci. Suppl., **8** : p. 251-272 (1987).

18. Folkman, J. and A. Moscona, Nature, **273** : p. 345-349 (1978).

19. Wang, N., J.P. Butler, and D.E. Ingber, Science, **260** : p. 1124-1127 (1993).

20. Adams, J.C. and F.M. Watt, Regulation of development and differentiation by the extracellular matrix, Development, **117** : p. 1183-1198 (1993).

21. Ratafia, M., Mammalian cell culture:worldwide activities and markets, Biotechnol. Bioeng., **5** : p. 692-694 (1987).

22. Goosen, M.F.A., ed. *Fundamentals of animal cell encapsulation and immobilization.*. 1991, CRC Press: Boca Raton.

23. Altman, J.J., A. Manoux, P. Callard, P. McMillan, B.A. Solomon, J. Rosen, and P. Galleti, Long term plasma glucose normalization in experimental diabetic rats with macroencapsulated implants of benign human insulinomas, Diabetes, **35** : p. 625 (1985).

24. Remes, A. and D.F. Williams, Immune response in biocompatibility, Biomaterials, **13** : p. 731-743 (1992).

25. Gristina, A.G., Biomaterial-centered infection: microbial adhesion versus tissue integration, Science, **237** (4822): p. 1588-95 (1987).

26. Korman, N.J., O. Sudilovsky, and D.F. Gibbons, J. Biomed. Mater. Res., **18** : p. 225 (1984).

27. Oakley, C. and D.M. Brunette, J. Cell Sci., **106** : p. 343 (1993).

28. Meyle, J., H. Wolburg, and A.F. von Recum, J. Biomat. Appl., **7** : p. 362 (1993).

29. Andrade, J.D., D.E. Gregonis, and L.M. Smith, in *Physicochemical Aspects of Polymer Surfaces*, K.L. Mittal, Editor. 1983, Plenum: New York.

30. Ruckenstein, E. and S.V. Gourisankar, Environmentally induced restructuring of polymer surfaces and its influence on their wetting characteristics in an aqueous environment, J. Coll. Interf. Sci., **107** (2): p. 488-502 (1985).

31. Schmitt, R.L. and J.A. Gardella, Study of surface composition and morphology of block copolymers of bisphenol A polycarbonate and poly)dimethlsiloxane) by x-

ray photoelectron spectroscopy and ion scattering spectroscopy, Macromolecules, **18** : p. 2675-2679 (1985).

32. Ulman, A., *An introduction to ultrathin organic films : from Langmuir-Blodgett to self-assembly*. 1991, Boston: Academic Press. xxiii, 442.

33. Nuzzo, R.Z. and D.L. Allara, J. Am. Chem. Soc., **105** : p. 4481 (1983).

34. Somorjai, G.A., *Chemistry in Two Dimensions-Surfaces*. 1982, Itaca: Cornell University Press.

35. Whitesides, G.M. and P.E. Laibinis, Langmuir, **6** (87) (1990).

36. Chidsey, C.E.D. and D.N. Loiacono, Langmuir, **6** : p. 709 (1990).

37. Chidsey, C.E.D., G.-Y. Liu, P. Rowntree, and G. Scoles, J. Chem. Phys., **91** : p. 4421 (1989).

38. Bain, C.D. and G.M. Whitesides, J. Am. Chem. Soc., **111** : p. 7164 (1989).

39. Hiley, S.L. and D.A. Buttry, Colloids and Surfaces A: Physicochem. Eng. Aspectets, **84** : p. 129 (1994).

40. Creager, S. and J. Clarke, Langmuir, **10** : p. 3675 (1994).

41. Atre, S.V., B. Leidberg, and D.L. Allara, Langmuir, **11** : p. 3882 (1995).

42. Tam-Chang, S.-W., H.A. Biebuyck, G.M. Whitesides, N. Jeon, and R.G. Nuzzo, Langmuir, **11** : p. 4371 (1995).

43. Haussling, L., B. Michel, H. Ringsdorf, and H. Rohrer, Angew. Chem. Int. Ed. Engl., **30** : p. 569 (1991).

44. Fritz, M.C., G. Hahner, and N.D. Spencer, Langmuir, **12** : p. 6074 (1996).

45. Delamarche, E., G. Sundarababu, H. Biebuyck, B. Michel, C.H. Gerber, H. Sigrist, H. Wolf, H. Ringsdorf, N. Xanthopoulos, and H.J. Mathieu, Langmuir, **10** : p. 4109 (1996).

46. Plant, A.L., Langmuir, **9** : p. 2764 (1993).

47. Mino, N., S. Ozaki, K. Ogawa, and M. Hatada, Thin Solid Films, **243** : p. 374-377 (1994).

48. Sondag-Huethorst, J.A., H.R. van Helleputte, and L.G. Fokkink, Appl. Phys. Lett., **64** : p. 285-287 (1994).

49. Wollman, E.W., D. Kang, C.D. Frisbie, I.M. Lorkovic, and M.S. Wrighton, J. Am. Chem. Soc., **116** : p. 4395-4404 (1994).

50. Rozsnyai, L.F. and M.S. Wrighton, J. Am. Chem. Soc., **116** : p. 5993-5994 (1994).

51. Abbott, N.L., A. Kumar, and G. Whitesides, Chem. Mater., **6** : p. 596-602 (1994).

52. Kumar, A., N. Abbott, E. Kim, H. Biebuyck, and G. Whitesides, Patterned Self-Assembled Monolayers and Meso-Scale Phenomena, Acc. Chem. Res., **28** : p. 219-226 (1995).

53. Jackman, R.J., J.L. Wilbur, and G.M. Whitesides, Fabrication of submicrometer features on curved substrates by microcontact printing, Science, **269** (5224): p. 664-6 (1995).

54. Ulman, A., *Characterization of organic thin films*. Materials characterization series. 1995, Boston Greenwich: Butterworth-Heinemann ; Manning. xvi, 276.

55. Mao, G., Ph.D Dissertation, (1998).

Chapter 2: Extracellular Matrix Proteins and Cells on Surfaces

2.1 INTRODUCTION

2.1.1. Protein adsorption at biomaterials interfaces

When any material is placed in a biological milieu, proteins from the aqueous phase readily adsorb onto its surface. Mass transfer mandates that proteins present in high concentration and that have high diffusion rates reach the surface first. Therefore, adsorption of abundant, small proteins, e.g., albumin, takes place immediately. Over time, these small proteins may be competitively exchanged for many other larger proteins like fibronectin or fibrinogen. This dynamic interfacial process is called the 'Vroman effect' [1]. Larger proteins are generally present in a lower concentration and have reduced diffusion coefficients, but may have structural and biochemical properties that enhance interfacial binding interaction with surfaces. Within milliseconds of exposure, these proteins form a layer on the biomaterial surface. While the layer can undergo time-dependent compositional and conformational changes, it becomes the biological interface that cells encounter when they approach the surface of implanted biomaterials. For this reason, the clinical success of biomaterials is largely determined by the local, molecular-level response of proteins to the interfacial properties of the materials.

Physiological fluids (e.g., plasma) contain numerous soluble proteins that spontaneously react with solid surfaces in very dynamic ways [2]. *In vivo* and *in vitro*, in

serum, cell adhesion to substrates is largely mediated by an ill-defined layer of adsorbed serum proteins. A complex and unelucidated competition between over 200 proteins in serum results in an adsorbed layer comprising proteins that facilitate cell adhesion and an array of others that do not actively interact with cells [2-4]. One predominant protein component adsorbed from serum is albumin, a globular soluble protein that does not promote cell adhesion. In much lower abundance are the extracellular matrix proteins (ECMs) including laminin, fibronectin (Fn), vitronectin and others that mediate cell attachment and spreading [2, 3, 5, 6].

2.1.2. Influence of Surface Properties on Protein Adsorption

Proteins interact with solid surfaces in a variety of ways. In general, the most important fundamental interactions include acid/base, hydrophobic, and electrostatic interactions. The additive effects of all of these interactions contribute to the overall composition and conformation of the protein layer adsorbed at the surface.

Proteins comprise arrays of linked hydrophobic and hydrophilic amino acids. Hydrophobic amino acid residues tend to cluster away from water, forming interior hydrophobic pockets in globular proteins. Hydrophilic amino acid residues will hydrate, forming the surface of a soluble protein. This is not absolute: hydrophobic amino acids are also present in hydrophobic domains on the surface of the proteins. The protein in aqueous milieu seeks a "global" energy minimum by forming a native, folded structure that achieves this lowest energy state. The interaction of hydrophobic areas of the protein and the substrate occurs at the interface: surface hydration, charging and protein folded stability are all involved.

Interaction of a soluble protein with a hydrophobic surface often involves removal of structural water from both surfaces to promote direct surface contact. Globular proteins alter their native conformation to expose interior hydrophobic pockets to the hydrophobic surface. Proteins will undergo these conformational changes spontaneously, often referred to as surface-induced denaturation, if the free energy increases. For this reason, protein adsorption onto hydrophobic surfaces is usually irreversible [7]. In general, proteins are more strongly bound to hydrophobic surfaces as a consequence of multiple hydrophobic interactions than to hydrated hydrophilic surfaces [8] [9]. Much larger adsorption energy has been measured for albumin adsorption onto hydrophobic silica than onto hydrophilic silica [9].

Electrostatic interactions between solid surfaces and proteins or between individual protein molecules may also have a large influence on protein adsorption. Protein net charge originates from additive charged, exposed side chains of amino acids, such as cationic amines (lysine) and anionic carboxylic acid groups (glutamate, aspartate). Interactions between charged or polar domains at a material's surface and charged or polar domains in a protein can influence the rate and amount of protein adsorption, the rate of protein-surface exchange [10], magnitude of protein-surface denaturation as well as the adsorbed protein conformation.

2.1.3. Conformation and Orientation of Proteins at Interfaces

Relative conformations of ECM molecules adsorbed on various surfaces have been determined directly using several methods. Attenuated total reflection Fourier transform infrared spectroscopy (FTIR/ATR) has been used to monitor surface

adsorption-induced changes in the amide and carbonyl regions of protein spectra [11, 12]. FTIR/ATR techniques were used to evaluate surface-dependent conformations in fibronectin adsorbed on SAMs of alkylsilanes on ATR germanium crystals. Results indicated that fibronectin adsorbed on all hydrophilic surfaces from single component buffer solutions showed similar spectra. Fibronectin adsorbed on all hydrophobic surfaces showed similar spectra to each other, yet distinctly different spectra from those observed on the hydrophilic surfaces. Correlations between surface chemistry and fibronectin conformation supported subsequent cell adhesion and spreading behaviors on each surface.

Antibody experiments probing adsorbed protein conformation have also been performed. Grinnell and Feld [13] used polyclonal Fn antibodies to assay Fn conformational changes in response to adsorption onto hydrophobic and hydrophilic polystyrene culture dishes. Their results demonstrated that the binding affinity of anti-Fn to adsorbed Fn was much higher on the hydrophilic surfaces than on the hydrophobic ones, suggesting different conformations of the adsorbed Fn. They also were one of the first groups to document the phenomena of "albumin rescuing", showing that, in the presence of small amounts of serum albumin, anti-Fn binding to plasma Fn adsorbed on hydrophobic surfaces increased markedly, indicating that a different, more favorable Fn conformation had been attained in competitive adsorption with albumin.

Many researchers in the biomaterials field have recognized the importance of the composition and conformation of the adsorbed protein layer in mediating cellular responses to material interfaces. Differences in cell activity are attributed to variable cell receptor reactivity to adsorbed ECM proteins. Compositional, conformational or

orientational changes in adsorbed proteins, particularly ECMs, modulate the availability and potency of these domains for integrin receptors. Cell-binding domains in ECMs directly interact with cell surface integrin receptors. These receptors are linked through transmembrane structures to cytoskeletal components involved in cell spreading and migration. Interactions between ECM domains and specific integrin receptors initiate signals that promote cell spreading and eventually growth and proliferation. It therefore seems feasible that modulation of an ECM conformation by a surface could alter or abolish specific interactions between these domains and cell receptors that ultimately lead to observed differential cell phenotypes.

2.1.4. The Role of Adsorbed Proteins in Cell Interactions with Solid Surfaces

Interactions of cells with surface-adsorbed proteins play a major role in cellular behavior. Specific oligopeptide domains conserved within the adsorbed ECM proteins (cell binding domains) act as ligands that are specifically recognized and bound by cell surface integrin receptors. Common motifs include the RGDS sequence [14-16], YIGSR , IKVAV [17, 18] and REDV [19] motifs found in various ECM proteins and fibrinogen. These motifs interact with cell surface receptors called integrins. Integrins have specificity for distinct cell-binding domain motifs.

Cell spreading has been shown to be mediated by adsorbed extracellular matrix proteins. Plow and coworkers demonstrated that BHK cells exhibit only 5% spreading in the absence of any fibronectin, but spreading increased to nearly 100% as the concentration of fibronectin is increased from 0.03 to 3 μg/ml [20]. Cell spreading effects due to interactions with RGDS sequences have been shown to be altered or complemented by engaging domains outside this region. Woods and Couchman et al [21]

observed that some normal fibroblasts attach and spread on the cell-binding domain of fibronectin but do not assemble focal contacts unless they also interact with either the amino- or carboxy-terminal heparin-binding domains of fibronectin. Assembly of focal adhesion contacts provides "anchors" to the underlying surface and is important in signal transduction to the cytoskeleton.

ECMs also control aspects of cell differentiation. A great deal of research has described the importance of interplay between ECM and differentiation and development of mouse mammary glands. In the resting state, ECM influence epithelial proliferation and ductal branching [22]. During pregnancy and lactation, ECM integrity is essential to the transition to a differentiated state [23]. Finally, after weaning, degradation of the ECM by metalloproteinases is essential to bring the mammary gland back to its resting state [24].

Culturing of hepatocytes has proven to be a difficult task. Differentiation of hepatocytes has been shown to be regulated *in vitro* by extracellular matrix as a substratum [25]. Numerous liver-enriched transcription factors have been isolated and determined to play important roles in maintaining liver-specific gene expression as well as liver differentiation. Many of these transcription factors have been shown to be regulated by signaling pathways initiated via cell-ECM interactions. For example, collagen substrates in the presence of growth factors facilitate growth of freshly isolated hepatocytes but also lead to a loss of liver-specific function [25]. This de-differentiation can be prevented in cells cultured on reconstituted basement membrane. Gene expression results indicate that collagen stimulates the expression of the AP-1 family of transcription factors and stimulates transition of cells from the G_0 to G_1 stage of the cell cycle. In

addition to stimulating AP-1 expression, collagen down-regulates expression of C/EBPα, a transcription factor responsible for up-regulation of liver-specific genes. Culturing hepatocytes on basement membranes has the opposite effect as culturing them on collagen: AP-1 expression is inhibited and cells are arrested in the G_0 state of growth arrest [26]. This G_0 arrest has been shown to be required for the expression of C/EBPα. For this reason, it is difficult to expand hepatocytes in culture without losing the liver-specific phenotype.

2.1.5. Cells on SAMs

Recent research has combined the surface-chemistry control provided by self-assembled organic monolayers with protein adsorption and cell culture studies. Lewandowska and coworkers [27, 28] showed that surface-functionalized alkylsilane films on glass varied in their ability to induce cell spreading and stress fiber formation in fibroblasts and neural cells. A series of silanizing agents containing various surface-exposed end groups, including apolar $-CH_3$ and $-CH=CH_2$ and polar -Br, -CN, -COOH, and $-CHOHCH_2OH$ were used to prepare surfaces. Swiss 3T3 fibroblasts and Platt neuroblastoma cells were allowed to attach in serum-free media to surfaces pre-coated with 20 μg/ml fibronectin (FN). Cell attachment and stress fiber organization was then determined. Results indicated that the hydrophilic -COOH surface, while supporting similar levels of cell attachment, showed reduced levels of cell spreading compared to the glass control. Opposite trends were observed for the hydrophobic surfaces. Experiments also showed, however, that spreading on hydrophobic surfaces could be "rescued" or restored by adding bovine serum albumin to the Fn attachment media.

Healy's group [29] used photolithography to pattern alkylsilane lines on quartz surfaces. Patterned surfaces were produced with dimethyldichlorosilane (DMS) and N-(2-aminoethyl)-3-aminopropyl-trimethoxysilane (EDS) in alternating parallel lines 100μm wide. Neuroblastoma, osteosarcoma and fibroblast -like cells were plated on these surfaces in media containing 15% fetal bovine serum and imaged with time-lapse microscopy. Results showed that cells plated on surfaces patterned with EDS/DMS in the presence of serum preferentially attached to the hydrophilic EDS regions in a time-dependent manner.

Whitesides' group [30-32] has used patterning of derivatized alkylthiol monolayers on gold to investigate cell attachment. They examined attachment of rat basophilic leukemia (RBL) and mouse embryonic carcinoma (P19) adherent cell lines to patterned SAMs. Results showed that in media containing 10% fetal bovine serum, cell attachment was reduced on hydrophobic -CH_3 patterned areas, and polyethylene oxide oligomer surface groups completely inhibited cell attachment. However, cells seemed to readily attach to the more hydrophilic -COOH and -$N(CH_3)_2$ areas from serum.

Ratner's group recently looked at the effect of specific chemical functionalities on the growth of bovine aortic endothelial cells (BAEC) using a set of derivatized alkanethiolate monolayers (SAMS) on gold surfaces [33]. Relative amounts of Fn and albumin in buffer-adsorbed competition experiments as well tightness of protein binding onto SAMs terminated in -CH_3, -CH_2OH, -CO_2CH_3 and -CO_2H were determined. These data were correlated with BAEC-SAM surface growth. Results indicated that –COOH terminated SAM surfaces, which were the best cell growth substrates in the panel,

demonstrated significantly higher Fn adsorption and albumin elutability than did poor growth SAM substrates (-CO_2CH_3 and -CH_3).

These results along with a variety of older studies on polymers show that variations in model surface chemistries, cells and culture conditions produce very different cellular responses to surfaces. An important distinction among the previous experiments lies in the composition of the serum proteins available to adsorb to culture surfaces. Culturing cells in single-component conditions (c.f., Lewandowska experiments using only fibronectin [27, 28]) as opposed to multiprotein component culture conditions (c.f., Healy experiments [29]) greatly affects resulting cell attachment. These results indicate that careful control of the quality, functionality and spatial nature of surface chemistry provides a convenient route to influencing and understanding the interactions between ECM proteins, cells and solid surfaces and the possibility to control physiological responses. Further study of cell-materials interactions with these model biomaterials surfaces can now exploit new, enhanced capabilities of molecular and cell biology assays to report the molecular details of gross cell behavior, lending even more intimate insight into how these interactions might be exploited in new biomaterials development.

2.2. Experimental

2.2.1. Fibronectin Adsorption to Derivatized SAM Surfaces

Adsorption of human Fn to SAM surfaces of different chemistries was determined in the presence and absence of a 100-fold excess of bovine serum albumin (BSA). Fn was isolated from fresh human blood, anticoagulated with acid/citrate/dextrose, by gelatin-

agarose (Pharmacia LKB Biotechnology) affinity chromatography using 1M arginine for elution [34]. After extensive dialysis against phosphate buffered saline (PBS), Fn was stored in solution aliquots at -70°C. Fn was then radiolabeled using a modified chloramine-T procedure as previously described [20]. SAM-assembled gold-coated Mylar disks (prepared as described in Chapter 1) were floated (SAM face down) on a solution of radiolabeled Fn (2 μg/ml (100 μl)) in PBS in both presence and absence of BSA (200 μg/ml) for a series of times at room temperature. Following incubation, surfaces were rinsed three times with PBS to remove loosely associated proteins. Samples were counted in a γ-counter and the amount of ^{125}I-Fn bound to each surface was calculated from its specific activity.

2.2.2. Availability of the Cell Binding Domain in Fibronectin Adsorbed on SAM Surfaces.

Relative exposure and integrin-binding accessibility of a specific cell-binding domain of Fn adsorbed on various SAM surfaces was also determined. Binding of monoclonal antibodies directed against the tenth (RGD-containing) type III repeat of Fn was used to assess the availability of the cell-binding domain in a surface-adsorbed Fn condition [35] . SAM-assembled disks were floated overnight on the surface of a solution of Fn at a concentration of 2μg/ml (100μl/disk) in PBS overnight at room temperature. After post-coating (masking) with 1% BSA, various concentrations of ^{125}I-labeled monoclonal antibody (mAb) in PBS + 0.1% BSA were added for 2 h. After washing with PBS + 0.05% Tween, bound mAb radioactivity was measured and the amount of bound mAB calculated, correcting for nonspecific binding to BSA controls. Levels of anti-RGD antibodies bound to Fn adsorbed under the different SAM surface

conditions at saturation were determined using Scatchard plots from dilution data sets. To determine total amounts of Fn bound to SAM disk surfaces in each mAb experiment, a set of SAM surface-coated disks of various chemistries were exposed to 2 μg/ml ^{125}I-Fn (100μl) and processed as described above for Fn adsorption to SAMs.

2.2.3. Fibroblast Adhesion to SAM Surfaces

Swiss 3T3 fibroblasts were maintained in Dulbecco's Modified Eagles Media (DMEM) supplemented with 10% fetal bovine serum (FBS). Freshly prepared SAM samples were soaked in 70% ethanol for 20 minutes, dried in a stream of nitrogen, and rinsed in phosphate-buffered saline (PBS) before being exposed to 5 mls of (1) DMEM supplemented with 10% FBS (Sigma) or (2) 3.5 μg/ml bovine Fn (Becton-Dickinson Collaborative Biomedical Products) in PBS or (3) 3.5 μg/ml Fn (Becton-Dickenson) in the presence of 100-fold excess (350 μg/ml) of bovine serum albumin (BSA) (Sigma) for 4 hours at 37 °C. Following this SAM substrate protein preadsorption step, samples were rinsed three times in PBS to remove any unbound proteins. Swiss 3T3 fibroblasts were then plated onto the surfaces at a concentration of 5.0 x 10^4 cells/cm^2 (1x10^5 cells/ml) in serum-free media. Following 4 hours of attachment, dishes were rinsed 3 times with PBS and cell attachment was quantified with a hemacytometer following trypsinization.

2.2.4. Fibroblast Growth on Derivatized SAM Surfaces

Swiss 3T3 fibroblast growth on derivatized SAM surfaces was quantified by cell number following 0-5 days in culture. SAM surfaces were prepared as described in Chapter 1 and cells were plated at a concentration of 5.0 x 10^4 cells/cm^2 in DMEM + 10% FBS (adhesion media). Following 0-5 days of exposure, surfaces were rinsed 3

times with PBS and cell number was determined by cell counting with a hemacytometer following trypsinization.

2.2.5. Primary Cell Line Experiments

Adhesion and growth experiments were performed on primary cell cultures of chick skin fibroblasts. Chick embryos (10 days old) were skinned, trypsinized to create a single celled suspension and cultured in DMEM + 10% FBS. Cells were then used in adhesion and growth experiments as previously described for Swiss 3T3 fibroblasts.

2.3. RESULTS

2.3.1. Fibronectin adsorption to SAM surfaces varies with surface chemistry.

Two protein factors are believed to affect cellular response to implanted biomaterials [27, 35]: 1) relative protein adlayer composition, and 2) conformation of adsorbed ECMs on different surface chemistries. To determine relative Fn levels adsorbed onto different SAM surface chemistries, Fn was radiolabeled with ^{125}I and exposed to $-CH_3$ and -COOH derivatized SAM surfaces as a function of time. These surfaces were chosen to represent the two extremes in cell/surface response as indicated by relevant adhesion and spreading data. Levels of adsorbed Fn from aqueous solutions of either Fn alone or Fn in 100-fold excess BSA were then determined by scintillation counting.

Figure 2.1 shows that after eight hours, single component Fn adsorption to the -COOH terminated SAM surface is significantly higher (0.778 $\mu g/cm^2$) than that seen on the $-CH_3$ terminated SAM surface (0.502 $\mu g/cm^2$). This relative difference was also observed for binary Fn solution in the presence of 100-fold excess BSA (i.e., simulating

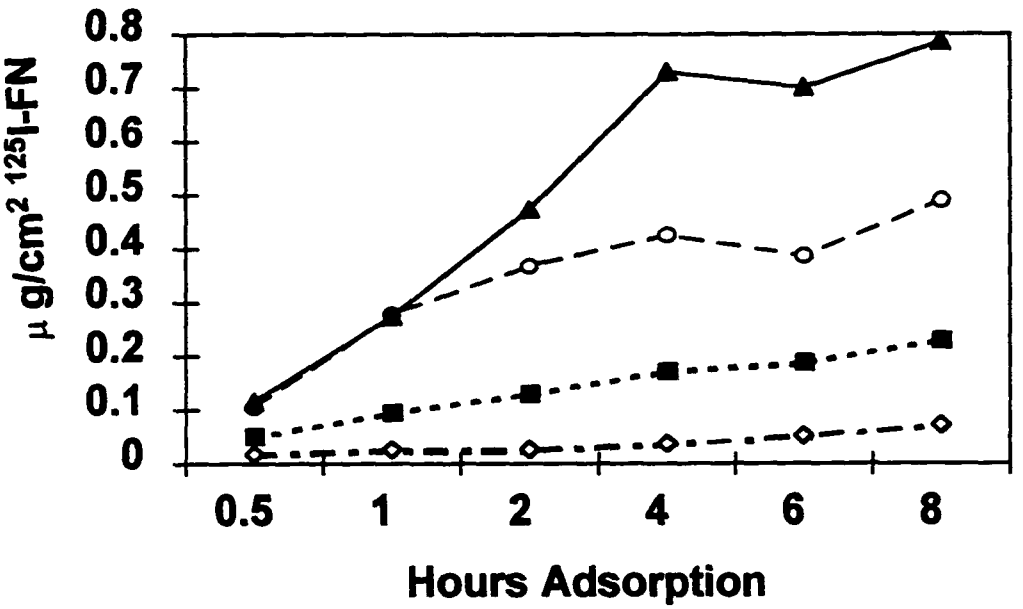

Figure 2.1 Fibronectin adsorption to derivatized SAM surfaces. SAM-assembled disks were exposed to a solution of ^{125}I-labeled Fn (2 μg/ml) in PBS in both the presence and absence of 100X BSA (200 μg/ml) for a series of times at room temperature. Surfaces were rinsed and radioactivity was determined in a γ-counter and the amount of ^{125}I-Fn bound to each surface was calculated from its specific activity.Legend: -▲- COOH SAM, FN (2 μg/ml), -O-- CH_3 SAM, FN (2 μg/ml), - -■ COOH SAM, FN (2 μg/ml) + 100X BSA (200 μg/ml) , - -◇ – CH_3 SAM, FN (2 μg/ml) + 100X BSA (200 μg/ml).

the protein competition conditions in FBS). However, under these competitive adsorption conditions, Fn adsorption is reduced drastically over that seen from single component solutions on both SAMs while Fn adsorption to the -COOH surface is over 3 times greater than that on the -CH_3 surface.

2.3.2. Adsorbed Fibronectin Conformation is Modulated by Surface Chemistry.

Conformation of Fn adsorbed on various SAM surfaces was also assessed by monitoring the exposure of a specific Fn epitope corresponding to an integrin recognition sequence in adsorbed Fn. A monoclonal antibody, directed against the tenth type III repeat in the cell binding domain of Fn (anti-RGD IgG), was labeled with ^{125}I and exposed at various concentrations to SAM surface-adsorbed Fn [35]. Scatchard plot analysis was performed to analyze binding of the ^{125}I-labeled anti-RGD antibody to Fn adsorbed at saturation under the different SAM surface conditions. Averages from 3 experiments are shown in Figure 2.2. Antibody binding amounts were divided by the amounts of total Fn adsorbed on each surface detected by radiolabeling to obtain ratios of bound antibody per adsorbed Fn molecule on each SAM surface. In the absence of surface-induced changes in Fn cell-binding domain availability to solution phase antibody, no significant difference in this binding ratio would be expected for the different surface chemistries. Results (summarized in Figure 2.3) indicate that Fn adsorbed on -CH_3 terminated SAMs in the absence of other proteins exhibits reduced anti-RGD antibody binding. This then correlates to reduced surface exposure of adsorbed Fn cell-binding domain on this SAM relative to Fn adsorbed on the -COOH SAM surface. In addition, in the presence of 100-fold excess of BSA, the affinities of antibodies for Fn sites adsorbed on both surfaces were increased. This indicates that a

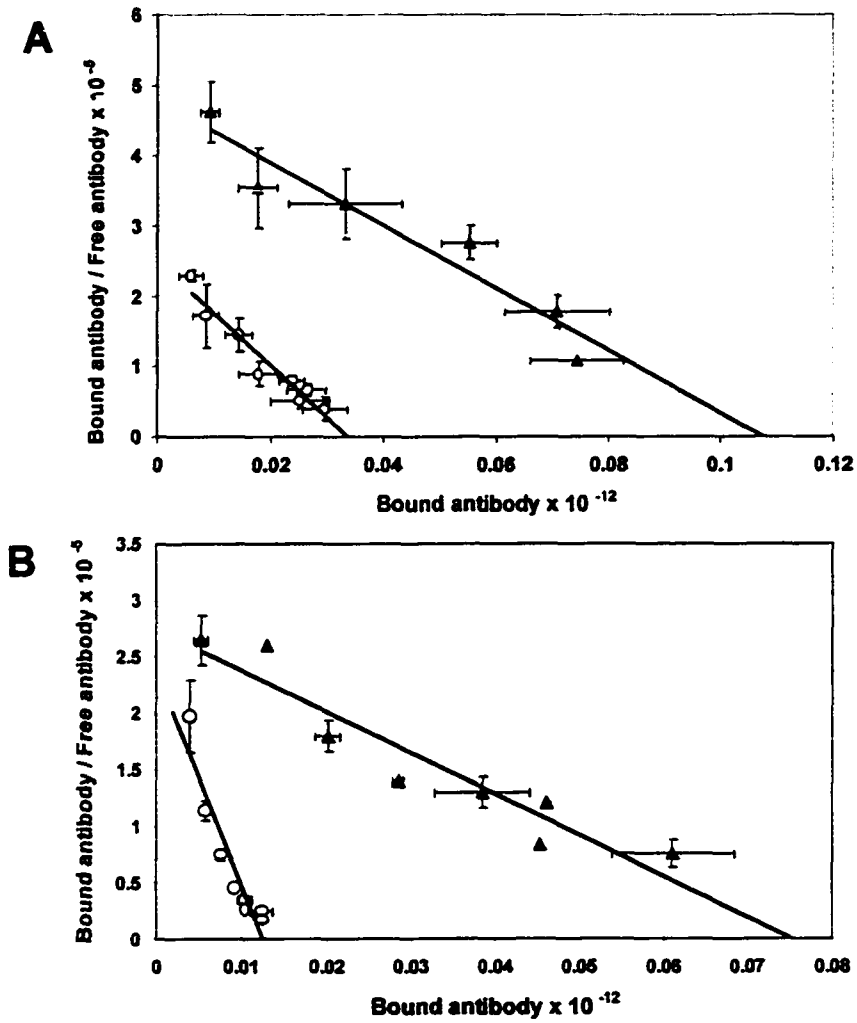

Figure 2.2 Scatchard plots of binding data for the interaction of anti-RGD antibody with SAM surface adsorbed Fn. -COOH (-▲-) and $-CH_3$ (-◯-) SAM-assembled disks were exposed to a solution of Fn (2 μg/ml) in PBS in both the absence A) and presence B) of 100X BSA (200 μg/ml) overnight at room temperature. Surfaces were rinsed, blocked and exposed for 2 hours to various concentrations of ^{125}I-labeled antibody directed against the tenth (RGD-containing) type III repeat of Fn (mAB). After washing, bound radioactivity was measured and the amount of mAB calculated from its specific activity, correcting for nonspecific binding to BSA controls. Levels of anti-RGD antibodies bound to Fn under the different surface conditions at saturation were determined using Scatchard plots. Averages from three experiments are presented in the figure. Fn levels were determined in concurrent experiments using ^{125}I-Fn coated disks processed as described in Materials and Methods.

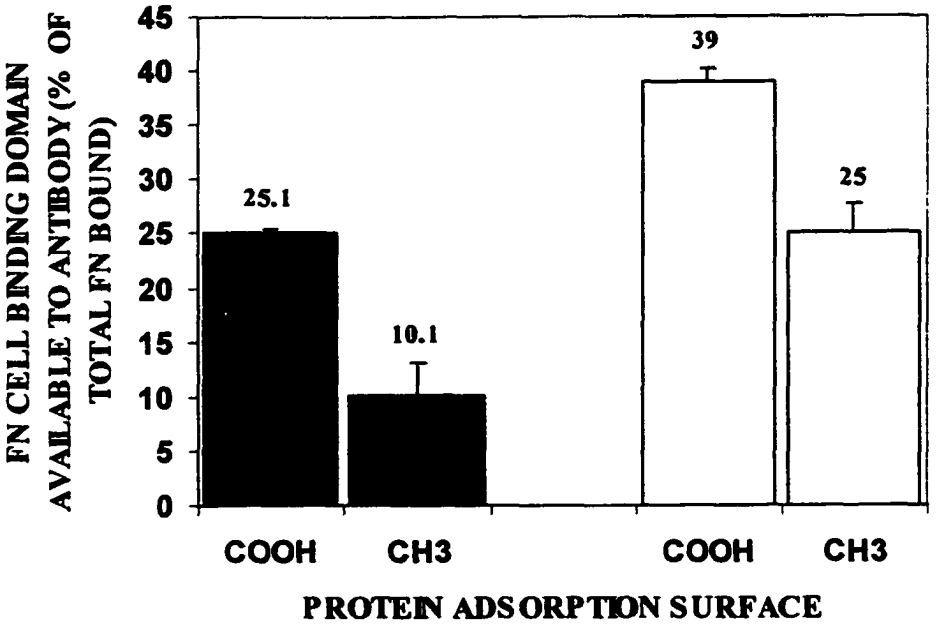

Figure 2.3 Summary of cell binding domain exposure in Fn adsorbed to SAM surfaces probed by monoclonal antibodies. Anti-RGD binding levels at saturation (obtained from the Scatchard plots in Figure 8) were divided by the amounts of total Fn adsorbed on each surface (detected by radiolabeling in concurrent experiments) to obtain ratios of bound antibody per adsorbed Fn molecule on $-CH_3$ and –COOH terminated SAM surfaces in both the presence (white bars) and absence (black bars) of 100X BSA. Results are reported as a percentage exposure of total cell binding domains present.

more favorable Fn cell-binding domain conformation is attained on both surfaces. Interestingly, levels of nonspecific ^{125}I -labeled antibody binding to BSA-adsorbed control -COOH terminated SAMs were greater than for the $-CH_3$ terminated SAM controls at all primary antibody concentrations. These values, however, were subtracted for each case to determine specific antibody binding levels and therefore do not affect the reported results.

2.3.3. Swiss 3T3 Fibroblast Adhesion and Growth on SAM Surfaces is Dependent Upon the Composition of the Pre-Adsorbed Protein Mixture

Effects of surface chemistry on the adhesion of cells to SAM surfaces preadsorbed with either FBS or specific, relevant isolated proteins from serum were determined. SAM surfaces of different functional group chemistries were preadsorbed (4 hours at 37°C) with 5 ml of either (1) DMEM + 10% FBS, (2) Fn alone, or (3) a mixture of Fn and 100-fold excess of BSA. Cell attachment was used to distinguish these conditions and surface effects.

Figure 2.4 shows patterns of attachment for Swiss 3T3 fibroblasts plated on derivatized SAM surfaces with various protein components preadsorbed. On SAM surfaces preadsorbed with DMEM + 10% FBS, cells attached in higher densities to the more hydrophilic -COOH terminated SAM, whereas minimal cell attachment was consistently observed on the hydrophobic $-CH_3$ terminated SAM. In contrast, on SAM surfaces preadsorbed with Fn alone, cells consistently attached to all SAM surface chemistries at similar densities, indicating that Fn coating apparently erases all surface chemistry-dependent effects on attaching cells. Interestingly, the data also shows that surface chemistry-dependent, differential cell-SAM surface attachment was recovered

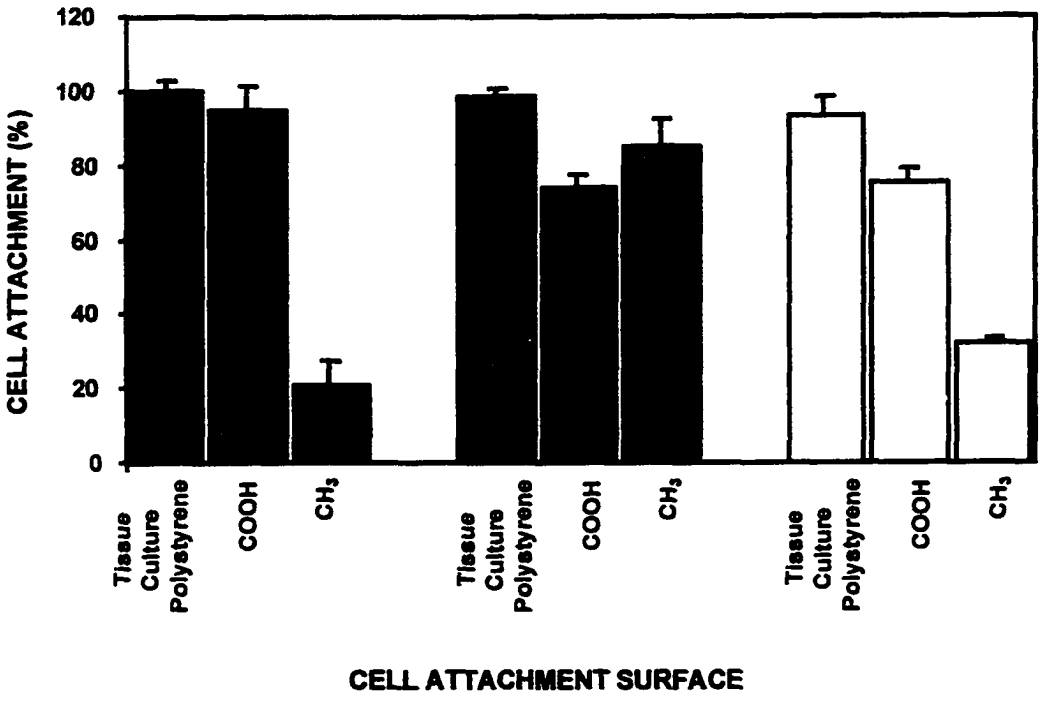

Figure 2.4 Fibroblast adhesion to derivatized SAM surfaces.
Swiss 3T3 fibroblasts were exposed for 4 hours to –COOH or $-CH_3$ terminated SAM surfaces preadsorbed with : DMEM + 10% FBS : (black bars) , Fn (3.5 μg/ml) (grey bars) and Fn (3.5 μg/ml) + 100X BSA (350 μg/ml) (white bars) , nonadherent cells were removed and adherent cells were trypsinized and counted with a hemacytometer. (n=3. Mean +/- std.dev.).

upon preadsorbing Fn in the competing presence of 100-fold excess of BSA (the approximate ratios of these proteins in FBS).

Figure 2.5 shows kinetic cell-growth plots of Swiss 3T3 fibroblasts plated in DMEM + 10% FBS on derivatized SAMs. Fibroblasts plated on tissue culture polystyrene (TCPS) showed the highest rate of cell proliferation. Cells plated on –COOH terminated SAMs displayed a proliferation rate comparable to that of TCPS, whereas cells plated on $-CH_3$ terminated SAMs displayed a reduced rate of proliferation. These results indicate that in multiprotein component media, proteins that facilitate cell adhesion and ultimately cell proliferation are differentially influenced by surface chemistry, in turn affecting short term cell proliferation rates.

2.3.4. Primary and Secondary Cell Line Responses to SAM Surfaces

Figures 2.6 and 2.7 show adhesion and growth comparisons of the trends observed with Swiss 3T3 fibroblast and chick skin fibroblast culture on SAMs. Figure 2.6 shows a comparison of chick skin fibroblast (CSF) adhesion on derivatized SAM surfaces with adhesion of Swiss 3T3 fibroblasts on the same surfaces. Similar differential cell adhesion trends are observed. On SAM surfaces preadsorbed with DMEM + 10% FBS, CSFs attached in similar densities to the hydrophilic -COOH terminated SAM and the control polystyrene surface, whereas minimal cell attachment was consistently observed on the hydrophobic $-CH_3$ terminated SAM. In comparison, CSFs appeared to tolerate adhesion conditions on $-CH_3$ surfaces slightly better than Swiss 3T3 fibroblasts as evidenced by a higher % cell attachment (28% versus 21% respectively).

Figure 2.7 represents comparative growth curves for CSFs and Swiss 3T3 fibroblasts plated in DMEM + 10% FBS on derivatized SAM surfaces. In general, cells

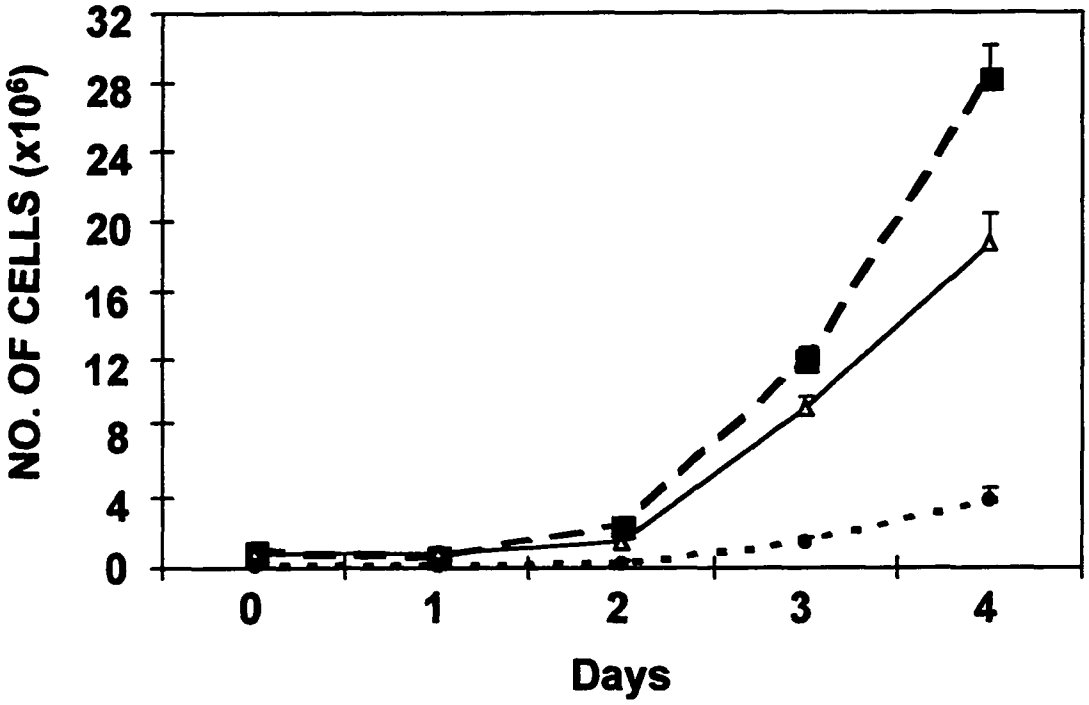

Figure 2.5 Fibroblast growth on derivatized SAM surfaces. Swiss 3T3 fibroblasts were plated at a concentration of 5.0 x 10^4 cells/cm^2 (1x10^5 cells/ml in DMEM +10% FBS. After 4 hours nonadherent cells were removed and a 0 time point was established. Every 24 hours thereafter representative samples were trypsinized and counted with a hemacytometer.
Legend: -■- Tissue culture polystyrene —△— COOH SAM, -●- - CH_3 SAM. (n=3, mean +/- std.dev.)

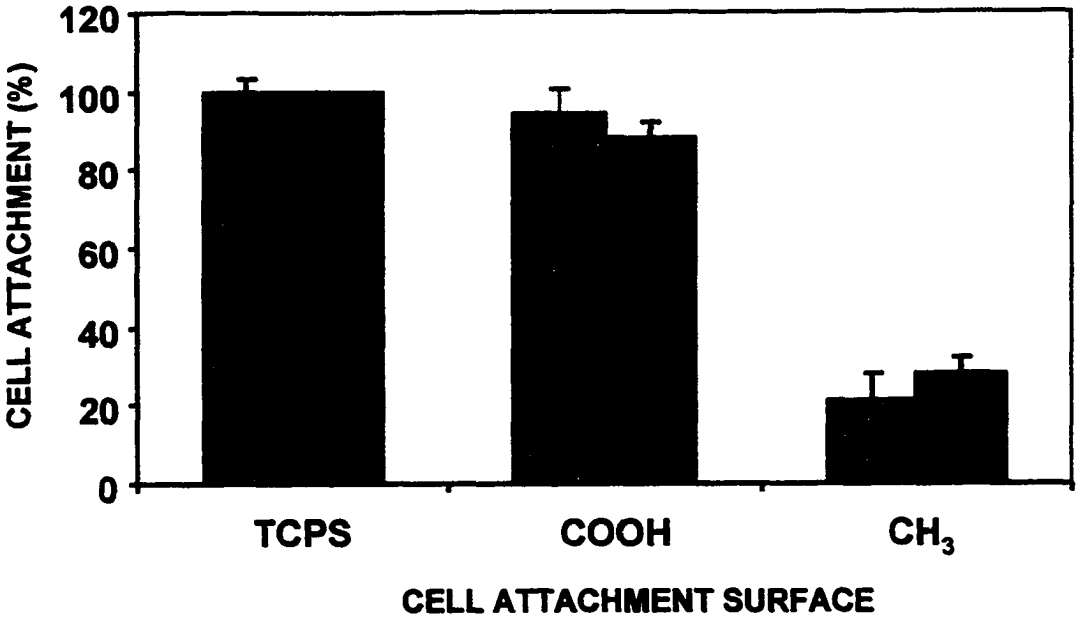

Figure 2.6 Comparison of Swiss 3T3 fibroblast and chick skin fibroblasts adhesion to derivatized SAM surfaces: Swiss 3T3 fibroblasts (grey) and chick skin fibroblasts (black) were plated in DMEM + 10% FBS on derivatized SAM surfaces. After 4 hours, surfaces were rinsed and cells were trypsinized and counted with a hemocytometer.

Figure2.7 Comparison of Swiss 3T3 fibroblast and chick skin fibroblast growth on derivatized SAMs: Swiss 3T3 fibroblasts (—O—) and chick skin fibroblasts (▪▪▪) were plated on DMEM + 10% FBS on derivatized SAM surfaces. After 4 hours, cells were rinsed and a representative sample was trypsinized and counted to establish a time 0 point. Cells were allowed to grow in culture and representative samples were tryspinized and counted at days 1, 2 and 3.

plated on –COOH terminated SAMs displayed a proliferation rate higher than that for cells plated on $-CH_3$ terminated SAMs. On the –COOH terminated SAM surfaces, the CSFs seem to attach and begin proliferating more rapidly than the Swiss 3T3 fibroblasts. However, by day 3, the cells have begun to proliferate at similar rates (as evidenced by the slopes of the lines on the graph). Both cell lines appear to exhibit a similar low growth phenotype on the $-CH_3$ terminated SAM surface.

2.4. DISCUSSION

Results presented here show that attachment, spreading and growth of Swiss 3T3 fibroblasts can be modulated by changing well-controlled SAM surface chemistry. While previous work led to similar conclusions regarding substrate-dependent cell behavior, substrate chemistries have rarely been consistent or controlled. Tissue culture polystyrene has at least five carbon surface chemistries. This study has used well-controlled, well-characterized, specific singular chemistries to correlate biological responses. Results demonstrate that molecular details in the surface chemistry translate to molecular changes in adsorbed ECM, influencing corresponding cell signaling responses.

The pivotal role of ECMs in the signaling pathways controlling cellular responses is part of a large body of evidence showing that composition and conformation of the absorbed protein layer controls cell-surface behaviors. The differential morphologies and growth kinetics observed in cells plated on the various SAM surfaces are consistent with Fn adsorption and conformational data on these SAM surfaces. For both singular and competitive adsorption scenarios tested, the -COOH terminated SAM surface displayed higher levels of Fn adsorption compared to the $-CH_3$ terminated surface (Figure

2.1). This difference between surfaces was much more pronounced in the presence of 100-fold excess of BSA (simulating the protein surface adsorption competition conditions present in FBS). The -COOH surface facilitates higher Fn binding in the presence of competitive excess BSA. In contrast, on the $-CH_3$ surface, BSA outcompetes Fn to a higher degree. Since BSA has no cell adhesive sites while Fn is critical for cell surface attachment, differences in relative BSA:Fn ratios on each SAM surface influences cell attachment, spreading and growth.

Several hypotheses have been forwarded claiming that surface chemistry may be capable of modulating adsorbed ECM protein conformation, thus modulating the biological exposure and reactivity of several critical ECM signaling domains. Differential availability/exposure of conserved ECM cell-binding domains containing the RGD sequence recognized by cell surface integrin receptors, could lead to distinct differences in a material's ability to support cell attachment, spreading and proliferation. A monoclonal antibody (mAb) directed against the tenth type III repeat (including the RGD motif) in Fn was used in this study to determine the cell-binding domain availability in Fn adsorbed to $-COOH$ and $-CH_3$ SAM surface chemistries. The exposure of this sequence has previously been demonstrated to be increased upon adsorption to tissue culture polystyrene surfaces [35]. This specificity was used as the basis to probe for differential epitope exposure as a function of SAM surface chemistry.

Data presented in Figure 2.3 represent the percentage of the total tenth type III sequences found in surface-adsorbed Fn exposed and recognized by the anti-Fn antibody. Levels of adsorbed Fn were determined in a concurrent ^{125}I-Fn adsorption experiment. Results showed that Fn adsorbed on the $-CH_3$ terminated SAM in the absence of other

proteins has a reduced level of anti-Fn antibody binding (10%), and thus a less accessible RGD cell-binding domain than Fn adsorbed on the –COOH surface (22%). Although no direct correlation can be made between Fn cell-binding domain availability probed this way and the observed cell spreading, these indirect results are consistent both with previous results for integrin-Fn surface behavior and the observed cellular responses on these SAMs.

Interestingly, in the presence of adsorption of 100-fold excess of BSA, the affinities of antibodies for Fn adsorbed on both surfaces was increased (-COOH: 39%, -CH_3: 25%). Previously, the interpretation of this finding has been that the presence of albumin changes the molecular folding/unfolding of Fn on surfaces, resulting in the expression of a more biologically active Fn conformation. Increased Fn cell-binding domain availability in the presence of albumin has been previously referred to as "albumin rescuing" [27]. Such a relationship is supported by the SAM data. Results in following chapters will support the enhancement of ECM presentation on –COOH SAMs more specifically.

To summarize, our data clearly show a relationship between controlled surface chemistry, Fn adsorption and conformation and subsequent of cell adhesion, spreading and growth. For the hydrophilic –COOH SAM surface, high levels of Fn cell-binding domain availability correlate with high degrees of cell attachment, spreading and growth. In contrast, -CH_3 SAM surfaces exhibit low levels of Fn adsorption and cell-binding domain accessibility, and also demonstrate reduced levels of cell interactions with these surfaces. Interestingly, on -CH_3 surfaces in the presence of competing BSA, Fn appears to adsorb in a more favorable cell binding conformation, consistent with albumin

rescuing. However, the presence of competing BSA leads to lower overall densities of Fn on this surface. Cell-based assays indicate that the more favorable Fn conformation cannot overcome the low adsorbed Fn density at this SAM surface to adequately facilitate cell-surface interactions. Fn adsorbed onto –COOH SAMs at higher density in the competitive presence of albumin, and also seems to adopt a more favorable conformation in the presence of BSA, improving the ability of this surface chemistry to serve as an efficient substrate for cell culture.

The ultimate goal of this research is to identify the specific surface determinants to control and modulate cell biological responses. This requires a careful assessment of the composition and conformation of the complex extracellular protein environment, as well as identifying the presence or absence of key outside-in receptor mediated cellular signaling events. These events include initiation of signal transduction pathways involved in progression through the cell cycle, as well as the subsequent induction of growth-associated gene expression downstream of the signal transduction cascades. Further chapters will explore these relationships.

2.5. Endnotes

1. Vroman, L. and A.L. Adams, Finding with the recording ellipsometer suggesting rapid exchange of specific plasma proteins at liquid/solid interfaces, Surface Sci., **16** : p. 438 (1969).

2. Andrade, J., ed. *Surface and Interfacial Aspects of Biomedical Polymers.* . Vol. 2. 1985, Plenum Press: New york.

3. Curtis, A.S. and J.V. Forrester, The competitive effects of serum proteins on cell adhesion, J Cell Sci, **71** : p. 17-35 (1984).

4. Mooney, M.A. and D.E. Ingber, Integrin Binding and Cell Spreading on Extracellular Matrix Act at Different Points in the Cell Cycle to Promote Hepatocyte growth, Molec. Biol. Cell, **5** : p. 967-979 (1994).

5. Mrksich, M., C.S. Chen, Y. Xia, L.E. Dike, D.E. Ingber, and G.M. Whitesides, Controlling cell attachment on contoured surfaces with self-assembled monolayers of alkanethiolates on gold, Proc Natl Acad Sci U S A, **93** (20): p. 10775-8 (1996).

6. Horbett, T.A. and J.L. Brash, eds. *Proteins at Interfaces II.* ACS Symposium Series. 1995, American Chemiscal Society: Washington D.C.

7. Andrade, J.D., V.L. Hlady, and R.A. Van Wagenen, Effects of plasma protein adsorption on protein conformation and activity, Pure & Appl. Chem., **56** : p. 1345 (1984).

8. Grinnell, F. and M.K. Feld, Adsorption characteristics of plasma fibronectin in relationship to biological activity., J. Biomed. Mat. Res., **15** : p. 363 (1981).

9. MacRitchie, F., The adsorption of proteins at the solid/liquid interface, J. Colloid Interface Sci., **38** : p. 484 (1972).

10. Vroman, L., A.L. Adams, G.C. Fischer, and P.C. Munoz, Interaction of high molecular weight kininogen, factor XII, and fibrinogen in plasma at interfaces, Blood, **55** : p. 156 (1980).

11. Liedberg, B., B. Ivarsson, and W.R. Salaneck, Fourier transform infrared reflection adsorption spectroscopy (FT-IRAS) of some biologically important molecules adsorbed on metal surfaces., Progr. Colloid & Polymer Sci., **70** : p. 67 (1985).

12. Cheng, S.K., K. Chittur, C. Sukenik, L. Culp, and K. Lewandowska, J. Coll. Interfac. Sci., **162** : p. 135-143 (1994).

13. Grinnell, F. and M.K. Feld, Fibronectin adsorption on hydrophilic and hydrophobic surfaces detected by antibody binding and analyzed during cell adhesion in serum-containing medium, J. Biol. Chem., **257** : p. 4888-4893 (1982).

14. Yamada, Y. and H.K. Kleinman, Functional domains of cell adhesion molecules, Curr Opin Cell Biol, **4** (5): p. 819-23 (1992).

15. Haas, T.A. and E.F. Plow, Integrin-ligand interactions: a year in review, Curr Opin Cell Biol, **6** (5): p. 656-62 (1994).

16. Pierschbacher, M.D. and E. Ruoslahti, Cell attachment activity of fibronectin can be duplicated by small synthetic fragments of the molecule, Nature, **309** (5963): p. 30-3 (1984).

17. Ranieri, J.P., R. Bellamkonda, E.J. Bekos, T.G. Vargo, J.A. Gardella, Jr., and P. Aebischer, Neuronal cell attachment to fluorinated ethylene propylene films with covalently immobilized laminin oligopeptides YIGSR and IKVAV. II, J Biomed Mater Res, **29** (6): p. 779-85 (1995).

18. Iwamoto, Y., F.A. Robey, J. Graf, M. Sasaki, H.K. Kleinman, Y. Yamada, and G.R. Martin, YIGSR, a synthetic laminin pentapeptide, inhibits experimental metastasis formation [published erratum appears in Science 1988 Jan 15;239(4837):245], Science, **238** (4830): p. 1132-4 (1987).

19. Massia, S.P. and J. Hubble, Vascular Endothelial Cell Adhesion and Spreading Promoted by the Peptide REDV of the IIICS Region of Plasma Fibronectin is Mediated by Integrin a4b1, J. Biol. Chem., **267** (2): p. 14019-14026 (1992).

20. Plow, E. and M. Ginsberg, J. Biol. Chem., **256** : p. 9477-9482 (1981).

21. Woods, A., J.R. Couchman, S. Johansson, and M. Hook, Adhesion and cytoskeletal organisation of fibroblasts in response to fibronectin fragments, Embo J, **5** (4): p. 665-70 (1986).

22. Silberstein, G.B., K.C. Flanders, A.B. Roberts, and C.W. Daniel, Regulation of mammary morphogenesis:evidence for extracellular matrix-mediated inhibition of ductal buddung by transforming factor beta-1, Dev. Biol., **152** : p. 354-362 (1991).

23. Sympson, C.J., R.S. Talhouk, C.M. Alexander, S.K. Chin, S.M. Clift, M.J. Bissell, and Z. Werb, Targeted expression of stromelysin-1 in mammary gland provides evidence for a role of proteinases in branching morphogenesis and the requirement for an intact basement membrane for tissue-specific gene expression., J. Cell Biol., **125** : p. 681-693 (1994).

24. Boudreau, N., C.J. Sympson, Z. Werb, and M.J. Bissell, Suppression of ICE and apoptosis in mammary epithelial cells by extracellular matrix and cytoskeleton, Science, **267** : p. 891-893 (1995).

25. Oda, H., Extracellular matrix regulates hepatocyte gene expression and differentiation, Connective Tissue, **30** : p. 225-232 (1998).

26. Rana, B., D. Mischoulon, Y. Xie, N.L. Bucher, and S.R. Farmer, Cell-extracellular matrix interactions can regulate the switch between growth and differentiation in rat hepatocytes: reciprocal expression of C/EBP alpha and immediate-early growth response transcription factors, Mol Cell Biol, **14** (9): p. 5858-69 (1994).

27. Lewandowska, K., N. Balachander, C.N. Sukenik, and L.A. Culp, Modulation of fibronectin adhesive functions for fibroblasts and neural cells by chemically derivatized substrata, J Cell Physiol, **141** (2): p. 334-45 (1989).

28. Sukenik, C.N., N. Balachander, L.A. Culp, K. Lewandowska, and K. Merritt, Modulation of cell adhesion by modification of titanium surfaces with covalently attached self-assembled monolayers, J Biomed Mater Res, **24** (10): p. 1307-23 (1990).

29. Healy, K.E., C.H. Thomas, A. Rezania, J.E. Kim, P.J. McKeown, B. Lom, and P.E. Hockberger, Kinetics of bone cell organization and mineralization on materials with patterned surface chemistry, Biomaterials, **17** (2): p. 195-208 (1996).

30. Singhvi, R., A. Kumar, G.P. Lopez, G.N. Stephanopoulos, D.I. Wang, G.M. Whitesides, and D.E. Ingber, Engineering cell shape and function, Science, **264** (5159): p. 696-8 (1994).

31. Lopez, G., M. Albers, S. Schreiber, R. Carroll, E. Peralta, and G. Whitesides, Convenient Methods for Patterning the Adhesion of Mammalian Cells to Surfaces Using Self-Assembled Monolayers of Alkanethiolates on Gold, J. Am. Chem. Soc., **115** : p. 5877-5878 (1993).

32. Kumar, A., N. Abbott, E. Kim, H. Biebuyck, and G. Whitesides, Patterned Self-Assembled Monolayers and Meso-Scale Phenomena, Acc. Chem. Res., **28** : p. 219-226 (1995).

33. Tidwell, C.D., S.I. Ertel, and B.D. Ratner, Endothelial cell growth and protein adsorption on terminally functionalized,self-assembled monolayers of alkanethiolates on gold, Langmuir, **13** : p. 3404-3413 (1997).

34. Vuento, M. and A. Vaheri, Purification of fibronectin from human plasma by affinity chromatography under non-denaturing conditions, Biochem J, **183** (2): p. 331-7 (1979).

35. Ugarova, T.P., C. Zamarron, Y. Veklich, R.D. Bowditch, M.H. Ginsberg, J.W. Weisel, and E.F. Plow, Conformational transitions in the cell binding domain of fibronectin, Biochemistry, **34** (13): p. 4457-66 (1995).

Chapter 3: Intracellular Signaling on Model Cell Culture Surfaces

3.1. INTRODUCTION

Regulation of cell behavior by extracellular factors is currently an intensely studied area in cell biology. Although the understanding remains incomplete, the understanding of how cells sense their environment has increased over the past few years to reveal considerable complexity at various levels. *In vivo*, cells are exposed to numerous extracellular stimuli at one time. The intracellular signals induced in response to these stimuli determine cell phenotypic outcomes.

3.1.1. Cell Integrin Receptors Are Involved in Cell-Surface Recognition of Adsorbed ECMs

The integrin family of cell transmembrane receptors appears to be the major cell signaling component involved in mediating cell attachment to adsorbed extracellular matrix proteins [1-6]. All integrins are membrane-localized $\alpha\beta$ heterodimers; both subunits of each integrin heterodimer are transmembrane glycoproteins, each with a single hydrophobic transmembrane segment. The N-terminal domains of the α and β subunits combine to form the extracellular ligand binding region that interacts with the ECM cell binding domains. These regions are connected by the two receptor membrane

spanning regions and terminate in two cytoplasmic domains believed to interact with an array of cytoskeletal proteins [4, 7]. Biochemical evidence exists for direct interaction of integrin cytoplasmic domains with the cytoskeletal proteins talin and α-actinin.

3.1.2. Early integrin-mediated intracellular events

Receptor signaling via integrins takes two forms, 1) regulation of the affinity and conformation of the receptor from inside the cell, commonly referred to as inside-out signaling, and 2) triggering of intracellular events by ligand occupation of the receptors, referred to as outside-in signaling. Given the wide variety of integrin subunits, individual cells can and frequently do vary their adhesive properties by selective expression of different integrin subunit combinations that have altered affinities for various ECM domains, or signal different processes. Regulatory versatility is introduced by the ability of cells to modulate the binding properties of their integrins. For instance, $\alpha_2\beta_1$ on platelets is specific for collagen, not laminin [8], whereas on other cells it recognizes both ligands [9]. Several intracellular events have been determined as indicators of effective outside-in signaling between surface-adsorbed ECMs and signaling mechanisms. These early integrin-induced events include changes in intracellular pH, production of calcium ion transients, activation of immediate early gene expression, formation of stress fibers and focal contacts, and widespread tyrosine phosphorylation.

Almost all cells require that pH_i be maintained within a narrow range for optimal growth [10]. Intracellular alkalinization, resulting from activation of a transmembrane Na^+/H^+ antiporter on the cell surface, appears to be a common early effect of cell adhesion to ECM proteins, specifically Fn [11]. Work by Schwartz et al [12] showed that

insoluble fibronectin activates the Na+/H+ antiporter by clustering and immobilizing integrin $\alpha_5\beta_1$.

Calcium ion transients are also early indicators of effective outside-in signaling between the extracellular environment and the cell. Integrin-mediated adhesion to Fn by fibroblasts induces a rapid increase in the phosphorylation of phosphatidylinositol 4-phosphate (4-PIP) to 4,5-$PIP_{2\,[13]}$. The 4,5-PIP_2 serves as a preferred substrate for phospholipase C (PLC), leading to the production of the second messengers diacylglycerol (DAG) and inositol triphosphate (IP_3), that leads in turn to the release of intracellular calcium stores [14]. The calcium transients induced upon cell adhesion were later shown to be mediated by the small molecular weight GTPase RhoA [15].

As discussed in Chapter 1, activation of immediate early genes, such as c-myc, c-fos and c-jun, in response to cell adhesion to substrates is another indicator of effective extracellular-intracellular communication. Dike and coworkers [16] showed that suspension of 3T3 fibroblasts for prolonged periods of time caused cells to enter a G_0 (quiescent) growth state, as demonstrated by a decrease in mRNA synthesis to approximately 20% of exponential levels and inhibition of DNA synthesis. However, a rapid induction of c-fos, c-jun and c-myc gene expression was observed following adhesion of suspension-arrested fibroblasts to tissue culture polystyrene in both the presence and absence of serum.

Formation of stress fibers, and thus cell spreading, is another common indicator of the effective outside-in communication between ECM proteins and cells. The small GTPase RhoA is a known, key regulator of stress fiber formation [17-19]. The formation of stress fibers is believed to be due to the Ser-Thr kinase p160ROCK, which interacts

with Rho in a GTP-dependent manner [20]. Two substrates for this kinase, myosin light chain phosphatase and myosin light chain, are known to regulate the assembly of actin-myosin filament bundles, and recent work has shown that Rho-induced stress fiber formation occurs primarily through bundling of preexisting filaments [21].

A complex signal transduction cascade is initiated that mediates the formation of stress fibers and associated cytoskeletal proteins in an adhesive complex, called a focal adhesion contact, that in turn facilitates cell spreading and migration. The current thinking is that following the binding of a typical integrin to ECMs, cytoskeletal actin-myosin contractility is induced. The cytoplasmic tails of the integrin subunits bind to talin and α-actinin, initiating the aggregation of the integrins into focal contacts. Subsequent to integrin aggregation, a variety of cytoskeletal proteins accumulate at the cytoplasmic membrane surface-side of the integrin cluster. Significantly, numerous proteins are found localized to intracellular focal adhesion sites. These include the actin-binding proteins α-actinin, talin, vinculin and tensin, as well as many proteins involved in growth factor signaling.

All β_1 and α_5 subunit-containing integrins share the ability to activate the focal adhesion associated kinase, FAK. FAK is a nonreceptor tyrosine kinase, which is expressed in almost all tissues. Although the exact mechanism by which integrins activate FAK is not completely understood, it is clear that the process is tightly coupled to the process of assembly of focal adhesions and associated stress fibers. Such activation of FAK has been shown to require the same segment of the β integrin subunit cytoplasmic tail region that is thought to interact with talin [22]. Thus it is possible that the initial recruitment of FAK to focal adhesions is indirect and mediated by talin.

However, other *in vitro* evidence indicates that FAK interacts directly with a portion of the β integrin subunit [23].

Vinculin is another protein that has been shown to be localized to focal contacts following ECM-coupled integrin aggregation. The important role of vinculin in cellular adhesion is illustrated by the findings that 1) disruption of the single gene encoding vinculin in *C. elegans* leads to embryonic death [24] and 2) microinjection of antibodies against vinculin into fibroblasts causes loss of adhesion [25]. Vinculin interacts *in vitro* with a variety of structural and regulatory proteins at the focal contact site including actin, α-actinin, talin, paxillin and numerous protein kinases [26].

Vinculin has been shown to have a masked carboxy-terminal actin-binding site [27]. It is believed that regulation of vinculin by integrin-dependent signaling cascades may induce head-tail intramolecular association in the vinculin protein and expose the actin binding site. The conformational change necessary for exposure of the site has been proposed to be dependent on vinculin's phosphorylation state [28]. Vinculin has also been shown to contribute to the attachment of actin filaments to integrin focal adhesions.

Paxillin is a 68 kDa cytoskeletal protein that has also been demonstrated to localize to focal adhesions. A number of observations suggest that paxillin is involved in transducing signals from growth factor receptors to focal adhesions. Paxillin has been shown to be phosphorylated in response to several growth factors including epidermal growth factor and platelet-derived growth factor [29, 30]. In vitro, paxillin has been shown to be phosphorylated by FAK [31]. However, this phosphorylation by FAK is not necessary for recruitment of paxillin to focal adhesions [32]. Paxillin has also been shown to interact with the carboxyl terminus of vinculin *in vitro* and *in vivo* [33].

Finally, protein phosphorylation is one of the earliest events detected following association between integrins and ECMs. Tyrosine kinase inhibitors block formation of focal contacts, implicating tyrosine phosphorylation in signaling pathways linked to integrin receptors. Kornberg and coworkers [34, 35] observed that antibody-mediated clustering of integrins leads to enhanced phosphorylation on tyrosine residues of many cytoplasmic proteins. In particular, tyrosine phosphorylation of two proteins, paxillin and focal adhesion kinase (FAK), is a critical step for adhesion-mediated signal transduction. Burridge and coworkers [36] also showed that paxillin and FAK both become tyrosine phosphorylated in response to adhesion on extracellular matrices. FAK, also a tyrosine kinase, appears to play a central role in integrin-mediated signal transduction.

The previously presented protein and cell data in Chapter 2 effectively describe an interesting interfacial scenario where SAM surface chemistry mediates cell behavior through the adsorbed ECM protein layer. These sequences of biological causes-and-effects form the basis to extend the investigations of biomaterials surface-cell response to the receptor-mediated intracellular signal transduction level. Such a strategy should provide valuable molecular and cellular biology evidence extending the understanding of the complex relationships between initial cell-biomaterials attachment phenomena and signaling pathways inside the cell.

3.2. EXPERIMENTAL

3.2.1. Immunocytochemistry

Cytoskeletal organization in adherent, cultured fibroblasts was observed as an indication of the relative degrees of cell spreading on various SAM chemistries. Staining

of filamentous actin (F-actin) with rhodamine phalloidin (Molecular Probes) was used to monitor stress fiber formation via fluorescence microscopy. Stress fiber formation was used as an indicator of the extent of cell spreading [37, 38]. Focal contact formation was determined *in situ* through localization of paxillin using an anti-paxillin monoclonal (Signal Transduction Laboratories) followed by a fluorescein labeled secondary antibody (Molecular Probes). Experiments were also performed to localize vinculin and FAK proteins to focal contacts using an anti-vinculin antibody (a gift from the laboratory of Dr. Joan Fox, Cleveland Clinic Foundation) or anti-FAK antibody (Signal Transduction Laboratories). Freshly prepared SAM surfaces (See Chapter 1) were soaked in 70% ethanol for 20 minutes, dried in a stream of nitrogen, and rinsed in phosphate-buffered saline (PBS) before being exposed to five ml of either (1) DMEM supplemented with 10% FBS (Sigma) or (2) 3.5 μg/ml Fn (Becton-Dickinson Collaborative Biomedical Products) in PBS or (3) 3.5 μg/ml Fn in the presence of 100-fold excess (350 μg/ml) of bovine serum albumin (BSA) (Sigma) for 4 hours at 37 °C. Following this substrate protein pre-adsorption step, samples were rinsed three times in PBS to remove any unbound proteins. Swiss 3T3 fibroblasts were then plated onto the surfaces in serum-free media for 12 hours. Following this time period, cells were fixed with a freshly prepared 3.7% paraformaldehyde/PBS solution, solubilized with 0.1% Tween 20 in PBS for 15 minutes and blocked with 4% goat serum (Sigma) in PBS for 4 hours at room temperature. Adherent cells were then incubated with the primary antibodies prepared in 4% goat serum in PBS for 1 hour at room temperature. The surfaces were then rinsed 3 times with PBS and incubated for 30 minutes with a 4% goat serum solution containing a fluorescein goat-anti-mouse antibody (Molecular Probes) and rhodamine phalloidin

(Molecular Probes Inc.) in PBS. Following rinsing with PBS, stained samples were then mounted on a microscope slide containing Prolong Antifade (Molecular Probes) and imaged using a 40X objective via fluorescence microscopy. Images were generated and analyzed using the Metamorph™ image analysis program (Universal Imaging Corp.).

3.2.2. Primary Cell Line Experiments

Immunocytochemistry experiments on focal contact and stress fiber formation were performed on primary cell cultures of chick skin fibroblasts as described above. Chick embryos (10 days old) were skinned, trypsinized to create a single-cell suspension and cultured in DMEM + 10% FBS. Cells were then used in immunocytochemistry experiments as previously described for Swiss 3T3 fibroblasts.

3.2.3. Analysis of Tyrosine Phosphorylation of Focal Adhesion Proteins

Immunocytochemistry experiments were performed to determine relative levels of tyrosine phosphorylation of focal contact proteins in cells plated on derivatized SAM surfaces. Fibroblasts were plated in DMEM + 10% FBS for 24 hours on the series of derivatized surfaces. Staining was performed as described above using a primary antibody directed against phosphorylated tyrosine residues (PY20- Signal Transduction Laboratories) followed by a fluorescein-labeled secondary antibody. To further analyze tyrosine phosphorylation of the focal adhesion proteins FAK and paxillin, immunoprecipitates from whole-cells extracts of cells plated on derivatized SAM surfaces were analyzed by Western blotting. Fibroblasts were plated in DMEM + 10% FBS for 24 hours on the series of derivatized surfaces. To obtain quiescence, cells were seeded on tissue culture polystyrene (Becton Dickenson) and maintained in DMEM with 10% FBS until they reached confluence. The cells were then extensively washed and

starved in serum-free culture medium for 2-4 hours. Quiescent, serum-starved cells were then either lysed as described below or stimulated with culture medium containing 2 μg/ml LPA (1-oleoyl-2-hydroxy-sn-glycero-3-phosphate, monosodium salt in water; Sigma). Cells were rinsed 3 times with PBS and lysed with 1 ml of buffer consisting of 1X PBS, 1% NP40, 0.5% sodium deoxycholate, 0.1% SDS, 10 μg/ml PMSF, 30 μg/ml apropotin and 100 mM sodium orthovanadate. Lysates were clarified at 15,000xg for 20 minutes at 4°C. To confirm specificity of the antibodies, 30 μg of blocking peptides (sequences complementary to the antigenic peptides for the paxillin and FAK antibodies) (Santa Cruz Biotechnology), were added to some samples to compete with native proteins. Supernatants were then incubated with either anti-paxillin or anti-FAK antibodies for 1 hour at 4°C, followed by Protein A/G PLUS-Agarose (Santa Cruz Biotechnology) incubation with mixing overnight at 4°C. Proteins bound to the agarose were rinsed with fresh RIPA buffer, dissolved in SDS-sample buffer, boiled for a minute, separated by electrophoresis on a 7.5% polyacrylamide gel (Laemmli, 1970) and transferred electrophoretically to polyvinylidene difluoride (PVDF) membranes (NEN Life Science Products). PVDF was blocked with 4% bovine serum albumin (BSA)(Sigma) in PBS overnight. The PVDF was then incubated for one hour with an anti-phosphotyrosine antibody, washed three times with TTBS (150 mM NaCl, 50 mM Tris-Cl, 0.05% Tween, pH 7.6), and incubated for one hour with a secondary antibody conjugated with alkaline phosphatase (Santa Cruz Biotechnology, Inc.) for 1 hour at room temperature. Following extensive washing with TTBS, enhanced chemiluminescence (Dupont NEN) was used to develop the blots.

Blots were stripped and reprobed with anti-FAK (Transduction Laboratories) or anti-paxillin (Transduction Laboratories) antibodies.

3.3. RESULTS

3.3.1. Swiss 3T3 fibroblast stress fiber and focal contact formation on SAM surfaces is dependent upon the composition of the pre-adsorbed protein mixture.

To determine effects of adsorbed protein components on induction of stress fiber and focal contact formation in cells plated on derivatized SAMs, Swiss 3T3 fibroblasts were plated as described above and allowed to attach and spread overnight at 37°C. Cells were then immunostained for the presence of filamentous actin and focal contacts, indicators of effective cell spreading [4]. Focal contacts were visualized within adherent cells using a monoclonal antibody for paxillin coupled with a fluorescein-labeled secondary antibody. Experiments were also performed using probe monoclonal antibodies for vinculin and FAK. Filamentous actin (F-actin) was visualized using rhodamine-labeled phalloidin [39].

Figure 3.1 shows fluorescent overlay images of cells plated on –COOH, -OH, -CH_3 and –CF_3 terminated SAM surfaces preadsorbed with either A) DMEM + 10% FBS, B) Fn or C) Fn + 100X BSA. Cells were stained with rhodamine phalloidin (red) and anti-vinculin (green). Overlay of the two stainings appear yellow in the images. Similar to the surface chemistry-independent effects on cell adhesion shown in Chapter 2, SAM surfaces preadsorbed with Fn alone (Figure 3.1B) support focal contact and stress fiber formation on **all** four surfaces. Localization of vinculin to the ends of filamentous actin networks indicates that effective outside-in signaling is achieved under these extracellular

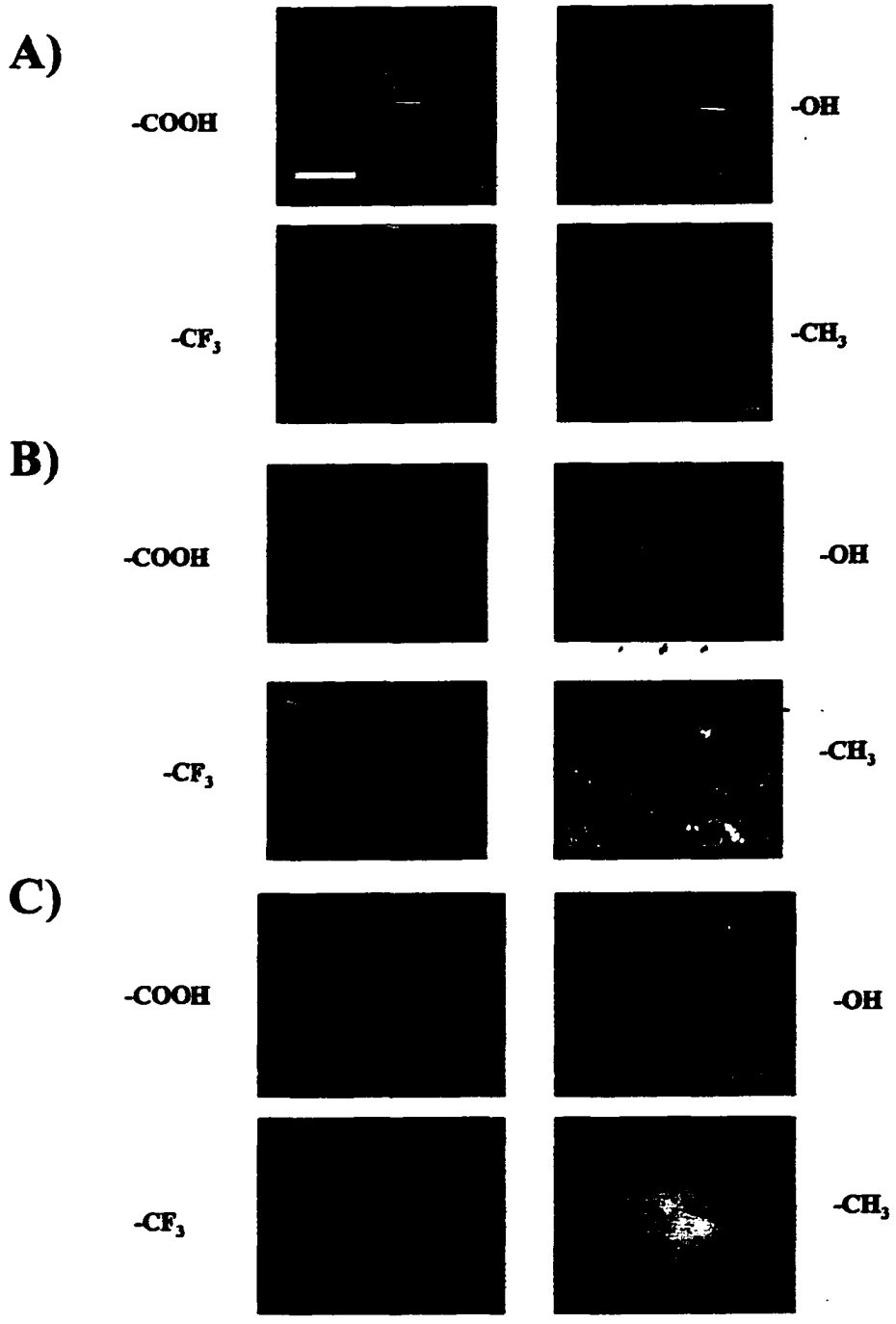

Figure 3.1 Vinculin and F-actin immunostaining in attached Swiss 3T3 fibroblasts on derivatized SAM surfaces. Swiss 3T3 fibroblasts were plated on –COOH, -OH, $-CF_3$ or $-CH_3$ (b,d,f) terminated SAM surfaces preadsorbed with (A) DMEM + 10% FBS, (B) Fn (3.5 μg/ml) or (C) Fn (3.5 μg/ml) + 100X BSA (350 μg/ml). Cells were cultured in respective conditions overnight at 37°C , fixed and stained for vinculin (green) and F-actin (red). Bar, 20μm.

conditions. Fn alone erases all effects of surface chemistry. Evidently sufficient lateral densities of Fn are deposited on all surfaces from Fn alone to support cell responses on all surfaces.

Differential cell spreading on derivatized SAMs preadsorbed with DMEM + 10% FBS (Figure 3.1A) was observed with trends similar to those observed in cell attachment: -COOH and –OH terminated surfaces support efficient cell spreading, as demonstrated by the formation of stress fibers capped by focal contacts. Focal contact formation was somewhat less on –OH terminated SAM surfaces when compared to –COOH, however, some localization of vinculin to the ends of stress fibers was observed. Minimal stress fiber and focal contact formation was observed on $-CH_3$ and $-CF_3$ terminated surfaces.

Finally, the presence of 100-fold excess BSA in the Fn mixture (Figure 3.1C) shows similar differential cell spreading on SAM surfaces in much the same pattern as that observed for cell attachment experiments. BSA:Fn competition in FBS and a simple binary mixture produce similar surface chemistry-dependent cell behaviors. The only significant difference between the results with the two mixtures was that cells plated on –OH terminated SAM surfaces preadsorbed with Fn +100X BSA showed less cell spreading and focal contact formation than on the same surfaces preadsorbed with DMEM + 10% FBS. Competition of adsorbing proteins, even that as simple as a binary Fn/BSA mixture, evidently produces surface-dependent cell behaviors.

As vinculin staining is not exclusively indicative of complete focal contact formation, the presence of other focal contact proteins in adhesion plaques in cells plated on derivatized SAM surfaces was also determined. Figures 3.2 and 3.3 represent paxillin and FAK staining for cells plated on $-CH_3$ and –COOH terminated SAM surfaces

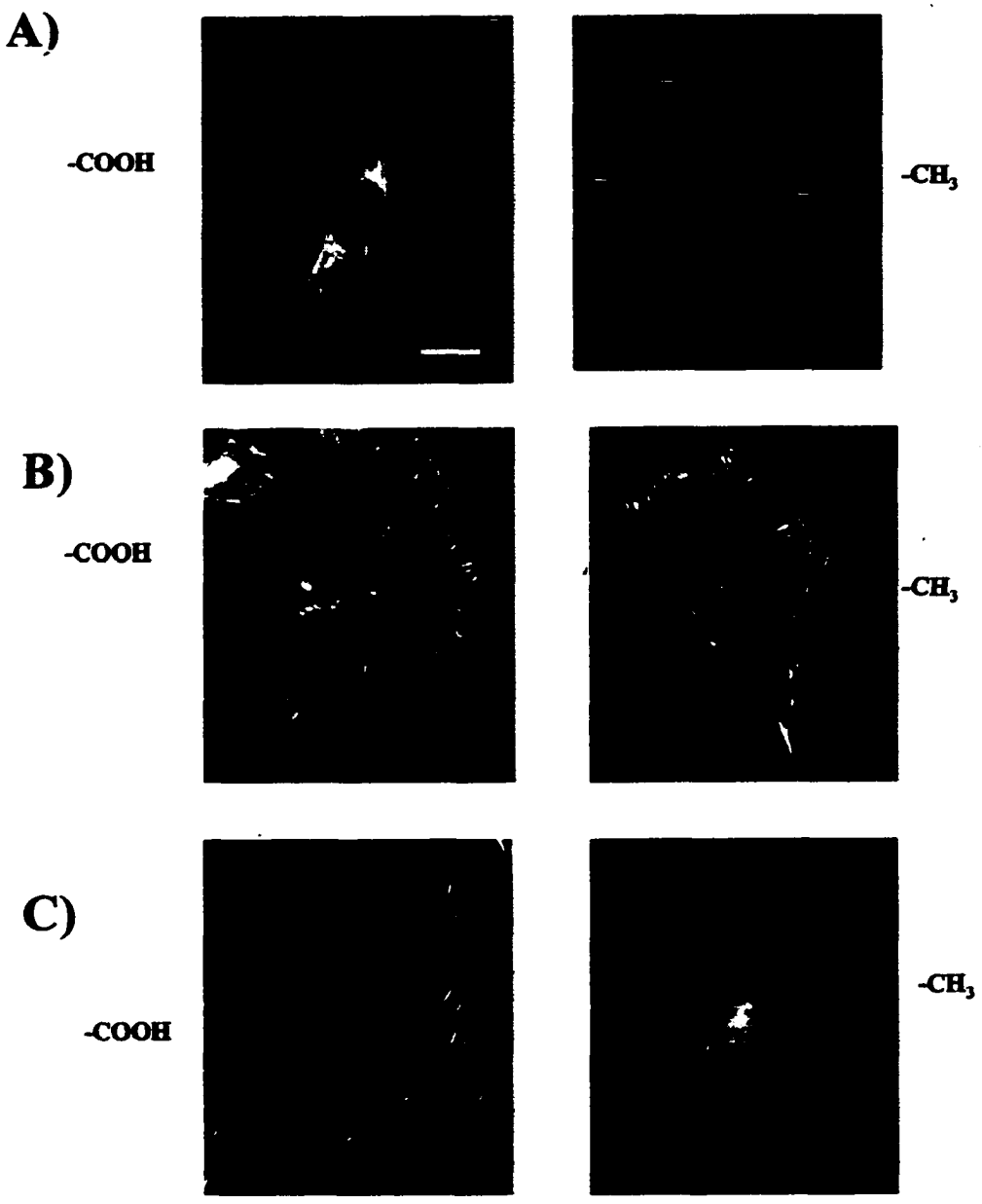

Figure 3.2 Paxillin immunostaining in attached Swiss 3T3 fibroblasts on derivatized SAM surfaces. Swiss 3T3 fibroblasts were plated on –COOH or $-CH_3$ terminated SAM surfaces preadsorbed with (A) DMEM + 10% FBS, (B) Fn (3.5 μg/ml) or (C) Fn (3.5 μg/ml) + 100X BSA (350 μg/ml). Cells were cultured in respective conditions overnight at 37°C , fixed and stained for paxillin. Bar, 20 μm.

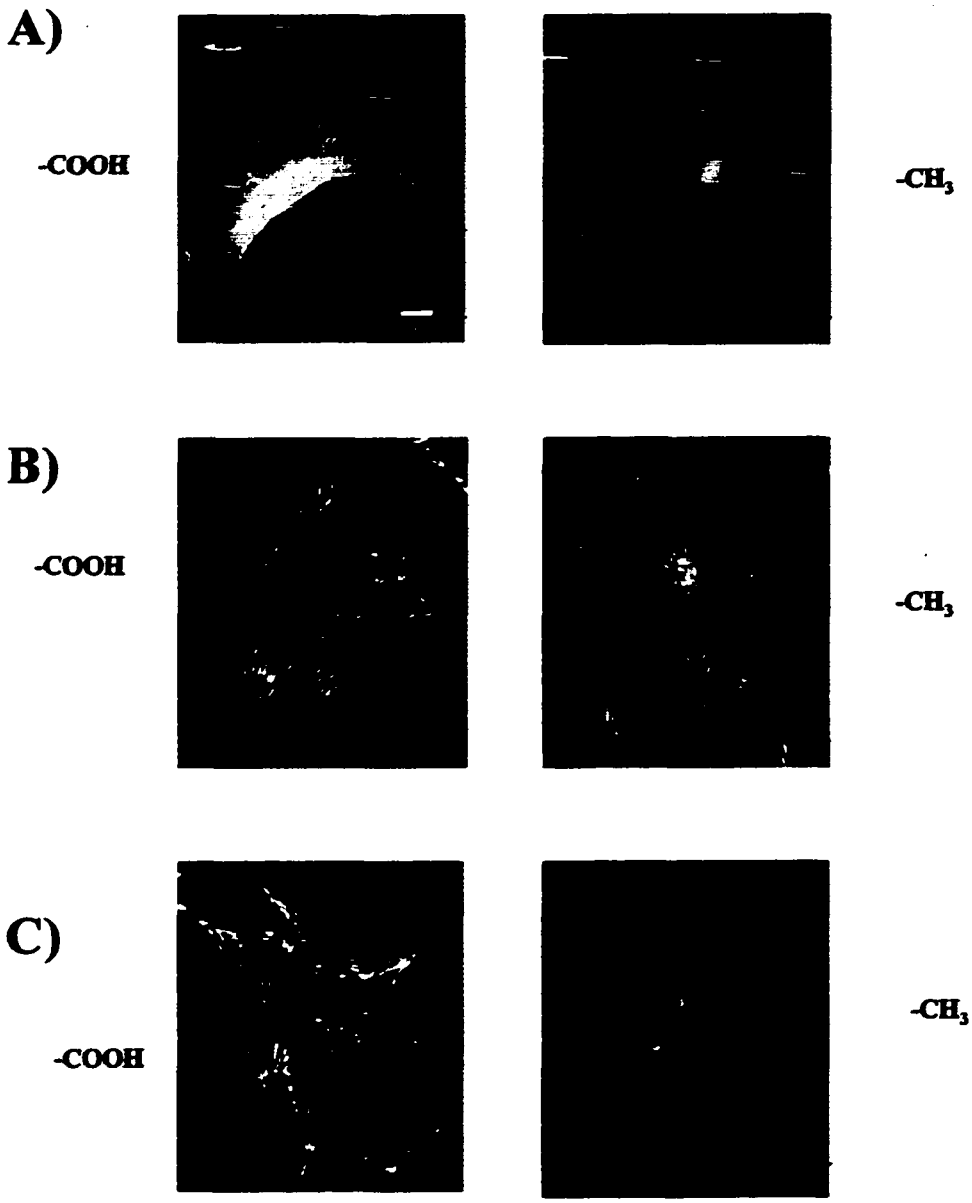

Figure 3.3 FAK immunostaining in attached Swiss 3T3 fibroblasts on derivatized SAM surfaces. Swiss 3T3 fibroblasts were plated on –COOH or $-CH_3$ terminated SAM surfaces preadsorbed with (A) DMEM + 10% FBS, (B) Fn (3.5 μg/ml) or (C) Fn (3.5 μg/ml) + 100X BSA (350 μg/ml). Cells were cultured in respective conditions overnight at 37°C , fixed and stained for FAK. Bar, 20 μm.

preadsorbed with the protein mixtures described above. These surfaces were chosen as they represented the two extremes in cell adhesion and spreading. Paxillin and FAK immunostaining exhibit identical patterns of staining of vinculin under the same extracellular matrix conditions. Specifically, fibroblasts plated on –COOH terminated SAM surfaces demonstrate focal contact formation from all assayed proteins on all surface conditions studied. In contrast, paxillin and FAK were shown not to localize to the plasma membrane in cells plated on $-CH_3$ terminated SAMs under conditions of protein competition, specifically DMEM + 10% FBS (Figures 3.2A and 3.3A) and Fn + 100X BSA (Figures 3.2C and 3.3C). However, focal contact formation, as demonstrated by the localization of paxillin and FAK to the ends of stress fibers, was observed when $-CH_3$ SAM surfaces were preadsorbed with Fn alone (Figures 3.2B and 3.3B).

3.3.2. Comparisons of Swiss 3T3 fibroblasts and Chick Skin fibroblast focal contact and stress fiber formation.

To ensure that differential stress fiber and focal contact formation as a function of surface chemistry was not exclusive to Swiss 3T3 fibroblast cell line, similar immunostaining experiments were performed on primary chick skin fibroblasts (CSFs). Figure 3.4 represents immunostaining of CSFs plated on derivatized SAM surfaces preadsorbed with DMEM + 10% FBS. The cells were stained with rhodamine-labeled phalloidin, to locate filamentous actin. Identical responses were observed with CSFs on SAMs as that observed with Swiss 3T3 fibroblasts. Although CSFs have a more spindly, extended morphology than Swiss 3T3 fibroblasts when plated on –COOH terminated SAM surfaces, they form focal contacts in a similar manner. In contrast to cells plated on –COOH terminated SAMs, but identical to the response displayed by Swiss 3T3

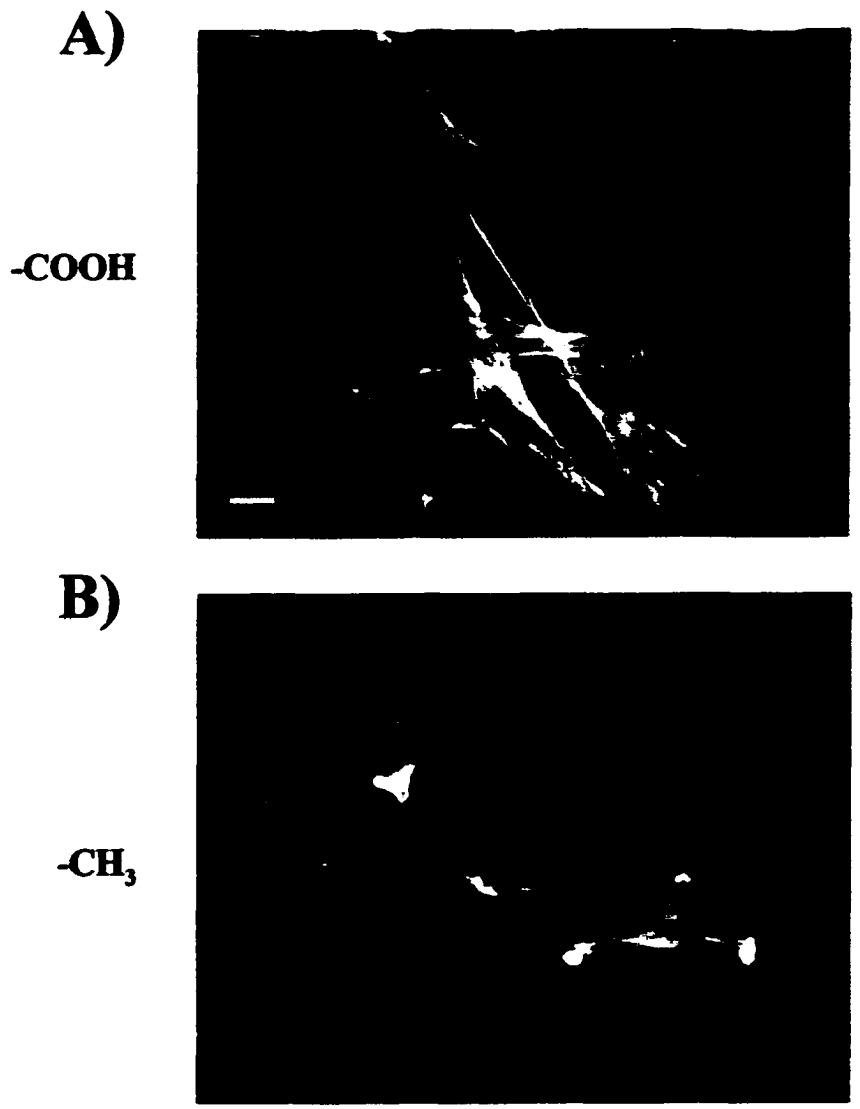

Figure 3.4 Filamentous actin staining in attached chick skin fibroblasts on derivatized SAM surfaces. Chick skin fibroblasts were plated on (A) –COOH or (B) $-CH_3$ terminated SAM surfaces in DMEM + 10% FBS overnight, fixed as described stained with rhodamine-phalloidin for filamentous actin. Bar, 20 μm.

fibroblasts, CSFs plated on $-CH_3$ terminated SAM surface lack the formation of visible stress fibers.

Figure 3.5 represents immunostaining of various focal contact proteins in CSF cells plated on derivatized SAM surfaces preadsorbed with DMEM + 10% FBS. The cells were stained with monoclonal antibodies for A) vinculin, B) paxillin and C) FAK. Results indicate that there is no detectable difference between observed focal contact formation in response to surface chemistry between the secondary Swiss 3T3 fibroblast cell line and primary cultures of chick skin fibroblasts. Both cells types show localization of vinculin, paxillin and FAK to the plasma membrane when plated on –COOH terminated SAM surfaces and a lack of this localization in cells plated on $-CH_3$ terminated SAM surfaces.

3.3.3. Tyrosine phosphorylation of focal contact proteins is surface chemistry-dependent.

Protein phosphorylation is another important intracellular signaling event following focal contact formation. To investigate the initiation of this event, fibroblasts plated on derivatized SAM surfaces preadsorbed with various protein components were immunostained with an antibody directed against phosphorylated tyrosine. Figure 3.6 represents results typically obtained. Swiss 3T3 fibroblasts capable of forming stress fibers and focal contacts on –COOH SAM surfaces also consistently exhibit tyrosine phosphorylation localized to the area of focal contacts. In contrast, rounded, unspread fibroblasts in $-CH_3$ SAM surfaces showed minimal localized tyrosine phosphorylation.

These immunofluorescence data correlate with biochemical analysis of tyrosine phosphorylation of several focal adhesion components under favorable and unfavorable

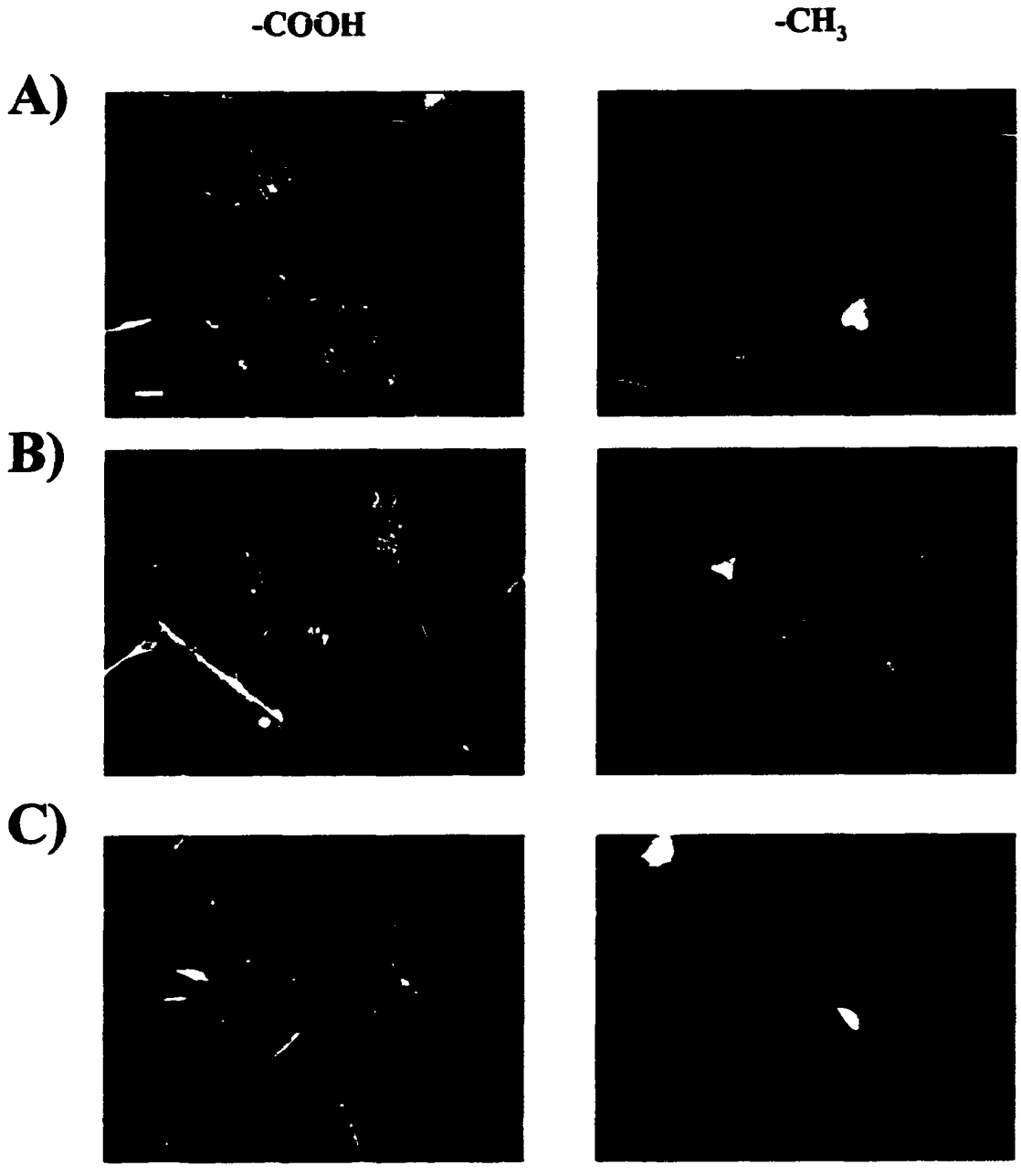

Figure 3.5 Immunostaining in attached chick skin fibroblasts on derivatized SAM surfaces. Chick skin fibroblasts were plated on –COOH or $-CH_3$ terminated SAM surfaces in DMEM + 10% FBS overnight., fixed and stained for (A) vinculin, (b) paxillin and (c) FAK. Bar, 20 μm.

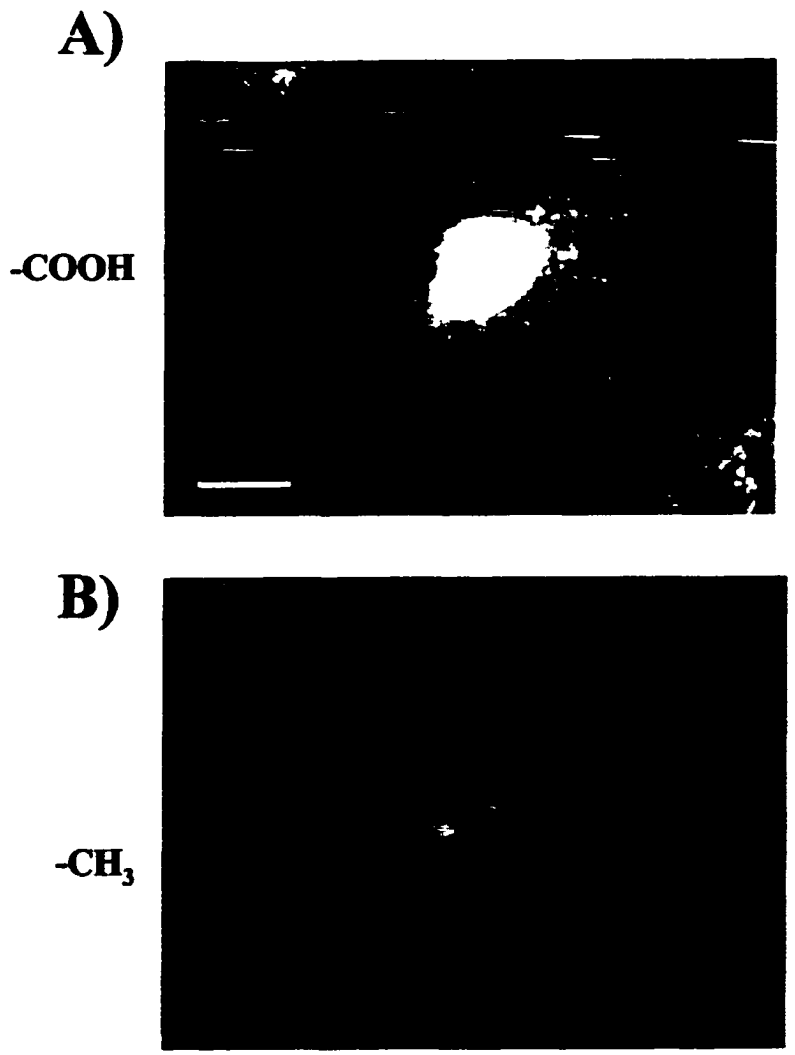

Figure 3.6 Phosphotyrosine immunostaining in attached fibroblasts on derivatized SAM surfaces. Swiss 3T3 fibroblasts were plated on –COOH (a) or –CH_3 (b) terminated SAM surfaces preadsorbed with DMEM + 10% FBS. Cells were cultured in respective conditions overnight at 37°C , fixed and stained for phosphotyrosine. Bar, 20 μm.

surface-induced adhesion conditions. Figure 3.7 is an example of a Western blot of tyrosine phosphorylation of two of the most prominent tyrosine phosphorylated focal adhesion proteins, paxillin and FAK. Proteins were immunopreciptated from cell extracts and the resulting proteins were probed with antibodies for paxillin (Figure 3.7A) and FAK (Figure 3.7B). Lane 2 represents extracts from serum-starved fibroblasts, which is a negative control for tyrosine phosphorylation. Lane 4 represents extracts from LPA-stimulated Swiss 3T3 fibroblasts. LPA stimulation has been shown to lead to extensive tyrosine phosphorylation of focal contact proteins [40]. Results show that equal amounts of both paxillin and FAK were precipitated from extracts of cells plated on –COOH (Lane 5) and $-CH_3$ (Lane 3) terminated SAMs and control conditions.

Figure 3.8 represents a control experiment for the specificity of the monoclonal antibodies used in the immunoprecipitation experiments. An antigenic peptide specific for FAK was available to use in competition experiments with endogenous FAK protein. Extracts were immunoprecipitated in the presence (Lanes 3,5,7 and 9) and absence (2,4,6 and 8) of the peptide. As expected, the presence of blocking peptide competed away the FAK protein binding, as evidenced by the loss of band intensity at approximately 125 kD.

Figure 3.9 represents a Western blot of the same cell extracts used in Figure 3.7, except this time probed with a monoclonal antibody directed against phosphorylated tyrosines. As expected, extracts from LPA-stimulated cells (Lane 4) show extensive phosphorylation of paxillin (Figure 3.9A) and FAK (Figure 3.9B) proteins. Lane 5 demonstrates that the paxillin and FAK proteins from extracts of cells plated on -COOH terminated SAMs are approximately twice as phosphorylated (46% and 55% more respectively) as those from cells plated on $-CH_3$ terminated SAMs (Lane 3). Lane 2,

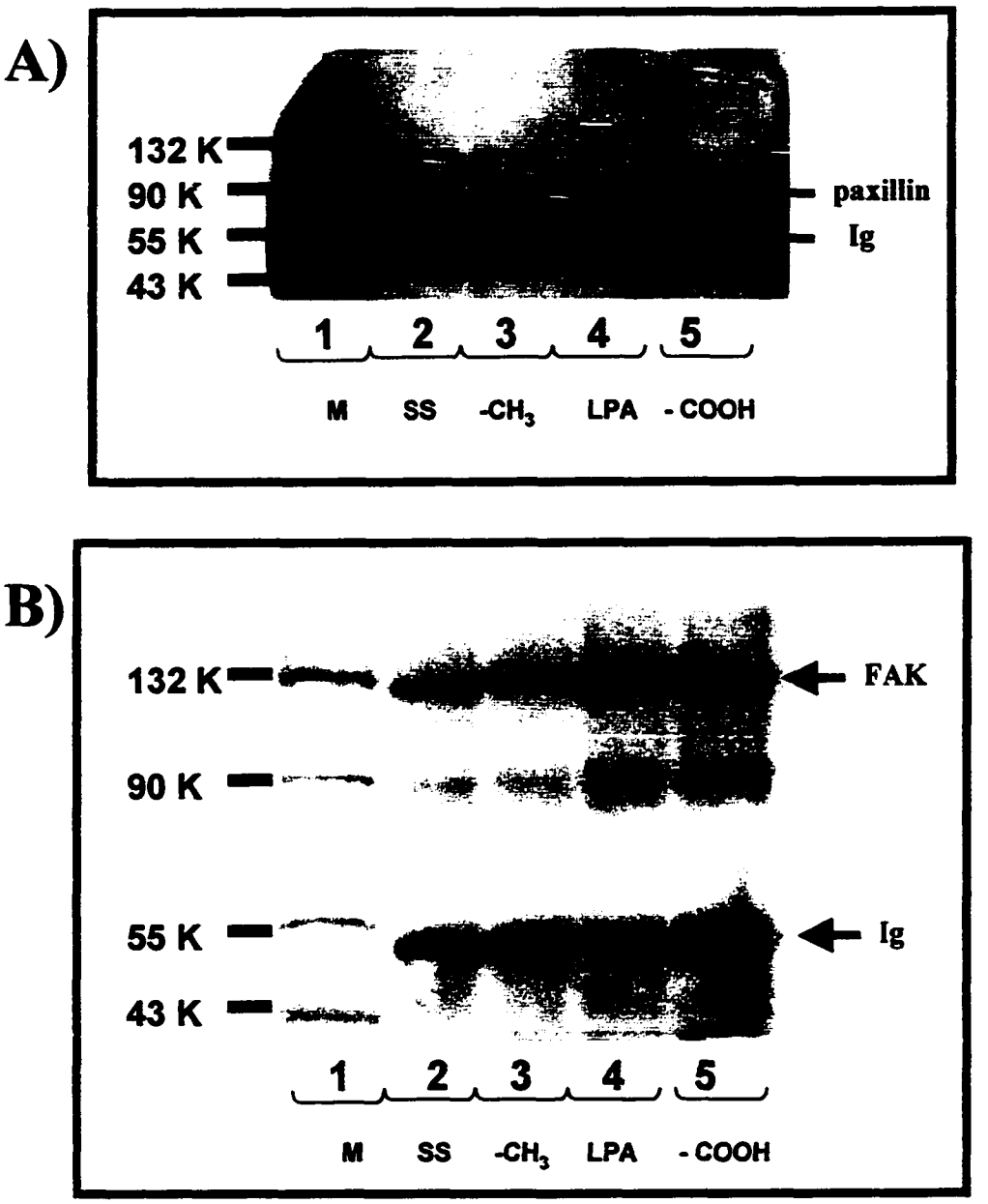

Figure 3.7 - Immunoprecipitations of paxillin (68 K) and FAK (125 K) from whole cell extracts of Swiss 3T3 fibroblasts plated on derivatized SAM surfaces: Swiss 3T3 fibroblasts were plated in DMEM + 10% FBS on $-CH_3$ (Lane 3) or -COOH (Lane 5) derivatized SAM surfaces overnight. Whole cell extracts were prepared and 500 μg of total protein were immunoprecipitated with monoclonal antibodies for paxillin (A) and FAK (B). Samples of cells serum starved for 4 hours (SS) (Lanes 2) and serum starved followed by LPA stimulation for 30 minutes (LPA) (Lane 4) were also taken. Following immunoprecipitations, samples were run on a 7.5% denaturing PAGE. Western blot were performed using monoclonal antibodies for FAK and paxillin and blots were developed by chemiluminesence. M= MW markers.

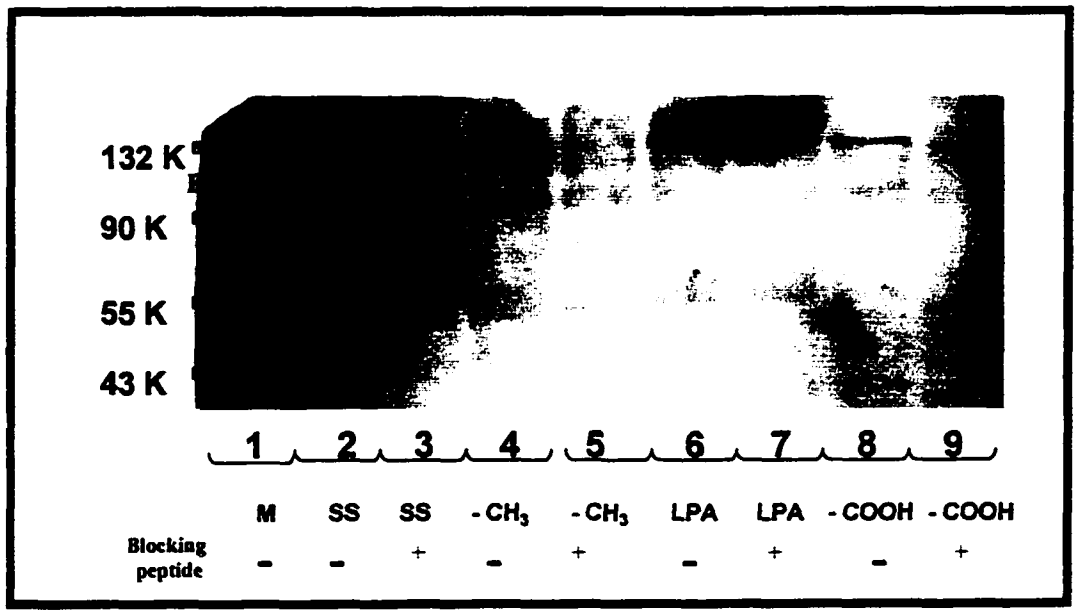

Figure 3.8 Westerns of FAK (125 K) immunoprecipitations of whole cell extracts of Swiss 3T3 fibroblasts plated on derivatized SAM surfaces: Swiss 3T3 fibroblasts were plated in DMEM + 10% FBS on -CH_3 (Lanes 4 and 5) or -COOH (Lanes 8 and 9) derivatized SAM surfaces overnight. Whole cell extracts were prepared and 500 ug of total protein were immunoprecipitated with a polyclonal antibodies FAK in presence (+) or absence (-) of competing antigenic blocking peptide. Samples of cells serum starved for 4 hours (SS) (Lanes 2 and 3) and serum starved followed by LPA stimulation for 30 minutes (LPA) (Lanes 6 and 7) were also taken. Following immunoprecipitations, samples were run on a 7.5% denaturing PAGE. A Western blot was performed using a monoclonal antibody for FAK and the blot was developed by chemiluminesence. M= MW markers.

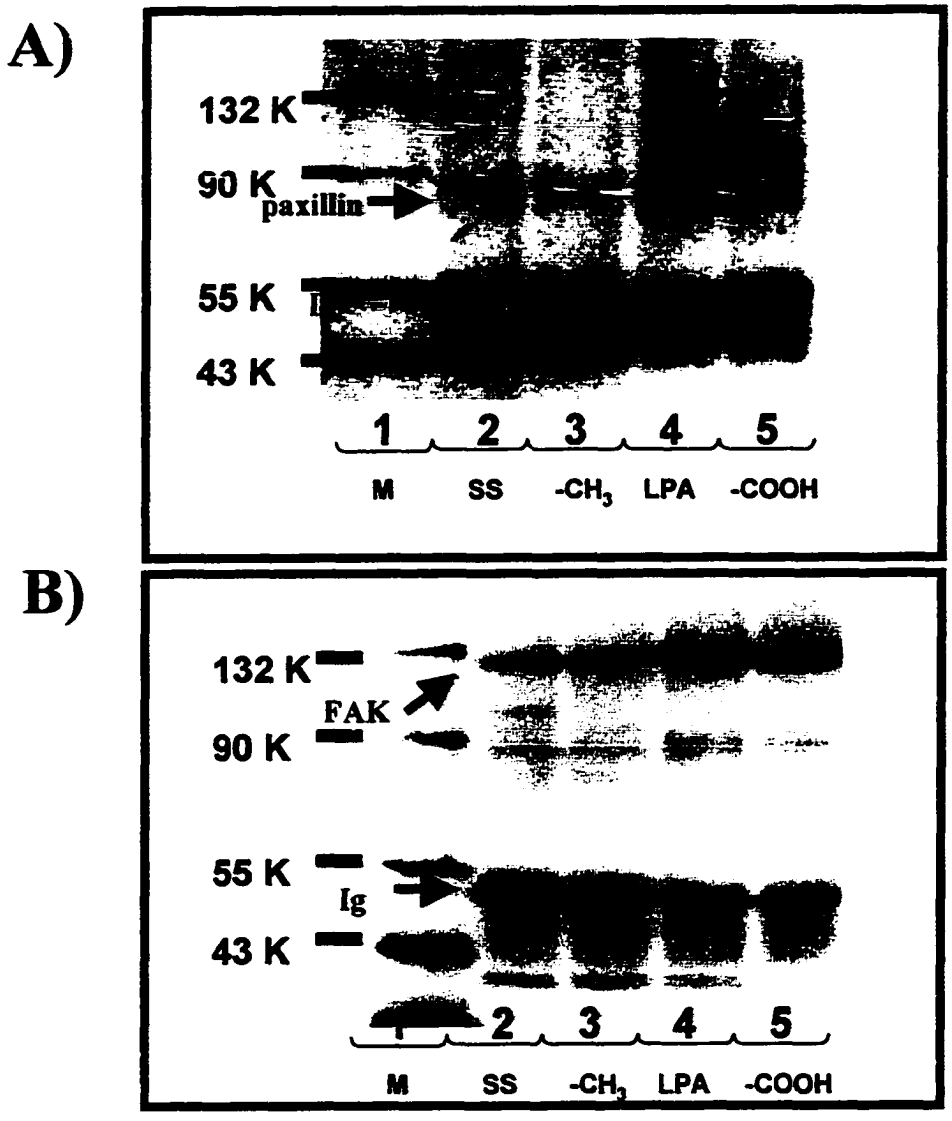

Figure 3.9 Phosphotyrosine Westerns of paxillin (68 K) and FAK (125 K) immunoprecipitations of whole cell extracts of Swiss 3T3 fibroblasts plated on derivatized SAM surfaces: Swiss 3T3 fibroblasts were plated in DMEM + 10% FBS on $-CH_3$ (Lane 3) or -COOH (Lane 5) derivatized SAM surfaces overnight. Whole cell extracts were prepared and 500 ug of total protein were immunoprecipitated with monoclonal antibodies for A) paxillin and B) FAK. Samples of cells serum starved for 4 hours (SS) (Lanes 2) and serum starved followed by LPA stimulation for 30 minutes (LPA) (Lane 4) were also taken. Following immunoprecipitations, samples were run on a 7.5% denaturing PAGE. A Western blot was performed using a monoclonal antibody for phosphorylated tyrosines (PY20) and blots were developed by chemiluminesence. M= MW markers.

extracts from serum-starved cells, serve as negative controls for tyrosine phosphorylation. However, in this experiment, some phosphorylation of both proteins was evident under serum starved conditions. The levels were comparable to those seen in cells plated on $-CH_3$ terminated SAM surfaces.

3.4. DISCUSSION

Results presented here demonstrate that outside-in signaling responsible for activation of intracellular signal cascades that promote initiation of stress fiber and focal contact formation and tyrosine phosphorylation can be modulated by changing well-controlled surface chemistry. Results demonstrate that molecular details in the surface chemistry and their influence on protein adsorption from serum translate to molecular changes in ECM detection by integrin cell receptors and corresponding cell signaling responses.

Results presented in Chapter 2 demonstrated that surface chemistry was capable of modulating macroscopic cellular properties including fibroblast adhesion and growth. Cell proliferation on surfaces is ultimately mediated by initiation of intracellular signaling mechanisms. As discussed in the introduction of this chapter, many intracellular events are initiated in response to cell surface integrin receptors with surface-adsorbed ECM proteins. One of the most prevalently used techniques for investigating effective outside-in communication is tracking the formation of stress fibers and focal contacts using immunocytochemistry.

Results described in this chapter demonstrate that formation of stress fibers and focal contacts can be linked with surface chemistry through protein adsorption results.

Formation of focal contacts and stress fibers, exhibited on the -COOH terminated SAM surface, indicates that effective outside-in transmembrane signaling is produced by integrin attachment to ECM proteins on this material's surface. However, this signaling is either absent or inefficient on the $-CH_3$ terminated SAMs. In addition to supporting minimal cell attachment, $-CH_3$ surfaces were also unable to support cell spreading, focal contact formation, and widespread tyrosine phosphorylation. These results indicate that outside-in signaling is modulated by surface chemistry in anchorage-dependent cells. The pivotal role of ECMs in this signaling pathway indicates that both composition and conformation of the adsorbed protein layer controls the differential morphologies observed in cells plated on various SAM surfaces.

The ultimate goal of this research is to identify the specific surface determinants to control and modulate cell biological responses. This requires a careful assessment of the composition and conformation of the complex extracellular protein environment, as well as identifying the presence or absence of key outside-in receptor mediated cellular signaling events. These events include initiation of signal transduction pathways involved in progression through the cell cycle, as well as the subsequent induction of growth-associated gene expression downstream of the signal transduction cascades.

The small molecular weight GTPase RhoA has been shown to play a role in several of the intracellular signals described herein, particularly the formation of focal contacts and stress fibers [19, 41, 42](48-50). Activation of RhoA following cell adhesion has been shown to be an essential step in the progression of these adhesion-dependent events [43]. RhoA activation is therefore hypothesized to be either absent or inefficient in

cells plated on the -CH_3 terminated SAMs, thus leading to the lack of stress fiber and focal contact formation observed in cells plated on these surfaces. The final chapter of this thesis outlines investigations into the relationships between SAM surfaces and RhoA. The connection relies on results from Chapter 2 and 3 and allows completion of a molecular-based understanding of how surfaces influence mechanisms of cell signaling.

3.5. Endnotes

1. Hynes, R.O., Integrins: versatility, modulation, and signaling in cell adhesion, Cell, **69** (1): p. 11-25 (1992).
2. Clark, E.A. and J.S. Brugge, Integrins and signal transduction pathways: the road taken, Science, **268** (5208): p. 233-9 (1995).
3. Ruoslahti, E. and M.D. Pierschbacher, New perspectives in cell adhesion: RGD and integrins, Science, **238** (4826): p. 491-7 (1987).
4. Damsky, C.H. and Z. Werb, Signal transduction by integrin receptors for extracellular matrix: cooperative processing of extracellular information, Curr Opin Cell Biol, **4** (5): p. 772-81 (1992).
5. Juliano, R.L. and S. Haskill, Signal transduction from the extracellular matrix, J Cell Biol, **120** (3): p. 577-85 (1993).
6. Richardson, A. and J.T. Parsons, Signal transduction through integrins: a central role for focal adhesion kinase?, Bioessays, **17** (3): p. 229-36 (1995).
7. Miyamoto, S., S.K. Akiyama, and K.M. Yamada, Synergistic roles for receptor occupancy and aggregation in integrin transmembrane function, Science, **267** (5199): p. 883-5 (1995).
8. Staatz, W.D., S.M. Rajpara, E.A. Wayner, W.G. Carter, and S.A. Santoro, The membrane glycoprotein Ia-IIa (VLA-2) complex mediates Mg++-dependent adhesion in platelets to collagen, J. Cell Biol., **108** : p. 1917-1924 (1989).

9. Elices, M.J. and M.E. Hemler, Thehuman integrin VLA-2 is a collagen receptor on some cells and a collagen/laminin receptor on others, Proc. Natl. Acad. Sci. USA, **86** : p. 9906-9910 (1989).

10. Grinstein, S., D. Rotin, and M.M. Mason, Na+/H+ exchange and growth-factor-induced cytosolic pH changes. Role in cellular proliferation, Biochem. Biophys. Acta, **988** : p. 73-97 (1989).

11. Ingber, D.E., D. Prusty, J.V. Frangioni, E.J. Cragoe, C. Lechene, and M.A. Schwartz, Control of intracellular pH and growth by fibronectin in capillary endothelial cells, J. Cell Biol., **110** : p. 1803-1811 (1990).

12. Schwartz, M.A., C. Lechene, and D.E. Ingber, Insoluble fibronectin activates the Na/H antiporter by clustering and immobilizing integrin a5b1, independent of cell shape, Proc. Natl. Acad. Sci. USA, **88** : p. 7849-7853 (1991).

13. McNamee, H.M., D.E. Ingber, and M.A. Schwartz, Adhesion to fibronectin stimulates inositol lipid synthesis and enhances PDGF-induced inositol lipid breakdown, J. Cell Biol., **121** : p. 673-678 (1992).

14. Rana, R.S. and L.E. Hokin, Role of phosphoinositides in transmembrane signaling, Phsiol. Rev., **70** : p. 115-164 (1990).

15. Chong, L.D., A. Traynor-Kaplan, G.M. Bokoch, and M.A. Schwartz, The small GTP-binding protein Rho regulates a phosphatidylinositol 4-phosphate 5-kinase in mammalian cells, Cell, **79** : p. 507-513 (1994).

16. Dike, L.E. and S.R. Farmer, Cell adhesion induces expression of growth-associated genes in suspension-arrested fibroblasts, Proc Natl Acad Sci U S A, **85** (18): p. 6792-6 (1988).

17. Ridley, A.J. and A. Hall, Cell, **70** : p. 389-399 (1992).

18. Miura, Y., A. Kikuchi, T. Musha, S. Kuroda, H. Yaku, T. Sasaki, and Y. Takai, J. Biol. Chem., **268** : p. 510-515 (1993).

19. Nobes, C.D. and A. Hall, Rho, rac, and cdc42 GTPases regulate the assembly of multimolecular focal complexes associated with actin stress fibers, lamellipodia, and filopodia, Cell, **81** (1): p. 53-62 (1995).

20. Leung, T., Q. Chen, E. Manser, and L. L., Mol. Cell Biol., **16** : p. 5313 (1996).

21. Machesky, L.M. and A. Hall, Role of actin polymerization and adhesion to extracellular matrix in Rac- and Rho-induced cytoskeletal reorganization, J Cell Biol, **138** (4): p. 913-26 (1997).

22. Lewis, J.M. and M.A. Schwartz, Mapping in vivo associations of cytoplamsic proteins with b1 cytoplasmic domains, Mol. Cell. Biol., **6** : p. 151-160 (1995).

23. Schaller, M.D., C.A. Otey, J.D. Hildebrand, and J.T. Parsons, Focal adhesion kinase and paxillin bind to peptides mimicking b integrin cytoplasmic domains, J. Cell Biol., **130** : p. 1181-1187 (1995).

24. Barstead, R.J. and R.H. Waterson, J. Cell Biol., **114** : p. 715-724 (1991).

25. Westmeyer, A., K. Ruhnau, A. Wegner, and B.M. Jockusch, EMBO J., **9** : p. 2071-2078 (1990).

26. Jockusch, B.M., Annu. Rev. Cell Dev. Biol., **11** : p. 379-416 (1995).

27. Johnson, R.P. and S.W. Craig, F-actin binding site masked by the intramolecular association of vinculin head and tail domains, Nature, **373** : p. 261-264 (1995).

28. Jockusch, B.M. and M. Rudiger, Crosstalk between cell adhesion molecules: vinculin as a paridigm for regulation by conformation, Trends in Cell Biol., **6** : p. 311-314 (1996).

29. Zachary, I., J. Sinnett-Smith, and E. Rozengurt, J. Biol. Chem., **267** : p. 19031-19034 (1992).

30. Zachary, I., J. Sinnett-Smith, and E. Rozengurt, J. Biol. Chem., **268** : p. 22060-22065 (1993).

31. Turner, C.E., M.D. Schaller, and J.T. Parsons, J.Cell Sci., **105** (637-645) (1993).

32. Bellis, S.L., J.T. Miller, and C.E. Turner, Characterization of tyrosine phopshorylation of paxillin in vitro by focal adhesion kinase, J. Biol. Chem., **270** (29): p. 17437-17441 (1995).

33. Wood, C.K., C.E. Turner, P. Jackson, and D.R. Critchley, J. Cell Sci., **107** : p. 709-717 (1994).

34. Kornberg, L.J., H.S. Earp, C.E. Turner, C. Prockop, and R.L. Juliano, Signal transduction by integrins: increased protein tyrosine phosphorylation caused by clustering of beta 1 integrins, Proc Natl Acad Sci U S A, **88** (19): p. 8392-6 (1991).

35. Kornberg, L., H.S. Earp, J.T. Parsons, M. Schaller, and R.L. Juliano, Cell adhesion or integrin clustering increases phosphorylation of a focal adhesion-associated tyrosine kinase, J Biol Chem, **267** (33): p. 23439-42 (1992).

36. Burridge, K., C.E. Turner, and L.H. Romer, Tyrosine phosphorylation of paxillin and FAK accompanies cell adhesion to extracellular matrix: A role for cytoskeletal assembly, J. Cell Biol., **119** (4): p. 893-903 (1992).

37. Heacock, C.S. and J.R. Bamburg, The quantitation of G- and F-actin in cultured cells, Anal Biochem, **135** (1): p. 22-36 (1983).

38. Heacock, C.S. and J.R. Bamburg, Levels of filamentous and globular actin in Chinese hamster ovary cells throughout the cell cycle, Exp Cell Res, **147** (1): p. 240-6 (1983).

39. Lewandowska, K., N. Balachander, C.N. Sukenik, and L.A. Culp, Modulation of fibronectin adhesive functions for fibroblasts and neural cells by chemically derivatized substrata, J Cell Physiol, **141** (2): p. 334-45 (1989).

40. Moolenaar, W.H., LPA: A novel lipid mediator with diverse biological actions, Trends Cell Biol., **4** : p. 213-219 (1994).

41. Hotchin, N.A. and A. Hall, Regulation of the actin cytoskeleton, integrins and cell growth by the Rho family of small GTPases, Cancer Surv, **27** : p. 311-22 (1996).

42. Nobes, C.D. and A. Hall, Rho, rac and cdc42 GTPases: regulators of actin structures, cell adhesion and motility, Biochem Soc Trans, **23** (3): p. 456-9 (1995).

43. Olson, M.F., A. Ashworth, and A. Hall, An essential role for Rho, Rac, and Cdc42 GTPases in cell cycle progression through G1, Science, **269** (5228): p. 1270-2 (1995).

Chapter 4: The Role of the Small Molecular Weight GTPase RhoA in Surface Chemistry-Induced Changes in Fibroblast Morphology

4.1. INTRODUCTION

Approximately 50 low molecular weight GTPases, responsible for signal transduction events in various cell types, have been described to date. Families of these enzymatic cell signal regulators are subdivided into five classes: Ras, Rab, Arf, Ran and Rho [1]. Rho family members -- CDC42, Rac and Rho -- have been shown to play dynamic roles in regulating the actin cytoskeleton. Rac is important in actin polymerization associated with membrane ruffling and lamellipodia formation [2, 3]. CDC42 is responsible for cell filopodia formation [2]. Rho activity is required for focal contact and stress fiber formation that facilitates cell spreading and adhesion on substrates [2, 4, 5]. Three different specific Rho protein sub-families (A,B and C) have been detected in all cell types examined to date [6] [7].

All Rho family members, like most G-proteins, cycle between GDP-bound inactive and GTP-bound active forms, aided by a number of intracellular regulatory proteins. Activation of RhoA has been shown to be an integrin- and growth factor-dependent event [8]. Although the mechanisms of Rho activation remain unclear, many have been proposed. Current models depict Rho in the GDP-bound, inactive form, complexed with a guanine nucleotide dissociation inhibitor (Rho-GDI) and found in the

cytoplasm of unstimulated, quiescent cells. Upon integrin receptor or growth factor stimulation, Rho is activated by conversion to GTP-Rho by a guanine nucleotide exchange factor (GEX) [9]. Because this activation is substrate-dependent for anchorage-dependent cell, RhoA modulation should exhibit a surface dependence, cued by integrin-surface coupling events.

RhoA is primarily known for its regulation of cell-surface induced focal contact and stress fiber formation [2, 4, 5]. Formation of stress fibers is linked to the Ser-Thr kinase, p160ROCK, that interacts with Rho in a GTP-dependent manner [10]. Two substrates for this kinase, myosin light chain phosphatase and myosin light chain, are known to regulate the assembly of actin-myosin filament bundles, and recent work has shown that Rho-induced stress fiber formation occurs primarily through bundling of preexisting filaments [11]. These signaled responses, as well as others, are important responses determining cell phenotype on surfaces. Clarification of how surfaces influence or direct these responses together with specific biological cues, is a significant issue.

Focal contact formation, creating adhesion plaques that regulate cell attachment to surfaces, is initiated following stress fiber formation. Rho activation is known to be upstream of activation of focal adhesion kinase (FAK). RhoA-stimulated bundling and contractility of actin-myosin complexes leads to the clustering of integrin receptors, thereby leading to the activation of FAK [12]. As FAK activation is a precursor to complete focal contact formation, Rho is essential to inducing focal contact formation and, thereby, also significant in cell-surface interactions.

Recent work has shown that culture surfaces comprising self-assembled monolayers (SAMs) of terminally derivatized alkylthiols on gold (see Figure 1.1)

modulate fibroblast morphological and growth characteristics[13]. Specifically, extracellular matrix protein (fibronectin) adsorption, conformation and subsequent ceil adhesion, spreading and growth are modified by varying terminal groups present on SAM surfaces. SAMs terminated in –COOH groups exhibit high levels of fibroblast attachment, spreading and growth, while these responses are minimized on $-CH_3$ terminated SAM culture surfaces. Fibroblasts plated on –COOH terminated SAM surfaces are capable of forming well-defined focal contacts and stress fibers, indicating effective communication between ECMs adsorbed on the SAM surface from serum and integrin-mediated intracellular signaling mechanisms. Cells attached to $-CH_3$ terminated SAM surfaces lack focal contact and stress fibers. These results suggest a possible role for Rho in the observed surface chemistry-influenced differences in cell behavior. Rho activation may be absent or inefficient in cells plated on the $-CH_3$ terminated SAMs, leading to the observed lack of stress fiber and focal contact formation observed in cells cultured on these SAM surfaces.

While a great deal of evidence implicates Rho-mediated, integrin-dependent regulation of numerous intracellular signaling pathways as a gatekeeper for induction of cell growth phenotypes in response to different surfaces, no systematic study has been reported that determines changes in these pathways as a function of surface chemistry. Such an integrated approach is both novel and a potentially valuable strategy to evaluate biomaterial surface-cell behavior at a level never before studied. This study probes the relationship between surface chemistry and RhoA, a member of the Rho family of proteins. The approach attempts to provide a better understanding of essential specific

surface requirements that prompt cell growth and proliferation, and begins to link key internal cell events to extracellular determinants.

4.2. EXPERIMENTAL

4.2.1. Cells and Culture Substrates

Swiss 3T3 fibroblasts (American Type Culture Collection) were grown in DME (Life Technologies, Inc.) with 100 U/ml penicillin and 100μg/ml streptomycin, supplemented with 10% fetal calf serum (complete medium). Asymmetric ω–functionalized alkylthiols bearing terminal methyl ($-CH_3$) and carboxylate (-COOH) functional groups were synthesized by well-known protocols as previously described [14-16]. Self-assembled monolayer (SAM) films of these compounds were fabricated on gold-coated Mylar surfaces (Courtalds Performance Films, FM-1 gold coating, 99.99% purity, deposited to 70-90 Å thickness by evaporative deposition on 0.0007 gauge tin-coated PET substrate) by a standard method [14-16]. These clean, gold-coated substrates were immersed in 1 mM solutions of the alkylthiol compounds in nitrogen-purged ethanol for 24 hours. Substrates were then rinsed in pure ethanol, blown dry in a stream of nitrogen gas and characterized by surface analysis techniques as previously described [13].

For C3 transferase experiments, cells were cultured as described above on –COOH terminated SAM surfaces in complete media. Following 24 hours of attachment, complete media was supplemented with 5μg/ml recombinant C3 exoenzyme (Calbiochem) and cells were incubated for 12 hours. Cells were then imaged using phase contrast microscopy.

4.2.2. Cytosolic/Membrane Fractionation

Fibroblasts cultured for 24 hours as described above were washed three times with PBS (0.1M phosphate, 0.15M NaCl, pH 7.2) and lysed in hypotonic buffer (10mM Tris, pH 7.5, 5mM $MgCl_2$, 1mM PMSF, 1mM apropotin, 100nM okadaic acid) on ice for five minutes. Plates were then scraped and resulting cell extracts were transferred to a microfuge tube. Extracts were frozen/thawed three times and then centrifuged at 15,000 rpm for five minutes at 4°C. Total protein concentration was determined using the Bradford assay and equivalent amounts of total protein were then ultracentrifuged at 100,000xg for 60 minutes. Supernatants (cytosolic fractions) were poured off and the pellet (membrane fraction) was washed two times in buffer.

4.2.3. Western Blot Analysis

Either whole cell extracts or fractionated extracts were chloroform/methanol precipitated as described by Wessel and Flugge [17]. Total protein levels were determined using a filter dye-binding assay [18]. Equivalent amounts of total protein were separated by electrophoresis on 10% polyacrylamide gels and transferred electrophoretically to polyvinylidene difluoride (PVDF) (NEN Life Science Products). PVDF was first blocked with 4% bovine serum albumin (BSA)(Sigma) in PBS overnight. The PVDF was then incubated for one hour with either anti-RhoA (Santa Cruz Biotechnology, Inc.) or anti-Rho-GDI (Santa Cruz Biotechnology, Inc.). Following incubation, blots were extensively washed with TTBS (150 mM NaCl, 50 mM Tris-Cl, 0.05% Tween, pH 7.6). Blots were then incubated with secondary antibody conjugated

with alkaline phosphatase (Santa Cruz Biotechnology, Inc.) for one hour at room temperature. Following extensive washing with TTBS, enhanced chemiluminescence (Dupont NEN) was used to develop the blots.

4.2.4. Mutant RhoA expression

Swiss 3T3 fibroblasts were plated on -CH_3 terminated SAMs precoated with ECM proteins from DMEM+10%FBS. The -CH_3 chemistry was chosen due to its demonstrated inability to support cell spreading under normal serum culture conditions [13]. Following 24 hours of attachment in complete media as described above, cells were transfected using LipofectAMINE™ Reagent (Life Technologies) with 7.5 μg each of pINDmycRhoAVal14, which expresses a myc-tagged constitutively active form of RhoA under control of an ecdysone-inducible expression system (Invitrogen) and pRXR, which produces the operator protein for the inducible system. The system is based on an insect regulatory mechanism [19]. Control transfections were also performed with the pIND vector alone. Following transfections, cells were rinsed and expression was induced with Ponasterone A for 48 hours. Cells were then fixed and stained for mutant RhoA expression using a fluorescein-labeled anti-PE10 (myc) monoclonal antibody, and for filamentous actin formation using rhodamine-labeled phalloidin as previously described [13].

4.3. RESULTS

4.3.1. Intracellular location of RhoA

The activation state of RhoA can be indirectly determined by examining the relative levels of RhoA proteins located in the cytosolic and membrane fractions, respectively, in cells plated on different SAM terminal chemistries. To determine the activation state of RhoA in cells plated on –COOH and $-CH_3$ derivatized SAM surfaces, cell extracts were obtained and fractionated into cytosolic and membrane fractions.

Figure 4.1 represents a RhoA Western blot of whole cell extracts from Swiss 3T3 fibroblasts plated on $-CH_3$ and -COOH terminated SAMs. Results show that the overall levels of RhoA present is two times less in cells plated on $-CH_3$ terminated SAMs than that in cells plated on -COOH terminated SAMs.

Figure 4.2 shows results for a RhoA Western blot of cytosolic and membrane fractions from cells plated on derivatized SAM surfaces. Cytosolic lanes represent 1/20th of the total cytosolic protein fraction and the membrane lanes represent the entire membrane protein fraction obtained, as membrane fraction levels equivalent to cytosolic levels are undetectable by Western blot analysis. RhoA was present both in the cytosolic and membrane fractions in cells plated on both $-CH_3$ and -COOH terminated SAMs. However, roughly half (44%) as much RhoA is localized to the membrane fraction in cells plated on $-CH_3$ terminated SAMs. This indicates that RhoA may be inefficiently activated and transported to the membrane in these cells, consistent with adherence and growth results reported on these same surfaces [13].

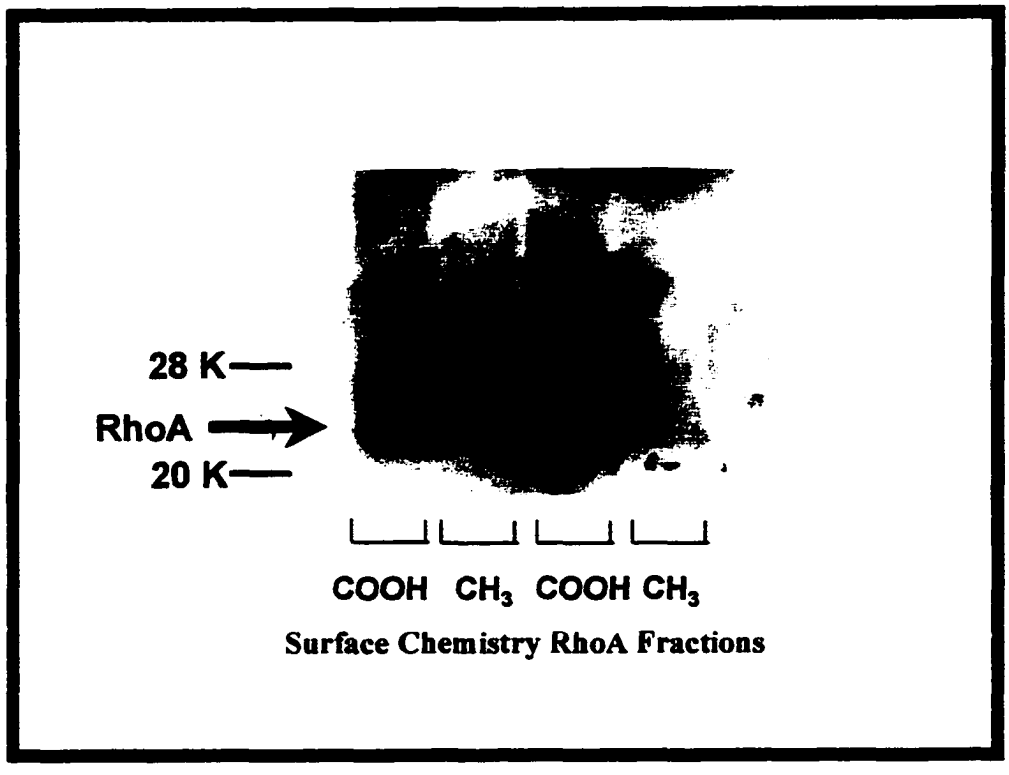

Figure 4.1 - RhoA levels are reduced in fibroblasts cultured on $-CH_3$ terminated SAM surfaces: Swiss 3T3 fibroblasts were plated in DMEM + 10% FBS on derivatized SAM surfaces overnight. Native whole cell extracts were prepared; total protein was normalized. Extract samples were separated using a 10% denaturing PAGE. A Western blot was performed using a monoclonal antibody for RhoA and blots were developed by standard chemiluminesence.

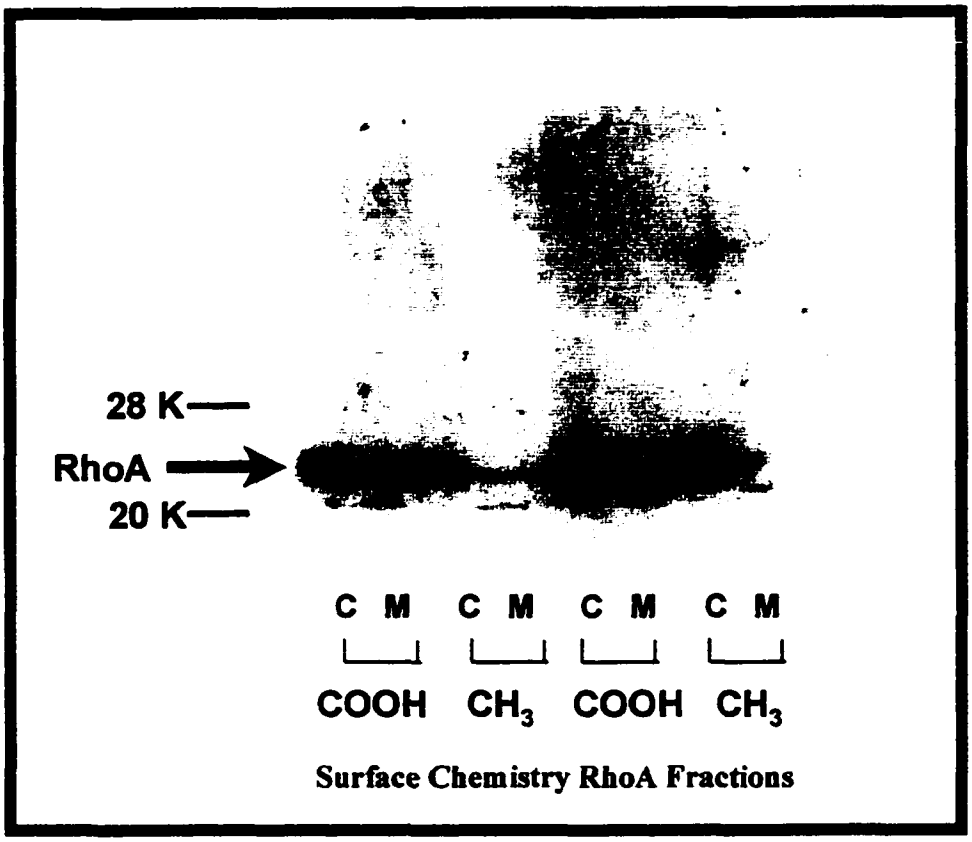

Figure 4.2 – Inactive, cytosolic RhoA is enriched in cells cultured on $-CH_3$ terminated SAM surfaces: Swiss 3T3 fibroblasts were plated in DMEM + 10% FBS on derivatized SAM surfaces overnight. Native whole cell extracts were isolated, normalized for total protein, and ultracentrifuged at 33,000 rpm to fractionate the cellular cytosolic and membrane protein fractions. Fractionated samples were then separated using a 10% denaturing PAGE. A Western blot was performed using monoclonal antibodies specific for RhoA; blots were developed by standard chemiluminesence. Duplicate lanes show cytosolic (C) and membrane (M) fractions marked for RhoA detection as a function of $-COOH$ or $-CH_3$ SAM surface chemistry.

4.3.2. Rho-GDI levels are higher in cells plated on $-CH_3$ terminated SAMs

Figure 4.3 shows a Western blot of whole cell extracts from cells on both surfaces probed with a monoclonal antibody specific for Rho-GDI. The different band intensities indicate that cells plated on the $-CH_3$ terminated SAM have 22% more Rho-GDI than cells plated on –COOH terminated SAM surface. This correlates with the higher level of inactivated, GDP-bound RhoA demonstrated to be present in these cells in Figures 4.1 and 4.2.

Figure 4.4 shows the same cell extracts separated into cytosolic and membrane fractions by ultracentrifugation. Results indicate that the cytosolic fraction of both extracts represent a larger proportion of Rho-GDI. However, cells plated on $-CH_3$ terminated SAM surfaces have four times as much RhoA in the cytosolic fraction as in the membrane fraction, whereas, this ratio is only three in cells plated on –COOH terminated SAM surfaces. This is consistent with Rho-GDI's known role in binding to cytosolic, inactive RhoA, which is present in a higher level in the cytosol in cells plated on $-CH_3$ terminated SAM surfaces.

4.3.3. C3 toxin inactivation of RhoA in cells plated on –COOH terminated SAM surfaces

C3 transferase irreversibly ADP-ribosylates RhoA on amino acid Asn-41and effectively inactivates RhoA [20]. This enzyme can be used as a tool to determine dependence of various cell functions on activated RhoA. Experiments were performed to confirm whether enhanced cell spreading demonstrated on –COOH terminated SAMs is RhoA dependent. To accomplish this, Swiss 3T3 fibroblasts plated on –COOH terminated SAM surfaces for 24 hours were exposed to C3 toxin for 12 hours and then

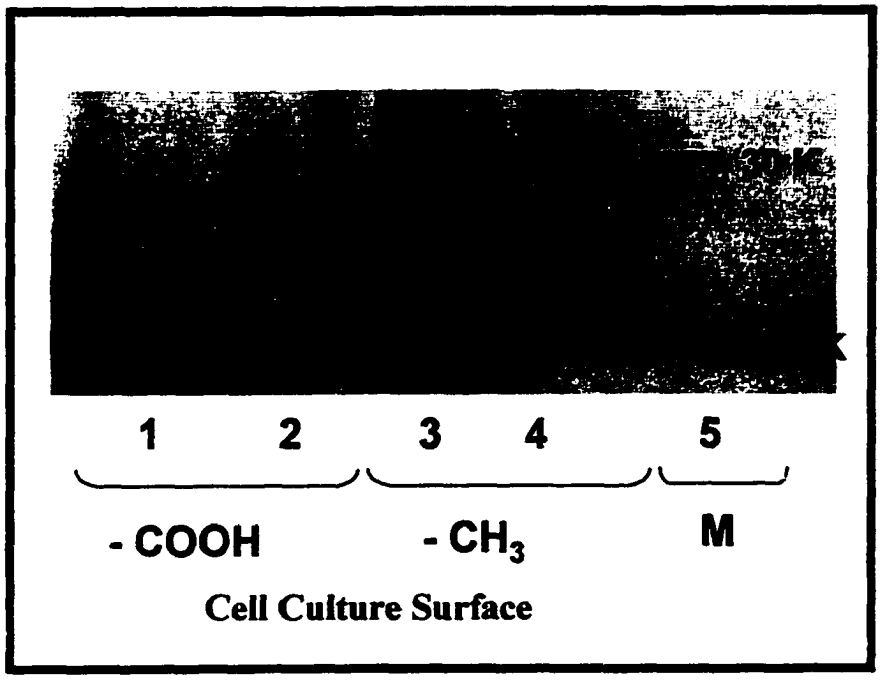

Figure 4.3 – Rho-GDI levels are enhanced in fibroblasts cultured on $-CH_3$ terminated SAM surfaces : Swiss 3T3 fibroblasts were plated in DMEM + 10% FBS on derivatized SAM surfaces overnight. Native whole cell extracts were isolated and normalized for total protein. Extract samples separated using a 10% denaturing PAGE. Western blotting was performed using monoclonal antibodies specific for RhoGDI; blots were developed by standard chemiluminesence. Lanes 1 and 2, and lanes 3 and 4, are duplicates, respectively, from cells cultured on –COOH and $-CH_3$ SAM surfaces.

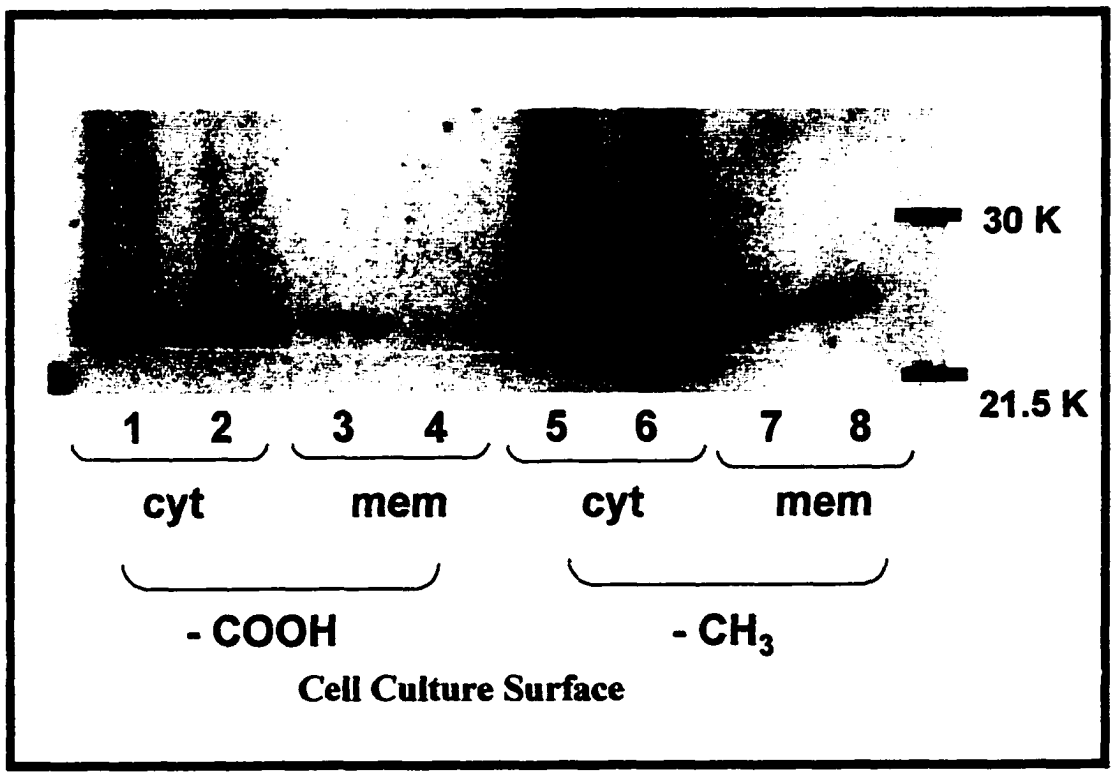

Figure 4.4 – Rho-GDI is enriched in the cytosolic fraction cells cultured on $-CH_3$ terminated SAM surfaces: Swiss 3T3 fibroblasts were plated in DMEM + 10% FBS on derivatized SAM surfaces overnight. Native whole cell extracts were isolated, normalized for total protein, and ultracentrifuged at 33,000 rpm to fractionate the cellular cytosolic and membrane protein fractions. Fractionated samples were then separated using a 10% denaturing PAGE. A Western blot was performed using monoclonal antibodies specific for Rho-GDI; blots were developed by standard chemiluminesence. Duplicate lanes show cytosolic (C) and membrane (M) fractions marked for Rho-GDI detection as a function of –COOH or $-CH_3$ SAM surface chemistry.

imaged using phase contrast microscopy. Figure 4.5 shows that exposure to C3 causes adherent cells on –COOH terminated SAM surfaces to retract cellular processes and begin to adopt a non-spread, low-growth phenotype.

4.3.4. Effects of mutant RhoA expression on transfected fibroblasts plated on derivatized SAM surfaces.

As described above, the GTPase Rho has been implicated in several integrin-mediated cellular responses. Figure 4.2 shows that cells plated on $-CH_3$ terminated SAMs fail to attach and spread, and show low levels of both RhoA activation and subsequent transportation to the membrane. This result suggests surface-induced activation of RhoA through integrin-signaling might be completely by-passed by expressing an inducible constitutively active form of RhoA that requires no surface induction.

Figure 4.6 represents a control experiment to understand the morphological effects of constitutively active RhoA expression in cells plated on –COOH terminated SAM surfaces, which already contain active RhoA. Figures 4.6A, B and C are fluorescence microscopy images from immunostaining experiments of mutant RhoA transfected cells plated on –COOH terminated SAM surfaces. Figure 4.6A represents the cells stained with polyclonal anti-myc and a fluorescein-labeled secondary antibody. This demonstrates that Swiss 3T3 fibroblasts plated on –COOH terminated SAM surfaces are capable of expressing the myc-tagged form of the protein. Figure 4.6B represents the same cells stained with rhodamine-labeled phalloidin, which is a toxin that bind to filamentous actin. Figure 4.6C represents the same cells as in 4.6A and 4.6B stained with a monoclonal antibody for paxillin, a focal adhesion protein and an Alexa 350-labeled

A)

B)

Figure 4.5 – RhoA inactivation leads to loss of growth phenotype in cells cultured on –COOH terminated SAM surfaces : Swiss 3T3 fibroblasts were plated on -COOH derivatized SAM surfaces in DMEM + 10% FBS. Following overnight incubation, cells were rinsed and exposed to 4μg/ml of C3 transferase in complete medium for 12 hours. Cells were then fixed as described and imaged using phase contrast microscopy. Images are of cells plated on –COOH terminated SAM surfaces A) before and B) after exposure to C3 transferase. Exposure to C3 transferase blocks RhoA activation irreversibly, causing initially adherent, spread cells on this surface chemistry to revert to a rounded, retracted morphology. Bar, 20 μm.

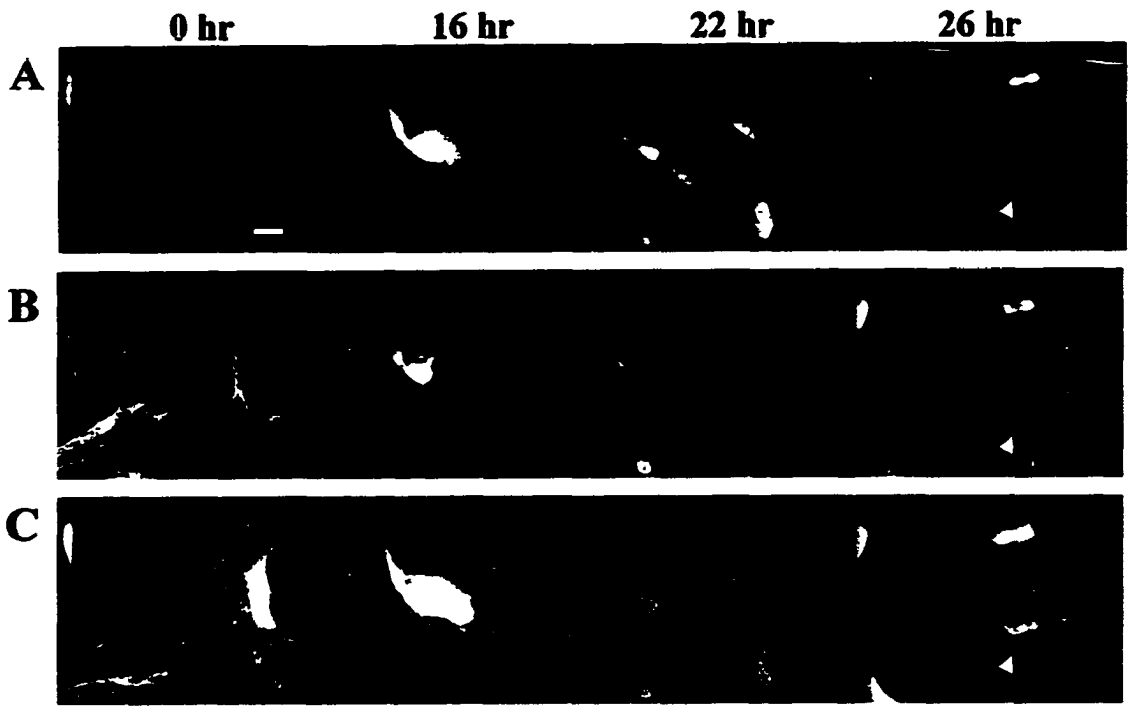

D

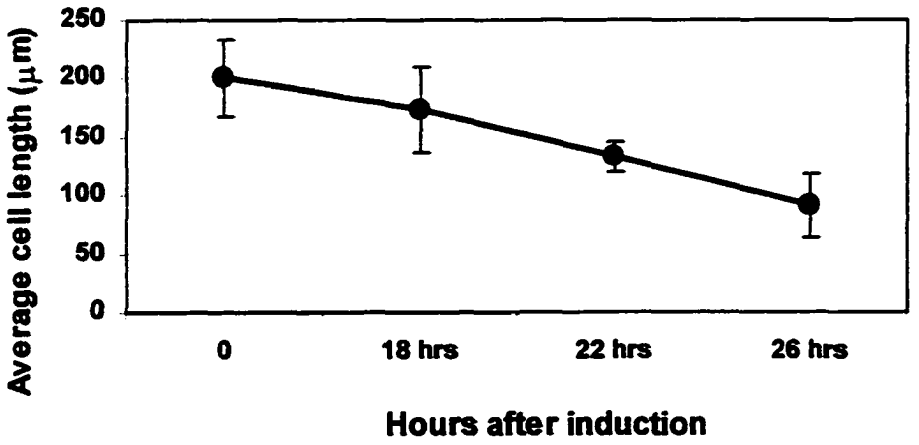

secondary antibody. Results reported above showed that RhoA is effectively activated in cells cultured –COOH terminated SAM surfaces. When a constitutively active form of the protein is expressed in these cells, they begin to retract and adopt a rounded morphology, lacking organized stress fibers. This response is commonly referred to in the literature as the "Rho phenotype [21]." All fibroblasts in the figures are transfected with constitutively active RhoA, with the exception of the cell indicated by an arrow in the figure. Figure 4.6D shows that the average cell length within the total cell population decreased over time as a function of mutant RhoA expression.

Figure 4.7 shows the morphological effects of constitutively active RhoA expression in cells cultured on $-CH_3$ terminated SAM surfaces. Figure 4.7A and 4.7B show that cells expressing mutant RhoA , as evidenced by positive staining with a fluorescently tagged myc antibody, are capable of achieving a spread morphology on - CH_3 terminated SAM surfaces -- a result that is the opposite of the morphological response observed with non-transfected cells. The staining observed in uninduced cells was a result of nonspecific staining by the fluorescein-conjugated secondary antibodies. Due to the compact nature of uninduced cells, nonspecific staining makes staining levels difficult to interpret in rounded, retracted cells. Similar to the results reported by Hall [8], rhodamine phalloidin staining, shown in Figure 4.7B indicates the presence of F-actin swirls, an intermediate actin organization response that is distinctly different from the complete lack of actin organization seen in non-transfected cells. By 26 hours, however, the cells retract and begin to adopt the characteristic Rho phenotype, as described above for cells plated on –COOH terminated SAM surfaces. Figure 4.7C shows that although cells are capable of attaining a spread morphology, no discernable focal contacts were

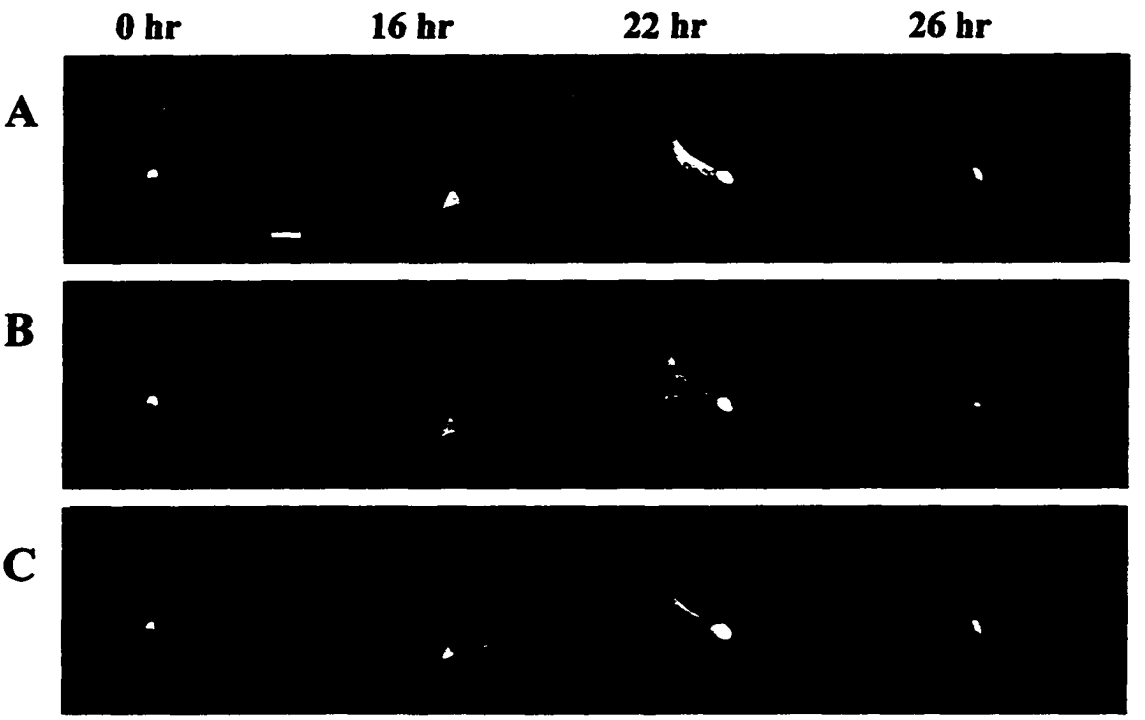

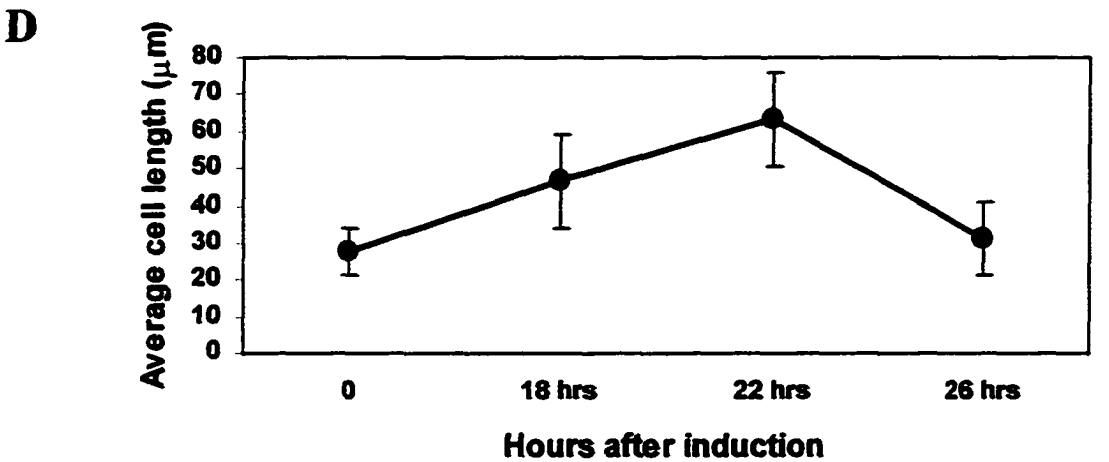

formed during the process. This correlates with the lack of available protein adhesion sites at the surface [13]. Figure 4.7D represents a summary of average cell length over time of fibroblasts plated–CH_3 terminated SAM surfaces transfected with constitutively active RhoA. Results show that there is an overall increase in cell spreading up to 22 hrs. After this time, cells begin to retract, similar to the observed response in transfected cells plated on –COOH terminated SAM surfaces. This response is characteristic of cells overexpressing active Rho protein [21].

4.4. DISCUSSION

In this work, we have attempted to address initial aspects of how RhoA contributes to surface chemistry-induced modulation of cell attachment and morphology. In addition, we show that artificially overriding the lack of surface-induced RhoA activation, such as that seen for cells cultured on –CH_3 terminated SAMs, by expressing a constitutively active form of RhoA is not sufficient to induce a growth phenotype in adherent cells.

These studies were motivated initially by our observations of focal contact and stress fiber formation in cells plated on derivatized SAM surfaces [13]. Fibroblasts cultured in serum on –CH_3 terminated SAMs do not form stress fibers and focal contacts. These structures are commonly used as indicators of effective outside-in signaling between surface-adsorbed ECM proteins (e.g., fibronectin) and intracellular, growth-stimulating signal transduction mechanisms. These observations combined with our previous findings that fibronectin-SAM surface adsorption and its RGD cell-binding

domain surface availability are less on -CH_3 SAMs when compared to –COOH terminated SAMs [13], led to the hypothesis that surface-dependent outside-in signaling was failing to activate RhoA on culture surfaces. This inactivation could then explain the lack of growth observed in fibroblasts cultured on –CH_3 terminated SAM surfaces. Significantly, proof of this hypothesis could establish an important link between cell biological responses and specific surface chemistry.

As described above, RhoA's activation state is believed to be modulated by both integrin and growth factor-dependent events [22]. Because RhoA mediates several cell attachment and spreading events investigated above, the activation state of RhoA is proposed to be directly influenced by integrin-specific events that are governed by ECM protein conformation and under surface chemistry control. Specifically, we contend RhoA is effectively activated and found in the GTP-bound,active form in cells cultured on the -COOH terminated SAM surfaces. Conversely, due to the low-growth phenotype observed in cells on -CH_3 terminated SAMs, RhoA is inefficiently activated in these cells and therefore found in the GDP-bound inactive state. At the present time, no anti-Rho-specific antibody is available to effectively precipitate Rho in its native form, thus allowing an analysis of the GTP/GDP state of the protein. However, the GTP-Rho form appears to be produced by receptors in response to extracellular signals, including integrin binding. Following this activation, RhoA is believed to be transported to the membrane [23] [24]. All known Rho proteins contain a carboxy-terminal CAAX box motif (C= cysteine, A= aliphatic amino acid, and X= any amino acid) shown to be geranyl-geranylated on the cysteine residue by the enzyme geranyl-geranyl transferase Type I [25]. This action was demonstrated to promote plasma membrane localization

[24]. After completing its action, GTP-Rho is hydrolyzed to GDP-Rho by Rho-GTPase activating protein (Rho-GAP) [26]. Rho is then bound by Rho-GDI, which inhibits GDP dissociation [27] and GTP binding [28], released from the membrane, and translocated back to the cytosol in its inactive form.

The activation state of RhoA was indirectly determined by examining the relative RhoA levels located in the cytosolic and membrane fractions in cells cultured on different terminal SAM surface chemistries. Translocation of RhoA to the membrane fraction, presumably following activation, correlates with several of the observed cell phenotypes indicating effective outside-in signaling between the cell and the extracellular environment. Consistent with this result was the observation that minimal amounts of RhoA are activated and localized to the membrane fractions in cells cultured on -CH_3 terminated SAMs due to the absence of these events. Total RhoA levels were reduced in cells cultured on –CH_3 terminated SAMs compared to those on the –COOH SAMs and significantly less RhoA was localized to the isolated membrane fraction, indicating inefficient RhoA activation and translocation.

Inactive RhoA is known to be sequestered in the cytoplasm by Rho-GDI. To strengthen the connection between RhoA's observed inactive state and the –CH_3 terminated SAM surface chemistry, comparisons of Rho-GDI's relative levels and localization in cells on the two different derivatized SAM surfaces were performed. Results indicated that consistent with the presence of a larger amount of inactive, GDP-bound, cytoplasmic RhoA in cells adherent to –CH_3 terminated SAM surfaces, Rho-GDI is also present in higher concentrations in the cytoplasm of these cells compared to

extracts from cells on -COOH SAMs. The connection between SAM surface chemistry, growth phenotype, and RhoA activation is tentatively established based on this evidence.

The role of RhoA in modulating surface-induced changes in adherent cell morphology was further addressed by artificially altering the activation state of RhoA in cells cultured on derivatized SAM surfaces. The first clues as to the biological function of Rho proteins came through the use of an exoenzyme produced by *Clostridium botulinum*, the C3 transferase, which irreversibly ADP-ribosylates Rho on amino acid Asn-41 [20]. When C3 transferase was introduced into a variety of cell types, they lost their actin stress fibers and rounded up [21, 29], thus implicating RhoA in these intracellular events. C3 transferase was used to correlate RhoA activation with adhesion and spreading in cells cultured on –COOH terminated SAM surfaces. Results show that inactivation of endogenous RhoA in spread cells plated on COOH terminated SAM surfaces results in a loss of growth phenotype, indicating a dependence on RhoA activation.

Additional alterations of RhoA activation in fibroblasts plated on –COOH terminated SAM surfaces were performed. An expression vector for constitutively active RhoA was introduced into fibroblasts plated on –COOH terminated SAM surfaces. RhoA has been shown to be effectively activated and transported to the membrane in these cells. Effects on cells morphology were monitored as a function of overexpression of mutant RhoA. Results show that overexpression of constitutively active RhoA in cells which contain adequate amounts of activated RhoA leads to a distinct morphology referred to in the literature as the Rho phenotype [21]. The cell body begins to retract and round up. This phenotype has also been shown to be induced after microinjection of normal Rho protein but higher concentrations are required [21].

The further role of RhoA in modulating surface-dependent cell morphologies was addressed by genetically compelling RhoA to remain active on $-CH_3$ terminated SAM surfaces and analyzing formation of intracellular stress fibers. An inducible, constitutively active, mutant form of RhoA was expressed in transfected fibroblasts plated on $-CH_3$ SAMs. Fibroblasts expressing this constitutively active RhoA mutant **are** capable of achieving a spread morphology on $-CH_3$ terminated SAM surfaces that is otherwise not observed on this surface. However, the rhodamine-phalloidin stress fiber staining indicated the presence of F-actin swirls, structures distinctly different from the fully organized stress fibers characteristic of cells plated on –COOH terminated SAMs. In the presence of mutant RhoA, the actin filaments appeared to lack contact with sites on the cell plasma membrane. These results are consistent with previous work with mutant active RhoA in adherent cells in culture Hotchin and Hall [8] showed that fibroblasts plated on surface-adsorbed poly-L-lysine (PLL), in the absence of extracellular matrix proteins formed actin swirls similar to those reported here when microinjected with constitutively active recombinant Rho protein. In addition, they concluded in the same paper that that functionally active Rho was not sufficient to trigger normal, complete focal contact assembly in the absence of extracellular matrix. Our results indicate not only is the **presence** of extracellular matrix essential for RhoA activation, but the **presentation** of surface adsorbed ECM proteins is also linked and critical. Specifically, extracellular matrix proteins responsible for integrin signaling must be present in the appropriate levels (density) and sufficiently recognizable conformation to lead to normal cell phenotypic responses in culture.

Our previous research [13] has demonstrated that fibronectin adsorbs to -CH_3 terminated SAMs at lower densities and in a less biologically active conformation than observed on –COOH terminated SAMs. Once adsorbed, fibronectin is known to be actively restructured by attached cells at the surface into a fibrillar matrix. This reorganization and restructuring plays an essential role in the biological activity of Fn [30]. The intracellular actin cytoskeleton is known to affect the assembly of Fn into a matrix. Newly assembled extracellular Fn fibrils align with intracellular actin-myosin bundles and focal adhesions [31]. In addition, disruption of actin filaments with the cytotoxin, cytochalasin, inhibits Fn matrix assembly [31]. Additionally, Rho-mediated actomyosin contractility is known to expose a cryptic assembly site in fibronectin [32]. Tension at the surface exerted by cells results in increased exposure of a self-assembly site in adsorbed Fn molecules. Exposure of this site has been demonstrated to induce fibronectin matrix reorganization and assembly.

Results presented here support the contention that RhoA is not being efficiently activated in cells adhering to –CH_3 terminated SAM surfaces. Lack of RhoA activation leads to the observed absence of actin filament bundling and subsequent reduction in contractility. Taken together, the sequence of events that emerges involves a surface chemistry dependence and regulation of these processes. Reduced levels of biologically active fibronectin adsorb on –CH_3 terminated SAM surfaces from serum; poorly recognized integrin binding sites compromise initial cell attachment. Signaling of RhoA on the intracellular side of the membrane is inefficient in this case, leading to a inefficient activation and translocation of RhoA to generate focal contacts and actin filament response. This then inhibits cell spreading, filament-induced tension, integrin clustering

and resultant extracellular fibronectin remodeling necessary for further phenotypic expression and cell growth responses.

Such an interpretation adds new molecular details involving the GTPase "gatekeeper" RhoA to a developing molecular model for the complex outside-in signal transduction process in adherent, anchorage –dependent cells. That Rho is highly conserved across a wide range of cells has profound implications for the generalized process of surface chemistry-modulated responses involving Rho proteins. Significantly, the capabilities demonstrated here to interrogate and manipulate the expression and activation of RhoA on surfaces should enhance further understanding of how cells precisely respond to adsorbed proteins and functional chemistry on surfaces. Correlations of molecular biological events associated with cell-surface signaling facilitate development of new biomaterials that integrate tissues using surface-tailored biological cues. Such rational approaches to needed materials improvements require full knowledge and control of signaling pathways to desired phenotypic endpoints. Study of RhoA modulation using well-controlled, albeit relatively simple surface chemistry, provides a new basis for assessing cell-surface interactions that contribute to such approaches.

The important intracellular signaling G-protein RhoA has been found to be influenced by cell culture surface chemistry. Using well-defined model organic surfaces in serum-based cell attachment experiments, the following conclusions are drawn:

1. RhoA becomes activated and membrane-localized in fibroblasts cultured on hydrophilic –COOH terminated surfaces, consistent with its known role in integrin-mediated cell signaling and growth responses. Such a result supports previous observations of greater cell attachment, proliferation and spreading, enhanced

fibronectin adsorption and greater integrin-binding motif availability on these surfaces over the more hydrophobic –CH3 terminated SAM surfaces [13].

2. Disabling the RhoA signaling process using C3 transferase (cytotoxin) produces an approximation of a low-growth, rounded-cell phenotype on surfaces, consistent with RhoA's known influence as a determinant for cell-surface association.
3. Transfection of low-growth phenotype, rounded cells on the poorly supportive $-CH_3$ terminated culture surface with a constitutively active RhoA mutant produces a transformation to a spread-cell phenotype with actin swirls, which is insufficient to facilitate a growth phenotype in these cells. Deficiencies in the attachment process are consistent with low cell attachment, spreading and proliferation, low fibronectin ECM densities and lack of RGD-integrin binding sites found previously on these surfaces [13]. F-actin assembly prompted by activated RhoA is not able to mature without sufficient integrin involvement.

4.5. Endnotes

1. Boguski, M.S. and F. McCormick, Nature, **366** : p. 643-654 (1993).
2. Nobes, C.D. and A. Hall, Rho, rac, and cdc42 GTPases regulate the assembly of multimolecular focal complexes associated with actin stress fibers, lamellipodia, and filopodia, Cell, **81** (1): p. 53-62 (1995).
3. Ridley, A.J., H.F. Paterson, C.L. Johnston, D. Diekmann, and A. Hall, Cell, **70** : p. 401-410 (1992).
4. Ridley, A.J. and A. Hall, Cell, **70** : p. 389-399 (1992).
5. Miura, Y., A. Kikuchi, T. Musha, S. Kuroda, H. Yaku, T. Sasaki, and Y. Takai, J. Biol. Chem., **268** : p. 510-515 (1993).
6. Maduale, P. and R. Axel, A novel ras-related gene family, Cell, **41** : p. 31-40 (1985).
7. Oloffson, B., P. Chardin, N. Touchot, A. Zahraoui, and A. Tavitan, Expression of the ras-related ral A, rho12 and rab genes in adult mouse tissues, Oncogene, **3** : p. 231-234 (1988).
8. Hotchin, N.A. and A. Hall, Regulation of the actin cytoskeleton, integrins and cell growth by the Rho family of small GTPases, Cancer Surv, **27** : p. 311-22 (1996).
9. Cerione, R.A. and Y. Zheng, Curr. Opin. Cell Biol., **8** : p. 216-222 (1996).
10. Leung, T., Q. Chen, E. Manser, and L. L., Mol. Cell Biol., **16** : p. 5313 (1996).

11. Machesky, L.M. and A. Hall, Role of actin polymerization and adhesion to extracellular matrix in Rac- and Rho-induced cytoskeletal reorganization, J Cell Biol, **138** (4): p. 913-26 (1997).

12. Chrzanowska-Wodnicka, M. and K. Burridge, Rho-stimulated contractility drives the formation of stress fibers and focal contacts., J. Cell Biol., **133** : p. 1403-1415 (1996).

13. McClary, K.B., T. Ugarova, and D.G. Grainger, Modulating fibroblast adhesion, spreading and proliferation with self-assembled monolayers of alkylthiolates on gold, J. Biomed. Mat. Res., (submitted Feb 1, 1999).

14. Ulman, A., *An introduction to ultrathin organic films : from Langmuir-Blodgett to self-assembly*. 1991, Boston: Academic Press. xxiii, 442.

15. Ulman, A., *Characterization of organic thin films*. Materials characterization series. 1995, Boston Greenwich: Butterworth-Heinemann ; Manning. xvi, 276.

16. Dubois, L.H. and R.G. Nuzzo, Synthesis, Structure and Properties of Model Organic Surfaces, Annu. Rev. Phys. Chem., **43** : p. 437-463 (1992).

17. Wessel, D. and U.I. Flugge, A method for the quantitative recovery of protein in dilute solution in the presence of detergents and lipids, Anal Biochem, **138** (1): p. 141-3 (1984).

18. Minamide, L.S. and J.R. Bamburg, A filter paper dye-binding assay for quantitative determination of protein without interference from reducing agents or detergents, Anal Biochem, **190** (1): p. 66-70 (1990).

19. No, D., T.-P. Yao, and R.M. Evans, Ecdysone-Inducible Gene Expression in Mammalian Cells and Transgenic Mice, Proc. Natl. Acad. Sci. USA, **93** : p. 3346-3351 (1996).

20. Aktories, K. and A. Hall, Botulinum ADP-ribosyltransferase C3: a new tool to study low molecular weight GTP-binding proteins, Trends Pharmacol Sci, **10** (10): p. 415-8 (1989).

21. Paterson, H.F., A.J. Self, M.D. Garrett, I. Just, K. Aktories, and A. Hall, Microinjection of recombinant p21rho induces rapid changes in cell morphology, J Cell Biol, **111** (3): p. 1001-7 (1990).

22. Hotchin, N.A. and A. Hall, The assembly of integrin adhesion complexes requires both extracellular matrix and intracellular rho/rac GTPases, J. Cell Biol., **131** (6): p. 1857-1865 (1995).

23. Fleming, I.N., C.M. Elliott, and J.H. Exton, Differential translocation of Rho family GTPases by lysophosphatidic acid, endothelin-1, and platelet-derived growth factor, J. Biol. Chem., **271** (51): p. 33067-33073 (1996).

24. Adamson, P., H. Paterson, and A. Hall, Intracellular localization of the $p21^{rho}$ Proteins, J. Cell Biol., **119** (3): p. 617-627 (1952).

25. Moores, S.L., M.D. Schaber, S.D. Mosser, E. Rands, M.B. O'Hara, V.M. Garski, M.S. Marshall, D.L. Pompliano, and J.D. Gibbs, Sequence dependence of protein prenylation, J. Biol. Chem., **266** : p. 14603-14610 (1991).

26. Lamarche, N. and A. Hall, GAPs for rho-related GTPases, Trends Genet, **10** (12): p. 436-40 (1994).

27. Ueda, T., A. Kikuchi, N. Ohga, and Y. Takai, J. Biol. Chem., **265** : p. 9373-9380 (1990).

28. Hart, M.J., Y. Maru, D. Leonard, O.N. Wittle, T. Evans, and R.A. Cerione, Science, **258** : p. 812-815 (1992).

29. Rubin, E.J., D.M. Gill, P. Boquet, and M.R. Popoff, Functional modification of a 21-kilodalton G protein when ADP-ribosylated by exoenzyme C3 of clostridium botulinum., Mol. Cell Biol., **8** : p. 418-426 (1988).

30. Mosher, D.F., Organization of the provisonal fibronectin matrix: control of products of blood coagulation, Thromb. Haemostasis, **74** : p. 529-533 (1995).

31. Wu, C.Y., V.M. Keivens, T.E. Otoole, J.A. McDonald, and M.H. Ginsberg, Integrin activation and cytoskeletal interaction are essential for the assembly of a fibronectin matrix., Cell, **83** (715-724) (1995).

32. Zhong, C., M. Chrzanowska-Wodnicka, J. Brown, A. Shaub, A.M. Belkin, and K. Burridge, Rho-mediated contractility exposes a cryptic site in fibronectin and induces fibronectin matrix assembly, J. Cell Biol., **141** (2): p. 539-551 (1998).

Chapter 5: Summary

5.1. Introduction

The research presented in this dissertation stems from two general observations. The first observation is that at the molecular level, most biomaterials have poorly-defined surface properties. As discussed in Chapter 1, this is primarily due to the historic use of polymeric materials [1]. Polymers are composed of multiple functional groups that are capable of dynamically restructuring at the surface in response to the environment [2]. This scenario makes it very difficult to actively design materials to elicit specific biological responses, due to the molecular level complexity present at the surface. And for this reason, there is a high rate of implant-centered infection and rejection that cannot be explained using cause and effect rationale [3].

The next observation that defined the research focus was that biological interactions such as protein adsorption and cell adhesion to solid surfaces are molecular level interactions. As discussed in Chapter 1, most cells are anchorage dependent, meaning that they require a solid substrate or proteinaceous scaffold to proliferate [4]. Cells adhere to biomaterials through interactions between receptors on the cell membrane and material surface-adsorbed proteins [5, 6]. These two observations led to the initial hypothesis that the ability to control surface chemistry at the molecular level would potentially lead to the ability to control molecular level biological responses. The primary goal of this research was to provide information to address implant infection and

rejection issues. Molecular level information would allow for the rational design of biomaterials that elicit predictable biological responses.

The model system used in this research utilizes self-assembly of alkylthiolates on gold. Self-assembly provides convenient, molecular level control of interfacial surface chemistry [7]. The first chapter of this dissertation describes the characterization of these films to ensure their composition and stability in cell culture conditions. Results show that SAMs of alkythiolates on gold have all the requisite properties for identifying molecular level determinants of biological responses.

Preliminary cell experiments indicated that SAM surface chemistry was capable of modulating cell morphology and growth. Specifically, cells plated on hydrophilic –COOH and –OH terminated SAM surfaces exhibited a well spread morphology and were able to proliferate. In contrast, cells plated on hydrophobic $-CH_3$ and $-CF_3$ terminated SAM surfaces remained rounded and were unable to proliferate. The research presented in this dissertation defines the molecular level determinants for these macroscopic biological responses.

Several signals exist which determine cellular fates when plated on materials. They can be grouped into extracellular signal and intracellular signals. Extracellular signals include growth factors and extracellular matrix proteins (ECMs). Intracellular signals include events induced upon interaction between surface-adsorbed ECMs and cell–surface integrin receptors.

As discussed in Chapter 2, the first biological contact with an implanted biomaterial occurs by proteins. Plasma contains a mixture of cell adhesive and cell non-adhesive proteins [1, 8]. In large abundance is the non-adhesive protein albumin, which

competes for surface occupancy with larger, adhesive ECMs. ECMs contain a cell-binding domain that interacts with cell-surface integrin receptors to facilitate cell adhesion to a material's surface. The chemistry at the surface can directly affect the relative levels of non-adhesive and adhesive proteins at the surface as well as the subsequent conformations of adsorbed proteins [9, 10]. For this reason, protein adsorption experiments were performed on hydrophilic –COOH and hydrophobic $-CH_3$ terminated SAM surfaces. When proteins adsorb onto surfaces, they unfold and adopt the most energetically favorable conformations. Numerous researchers in the field have demonstrated that surface chemistry can directly affect protein conformations at the surface [9, 10]. This affect could be particularly important for ECMs, which have the cell binding domain sequence that is recognized by cells. The hypothesis was that on surfaces that support cell growth, fibronectin would be present in a conformation which exposes the cell binding domain, whereas on the $-CH_3$ terminated SAM, which supports only minimal cell growth, this sequence may be less accessible. To test this hypothesis, we used a monoclonal antibody directed against the cell binding domain sequence in fibronectin. We performed Scatchard plots analysis to determine the relative affinities of the antibodies to cell binding domain sequences and determined the percent cell-binding domain available in fibronectin adsorbed onto methyl and carboxyl terminated SAM surfaces.

Protein adsorption and conformation experiments were performed in both competitive and non-competitive conditions. To summarize the extracellular signaling data, results showed that there is less fibronectin adsorption on methyl terminated SAM surfaces. This results in an overall decrease in the lateral density of fibronectin at the

surface. In addition, the fibronectin that is adsorbed is in a conformation that makes the cell-binding domain less accessible to approaching cells. This decrease in overall cellular anchors at the surface leads to low cellular adhesion and subsequent cell growth. This is in contrast to the scenario on carboxyl terminated SAM. Fibronectin adsorbs at high levels and in favorable conformation to these surfaces, facilitating a high level of cell adhesion and growth.

Chapter 3 describes the effects of surface chemistry on intracellular signals initiated in response to cell surface integrin attachment to material's surface adsorbed ECM proteins. Several indicators exist of effective outside-in communication between the extracellular environment and the cell. These indicators include the formation of stress fibers and focal contacts [11-15] and the phosphorylation of the focal contact proteins, FAK and paxillin [16]. To investigate the effects of surface chemistry on the activation of these intracellular events, immunocytochemistry experiments were performed.

Immunocytochemistry results showed that intracellular signaling events were modulated by surface chemistry. Cells plated on –COOH terminated SAM surfaces are well spread. They have extensive stress fiber formation and show localization of various focal contact proteins to the ends of the stress fibers, including FAK, paxillin and vinculin. In addition, several focal contact proteins are phosphorylated in response to plating on –COOH terminated SAM surfaces as demonstrated by phosphotyrosine staining at the ends of stress fibers as well as immunoprecipitation experiments. . In contrast, cells plated on $-CH_3$ terminated SAM surfaces exhibit very little cell spreading. They show minimal if any stress fiber formation and lack localization of focal adhesion

proteins to the cell membrane. In addition, reduced levels of tyrosine phosphorylation of focal contact proteins is seen in extracts from these cells.

To summarize, the research presented in this dissertation began by looking at protein adsorption and conformation on derivatized SAM surfaces and showed that there is less fibronectin adsorption and less cell binding domain available in Fn adsorbed on $-CH_3$ terminated SAM surfaces. Intracellular signaling data shows that these unfavorable protein conditions lead to inefficient activation of the intracellular signals which lead to stress fiber and focal contact formation. This is in contrast to the scenario in cells plated on carboxyl terminated SAM surfaces, where the protein conditions facilitate effective intracellular signaling.

Chapter 4 looks at the primary player in the induction of early signaling events, the small GTPase RhoA. The small molecular weight GTPase RhoA is involved in the formation of stress fibers and focal contacts, shown to be regulated by surface chemistry [13, 14, 17, 18]. Like all GTPases, RhoA is interconvertible between and active, GTP bound and inactive GDP bound state. The activation state of the protein is regulated by numerous proteins including guanine nucleotide exchange factors and GTPase activating proteins [19]. Upon activation, RhoA is transported to the membrane, where it is inserted via the isoprenyl group on its C-terminal end [20]. After providing its function, the protein is inactivated, released from the membrane and transported to the cytoplasm by the Rho guanine nucleotide dissociation inhibitor, until it is reactivated [21].

Based on the previously presented results, our hypothesis was that the activation state of RhoA was being modulated by surface chemistry. Specifically, we believed that on the -COOH terminated SAM surfaces, where cell growth was supported, RhoA would

be found primarily in an active, GTP-bound, membrane localized state, whereas on $-CH_3$ terminated SAM surfaces, which supported minimal cell growth, RhoA would be found primarily in an inactive, GDP-bound, cytosolic state. To determine the activation state of RhoA indirectly, extracts from cells plated on derivatized SAM surfaces were fractionated into cytosolic and membrane fractions and Western blots were performed for the presence of RhoA.

Results indicated that membrane extracts from cells plated on methyl terminated SAMs contain less RhoA than extracts from cells plated on carboxyl terminated SAM surfaces. This indicates that RhoA is inefficiently activated and transported to the membrane in cells plated on methyl terminated SAM surfaces. This directly correlates with the absence of stress fibers and focal contacts in these cells, as this response in due to the action of activated RhoA.

To further correlate the surface chemistry effects on RhoA, Rho-GDI levels in cytosolic and membrane fraction were determined. Recall that in its inactive form RhoA is sequestered in the cytoplasm by Rho-GDI [21]. As expected, cytosolic extracts from cells plated on $-CH_3$ terminated SAM surfaces contain more Rho-GDI than extracts from cells plated on –COOH terminated SAMs. This is concurrent with its role in sequestering the large amounts of inactive RhoA present in this fraction.

Finally, the effect of introducing active RhoA into cells plated on methyl terminated SAMs, which lack activated RhoA to begin with was determined by introducing a mutant, constitutively active form of RhoA into cells plated on $-CH_3$ derivatized SAM surfaces. Constitutively active RhoA expression in cells plated on $-CH_3$ terminated SAM surfaces leads to an increase in cell length, however, this increased

spreading was not accompanied by the formation of characteristic stress fibers or focal contacts.

To summarize the conclusions of this dissertation research, Chapter 2 looked at protein adsorption on different surface chemistries and found that surfaces that supported cell growth, such as the carboxy terminated SAMs exhibited high fibronectin adsorption and high cell binding domain availability. In contrast, surfaces like the methyl terminated SAM surfaces, which display limited cell growth capabilities, exhibit low levels of fibronectin adsorption and cell binding domain availability. The low density of protein anchors at the surface leads to inefficient activation of intracellular signal like RhoA, that lead to focal contact and stress fiber formation in cells plated on the methyl terminated SAM surface, whereas these signals are present in cells plated on carboxyl terminated SAMs.

Finally, overridding the surface activation step in cells plated on methyl terminated SAMs by introducing a constitutively active version of the protein is unable to induce a growth morphology in these cells. This can be attributed to the lack of available cell adhesion sites on this surface. The ultimate conclusion of this experiment is that despite the activation of intracellular mechanisms to facilitate cell spreading and growth, without coordination of extracellular factors, desirable growth phenotype cannot be achieved.

Ultimately, this research has demonstrated the ability to predictably control biological responses using well-defined surface chemistry. As discussed earlier, the design of biomaterials has been hindered by the lack of identifiable cause and effect

correlations between surface chemistry and cells. The results presented here represent a step in this direction.

5.2. Future Directions

To begin, several of the problems encountered in the experiments outlined in this dissertation could be addressed by considering alternative methodologies. The primary area of difficulty lies in the immunocytochemistry experiments presented. In cells plated on $-CH_3$ terminated SAM surfaces, the cell appear rounded. Non-specific staining by the fluorescently-labeled secondary antibodies make it difficult to identify specific, localized staining, as the non-specific staining in the cells is too high to identify any specific staining present. This led to difficulty in distinguishing cells expressing mutant RhoA from those not expressing the protein, as both were brightly stained. Alternatives to the methodology used to obtain the data presented include confocal microscopy and microinjection of recombinant protein. Confocal microscopy allows for imaging sections of cells. This could possibly reduce the cumulative effects of layers of nonspecific staining and allow for the identification of specific staining. Finally, microinjection of recombinant, mutant RhoA protein would allow for the tracking of morphological progression of only cells which have been injected.

The results presented in this dissertation provide information on biological responses to well-defined, uniform surface chemistries. An obvious progression of this model system would be to produce binary mixtures of derivatized alkylthiol on gold. For example, mixtures of –COOH derivatized SAM surfaces, which facilitate cell growth, and $-CH_3$ terminated SAM surfaces, which inhibit cell growth. Possibly by varying the

percentage of each alkythiol in the SAM, cell adhesion could be modified more precisely. These experiments would add another level of complexity to the system. It could potentially begin to address the question of why tissue culture polystyrene, which consists of a variety of surface functional group, facilitates unrivaled cell adhesion, spreading and growth.

The actin cytoskeleton of mammalian cells maintains cellular shape and plays a pivitol role in cell motility, phagocytosis and intracellular transport processes [14]. As discussed in the introduction section in Chapter 4, numerous members of the family of small molecular weight GTPases have been implicated in regulating cytoskeletal events essential for cell progression through the cell cycle [17]. Specifically, the Rho family of proteins include Rho, Rac and cdc42. Rac is important in actin polymerization associated with membrane ruffling and lamellipodia formation and cdc42 is responsible for cell filopodia formation [22]. Lamellipodia and filopodia are essential for cell motility and division and therefore essential for cell growth and survival on solid surfaces. Significantly, significant cross-talk exists between GTPases of the Rho subfamilies. For instance, cdc42 can activate Rac, hence filopodia are intimately associated with lamellipodia and Rac can activate Rho [23, 24]. Although the details of these interactions remain unclear, investigations of the interplay of these molecules in response to cell adhesion on different surface chemistries could be useful.

5.3. Endnotes

1. Andrade, J., ed. *Surface and Interfacial Aspects of Biomedical Polymers.* . Vol. 2. 1985, Plenum Press: New york.
2. Schmitt, R.L. and J.A. Gardella, Study of surface composition and morphology of block copolymers of bisphenol A polycarbonate and poly)dimethlsiloxane) by x-ray photoelectron spectroscopy and ion scattering spectroscopy, Macromolecules, **18** : p. 2675-2679 (1985).
3. Gristina, A.G., Biomaterial-centered infection: microbial adhesion versus tissue integration, Science, **237** (4822): p. 1588-95 (1987).
4. MacPherson, I. and L. Montagnier, Virology, **23** : p. 291-294 (1964).
5. Curtis, A.S. and J.V. Forrester, Cell interactions: some critical reappraisals, Biochem Soc Trans, **12** (3): p. 538-9 (1984).
6. Mooney, M.A. and D.E. Ingber, Integrin Binding and Cell Spreading on Extracellular Matrix Act at Different Points in the Cell Cycle to Promote Hepatocyte growth, Molec. Biol. Cell, **5** : p. 967-979 (1994).
7. Ulman, A., *An introduction to ultrathin organic films : from Langmuir-Blodgett to self-assembly*. 1991, Boston: Academic Press. xxiii, 442.
8. Mrksich, M., C.S. Chen, Y. Xia, L.E. Dike, D.E. Ingber, and G.M. Whitesides, Controlling cell attachment on contoured surfaces with self-assembled

monolayers of alkanethiolates on gold, Proc Natl Acad Sci U S A, **93** (20): p. 10775-8 (1996).

9. Garcia, A.J., M.D. Vega, and D. Boettiger, Modulation of cell proliferation and differentiation through substrate-dependenet changes in fobronectin conformation, Mol. Biol. Cell, **10** (1999).

10. Lewandowska, K., N. Balachander, C.N. Sukenik, and L.A. Culp, Modulation of fibronectin adhesive functions for fibroblasts and neural cells by chemically derivatized substrata, J Cell Physiol, **141** (2): p. 334-45 (1989).

11. Ridley, A.J. and A. Hall, Signal transduction pathways regulating Rho-mediated stress fibre formation: requirement for a tyrosine kinase, Embo J, **13** (11): p. 2600-10 (1994).

12. Miura, Y., A. Kikuchi, T. Musha, S. Kuroda, H. Yaku, T. Sasaki, and Y. Takai, J. Biol. Chem., **268** : p. 510-515 (1993).

13. Nobes, C. and A. Hall, Regulation and function of the Rho subfamily of small GTPases, Curr Opin Genet Dev, **4** (1): p. 77-81 (1994).

14. Nobes, C.D. and A. Hall, Rho, rac, and cdc42 GTPases regulate the assembly of multimolecular focal complexes associated with actin stress fibers, lamellipodia, and filopodia, Cell, **81** (1): p. 53-62 (1995).

15. Nobes, C.D. and A. Hall, Rho, rac and cdc42 GTPases: regulators of actin structures, cell adhesion and motility, Biochem Soc Trans, **23** (3): p. 456-9 (1995).

16. Burridge, K., C.E. Turner, and L.H. Romer, Tyrosine phosphorylation of paxillin and FAK accompanies cell adhesion to extracellular matrix: A role for cytoskeletal assembly, J. Cell Biol., **119** (4): p. 893-903 (1992).

17. Hall, A., Ras-related GTPases and the cytoskeleton, Mol Biol Cell, **3** (5): p. 475-9 (1992).

18. Hall, A., Rho GTPases and the actin cytoskeleton, Science, **279** (5350): p. 509-14 (1998).

19. Cerione, R.A. and Y. Zheng, Curr. Opin. Cell Biol., **8** : p. 216-222 (1996).

20. Moores, S.L., M.D. Schaber, S.D. Mosser, E. Rands, M.B. O'Hara, V.M. Garski, M.S. Marshall, D.L. Pompliano, and J.D. Gibbs, Sequence dependence of protein prenylation, J. Biol. Chem., **266** : p. 14603-14610 (1991).

21. Lamarche, N., N. Tapon, L. Stowers, P.D. Burbelo, P. Aspenstrom, T. Bridges, J. Chant, and A. Hall, Rac and Cdc42 induce actin polymerization and G1 cell cycle progression independently of p65PAK and the JNK/SAPK MAP kinase cascade, Cell, **87** (3): p. 519-29 (1996).

22. Hall, A., H.F. Paterson, P. Adamson, and A.J. Ridley, Cellular responses regulated by rho-related small GTP-binding proteins, Philos Trans R Soc Lond B Biol Sci, **340** (1293): p. 267-71 (1993).

23. Hall, A., Rho GTPases and the actin cytoskeleton, Science, **279** : p. 509-514 (1998).

24. Hall, A., ras and GAP--who's controlling whom?, Cell, **61** (6): p. 921-3 (1990).